



Technische Universiteit Delft

Sediment Transport Pathways in Burrard Inlet

MSc Thesis
Carlijn Meijers

Sediment Transport Pathways in Burrard Inlet

by

Carlijn Meijers

to obtain the degree of Master of Science
at the Delft University of Technology,
to be defended publicly on Wednesday December 1, 2021 at 16:00

Student number: 5064783
Project duration: March 10, 2021 – December 1, 2021
Thesis committee: Prof. dr. ir. Z.B. Wang, TU Delft & Deltares, chair
Dr. ir. B.C. van Prooijen, TU Delft
Dr. ir. E.P.L. Elias, Deltares
Ir. S.G. Pearson, TU Delft & Deltares

An electronic version of this thesis is available at <http://repository.tudelft.nl/>.

Abstract

Burrard Inlet (Vancouver, Canada) has been the home of the Tsleil-Waututh Nation (TWN) for thousands of years. Over the past decades, ongoing erosion has been observed along the shores of Burrard Inlet and the TWN reserve specifically. This leads to loss of land for the TWN community, damage to infrastructure, and exposure of historic sites with cultural value. Currently, there is insufficient knowledge concerning both the governing processes for sediment transport and transport pathways into, within, and out of Burrard Inlet. This knowledge is needed to propose and evaluate effective measures to prevent further erosion. This study aims to investigate the transport pathways in Burrard Inlet and give more insight into the mechanisms governing sediment transport in this inlet.

For this purpose, a Delft3D FM model of the area is set up and calibrated. This model is used to analyze sediment transport in the inlet under various forcing conditions. Transport pathways are visualized using SedTRAILS.

The model shows that flows and sediment transport in Burrard Inlet are tide-dominated and governed by the topography. Flows are strongly accelerated in constricted areas (First Narrows and Second Narrows), which leads to large velocity differences. Following the velocity field, sediment transport patterns are correspondingly dominated by these topographical restrictions. In the wider basins, flows slow down and form eddies. The model results suggest that these eddies act as sediment sinks. Additionally, sediment is lost into Indian Arm, a deep fjord with low flow velocities at the eastern end of Burrard Inlet. The possible pathways for sediment originating from the eroding shorelines at the TWN reserve are visualized. As soon as sediment from these banks is mobilized, it tends to move away from the shore with a final destination either in one of the eddies or in Indian Arm. The impact of wind and waves on the sediment transport patterns is limited.

Since first European contact in 1792, the shoreline of Burrard Inlet has changed significantly due to dredging activities, land developments, and industrial development as the city of Vancouver was built. Reconstructed historic shorelines are implemented in the model to assess the consequences of these shoreline changes on the sediment transport. Model results show that the tidal prism and the velocities in the Narrows have decreased since 1792, while the tidal range has increased. Moreover, sediment mobilized along the eroding shorelines showed greater potential for deposition along these same shores in 1792, compared to the present-day situation.



Figure 1: The study site: Burrard Inlet, located in Vancouver, British Columbia, Canada. The location of Tsleil-Waututh Nation's main community is indicated in the map.

Preface

Over the past 10 months, I have been able to dive into the world of sediment transport. As I learned more about the study site, I was fascinated by its complexity, by the many different processes that are brought together and interact with each other. In this thesis, I try to unravel some of it by exploring the sediment dynamics in Burrard Inlet, in a highly relevant cultural context. I really enjoyed working on this thesis, and I hope you enjoy reading it.

This thesis would never have been possible without the help of my committee. Thank you Stuart, for your never-ending enthusiasm and positivity, for always taking the time to read my drafts and provide me with feedback, and for regularly updating me with the latest Vancouver news. Edwin, you were always there when I needed you, and your valuable advice and critical questions have made this thesis a lot better. I want to thank Professor Wang for chairing the committee and Bram for the useful feedback. I am also grateful to the people supporting my thesis from Vancouver: Patrick, Spencer, and Eric, for introducing me to an area on the other side of the world with the stories and information you shared with me, and for your input to the project.

During the project, I got a lot of support from the people at Deltares and my fellow students. Thanks to Mick and Julien for all the help with modeling. Thank you, Denzel, Paula, and Sterre for thinking along with me and answering my questions.

I have worked on this thesis during the Covid-pandemic, which meant a lot of working from home. I want to thank all my friends for keeping me sane in these sometimes challenging times. Thank you, Nomi and Marthe for our regular walks and swimming sessions during the lockdown. Anton, for our daily morning coffee ritual. Thanks to Rieneke, Michiel, Twan, Tjerk, Charlotte, and Gabriela for all the coffees and lunches together, and drinking champagne from paper cups whenever someone reached a milestone in their project. Once we were able to study on campus again, you made the last few months of working on my thesis so much more enjoyable. And last, but certainly not least, I want to thank my parents, Rik, and Isa, for always being there for me and supporting me in everything I do.

Enjoy reading!

Carlijn Meijers
Delft, November 2021

Contents

1	Introduction	1
1.1	Context	1
1.2	Problem Statement	3
1.3	Research questions	3
1.4	Approach	4
1.5	Thesis outline	4
2	Literature Review	7
2.1	Cultural perspective	7
2.1.1	First Nations in Canada	7
2.1.2	Tsleil-Waututh Nation	7
2.2	Burrard Inlet	9
2.2.1	Inlet characteristics	9
2.2.2	Hydrodynamics	9
2.2.3	Salinity	10
2.2.4	Wind and waves	10
2.2.5	River discharge	11
2.2.6	Strait of Georgia and Fraser River	12
2.2.7	Environment	13
2.3	Sediment availability	14
2.4	Sediment transport patterns	15
2.4.1	Large scale transport patterns	15
2.4.2	Central Harbour	16
3	Model Set-up	19
3.1	Model Set-up	19
3.1.1	Model domain	19
3.1.2	Grid	19
3.1.3	Bed level	20
3.1.4	Rivers	21
3.1.5	Boundary conditions	21
3.1.6	Wind	22
3.2	Waves	23
3.2.1	Wave input	24
3.3	Representative tidal cycle	24
3.4	Limitations	26
3.5	Post-processing of the results using SedTRAILS	28
3.5.1	Description of the method	28
3.5.2	Limitations of the approach	28
3.5.3	Application	29
4	Model calibration and validation	31
4.1	Salinity	32
4.2	Roughness coefficient	33
5	Results	35
5.1	Hydrodynamics	35
5.1.1	Hydrodynamic particle trajectories	37
5.2	Sediment transport vectors	39
5.2.1	Sediment transport in Central Harbour	41

5.3	Sediment transport pathways using SedTRAILS	41
5.3.1	Central Harbour.	43
5.4	Sediment sources	45
5.4.1	Rivers in Burrard Inlet	45
5.4.2	Fraser River.	46
5.5	Influence of wind and waves	46
5.5.1	Wind.	46
5.5.2	Waves.	47
6	Human interventions	49
6.1	Implementation of shoreline changes in the model	49
6.2	Hydrodynamic changes	50
6.3	Changes in sediment transport	51
6.4	Changes in transport pathways	53
7	Discussion	57
7.1	Interpretation of the results.	57
7.2	Sensitivity	60
7.3	Effect of human interventions	61
7.3.1	Modeled shoreline changes	61
7.3.2	Other human interventions	62
7.4	Comparison to existing knowledge	64
7.4.1	Full inlet/larger scale patterns	64
7.4.2	Central Harbour.	65
8	Conclusion and recommendations	67
8.1	Conclusion	67
8.2	Recommendations	69
8.2.1	Data collection	69
8.2.2	Model improvements	70
8.2.3	Application of the existing model	71
8.2.4	Possible measures to counteract erosion	72
A	Calibration	77
B	Morphological tide	79
B.1	Selection of the morphological tide	79
B.2	Sensitivity runs for tidal cycles	81
C	Velocity analysis	85
D	SedTRAILS for hydrodynamics	87
E	Sediment Transport Pathways	93
F	Fraser river	97
G	Waves	101
G.1	Wave heights	101
G.2	Wave-driven changes to net transport.	104
G.3	SedTRAILS pathways for waves	107
H	Human Interventions	109

Introduction

1.1. Context

Burrard Inlet is a fjord in British Columbia, Canada, flowing out into the Strait of Georgia just north of the Fraser River. The fjord is located in the city of Vancouver (for the location, see Figure 1.1).

The Tsleil-Waututh Nation (TWN) has lived along the shores of Burrard Inlet for thousands of years. They are a First Nation, a recognized group of indigenous people in Canada. First Nations people are the original inhabitants of the land that is now Canada, and were the first to encounter European contact, settlements, and trade. The name Tsleil-Waututh means 'People of the Inlet' and the Nations cultural and historical identity is strongly connected to the inlet. Archaeological findings have confirmed that the inlet has been the center of their traditional territory for thousands of years (Tsleil-Waututh Nation, 2020).

Historically, Tsleil-Waututh lived from the natural resources of the inlet, especially through fishing and harvesting shellfish. TWN has a long-held stewardship obligation to protect and care for the water, land, air, and resources in Burrard Inlet. However, following the first European contact in 1792 and the urban and industrial developments in the city of Vancouver that followed, the resources of the inlet have been depleted and contaminated (Lilley et al., 2017). TWN is actively investing in efforts to restore the health and environment of Burrard Inlet. They participate in environmental restoration projects and commission scientific research projects on the current state of the inlet.

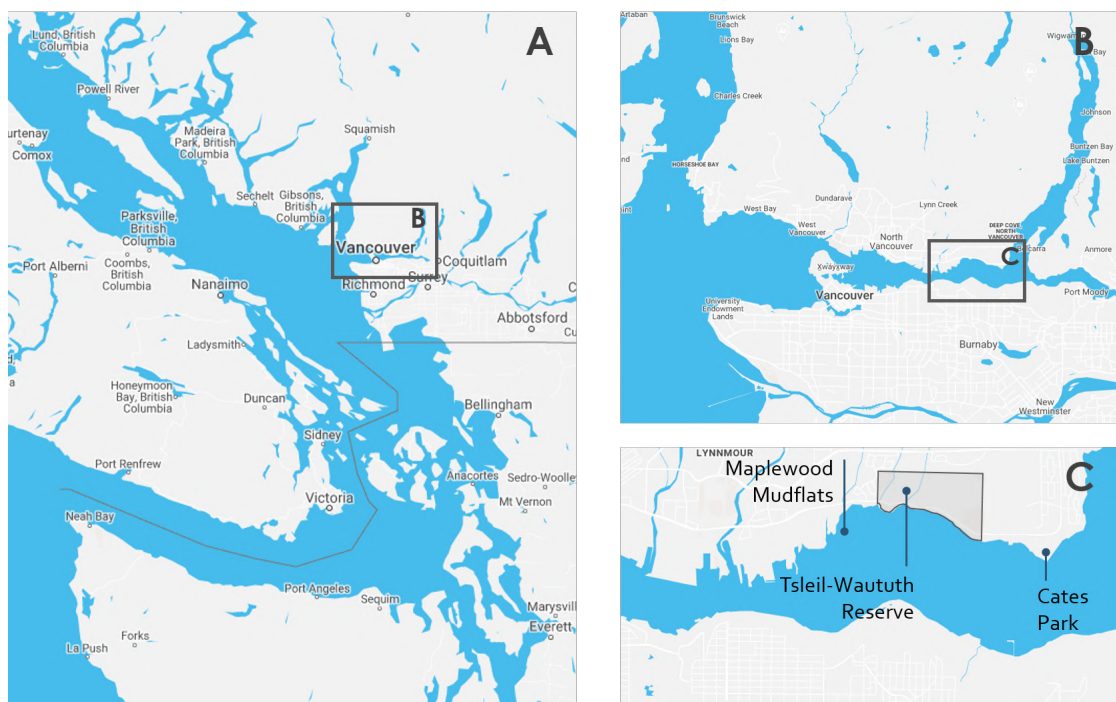


Figure 1.1: A) The location of Burrard Inlet within the Strait of Georgia. B) Burrard Inlet and the location of the Central Harbour. C) The Central Harbour, including the Tsleil-Waututh Reserve, Maplewood Mudflats and Cates Park.

Tsleil-Waututh members have observed ongoing erosion and a changing sediment composition along the shores of Burrard Inlet and their territory specifically. In cooperation with the Canadian consulting firm Kerr Wood Leidal Associates Ltd. (KWL), they have issued a research project to identify the sediment transport patterns and the mechanisms playing a role in the erosion.

Unlike many other west coast fjords, Burrard Inlet is relatively shallow, with a mean depth of 21m (Nijman and Swain, 1990). At the eastern end of the inlet, a deep fjord with steep cliffs extends northwards: Indian Arm. The inlet receives freshwater from several rivers, including Indian River, Capilano River and Seymour River. However, in the largest part of the inlet, the flow is dominated by tidal motion (Thomson, 1981).

The natural shoreline consists of rocky areas, combined with sand and gravel beaches (Coastal and Ocean Resources, 2018). Most of the shoreline area is highly developed due to residential and industrial activities in the city of Vancouver. The inlet is busy with shipping, since the industrial port of Vancouver is located in the Inner Harbour (Figure 1.2, Image 1).

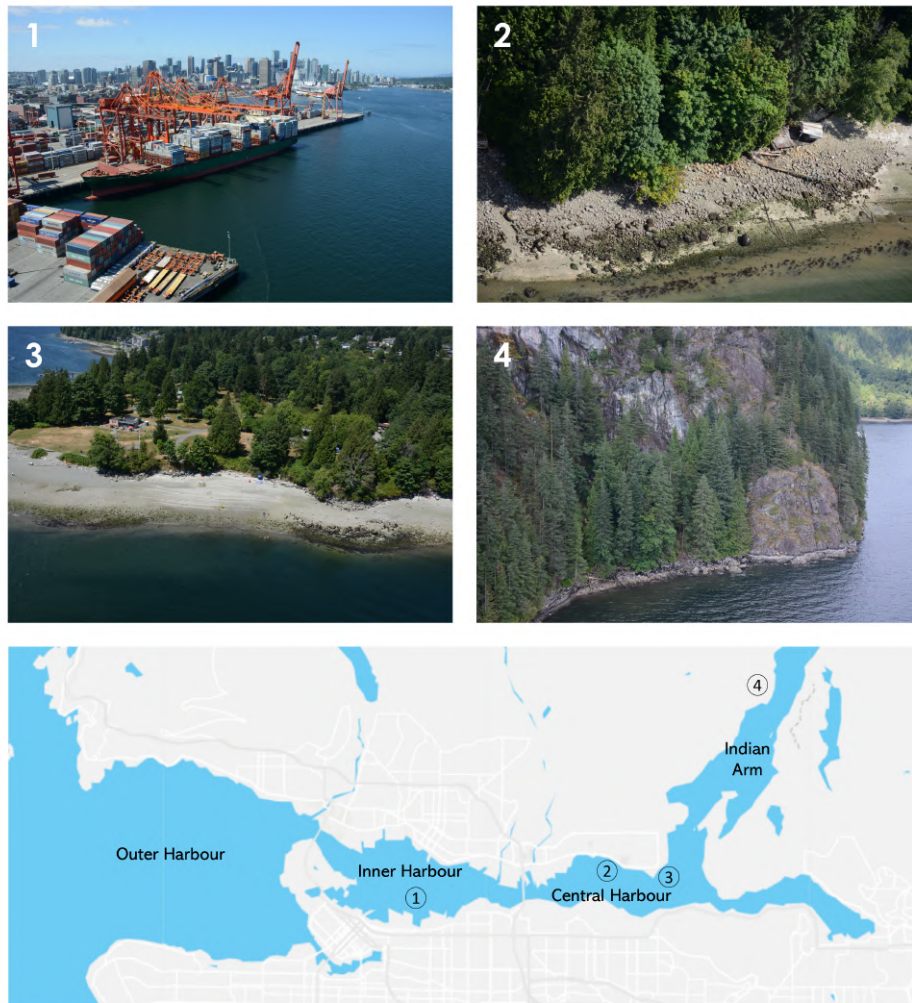


Figure 1.2: 1) The industrial port in Inner Harbour. 2) Eroding shorelines and coarse beaches in front of the Tsleil-Waututh reserve. 3) Eroding beaches at Cates Park. 4) Steep and rocky shorelines in Indian Arm. Images by Coastal and Ocean Resources (2018).

1.2. Problem Statement

TWN has long observed changes and impacts to their shorelines due to erosional processes. Shorelines in front of the TWN reserve and at culturally important locations, such as the archaeological site at Whey-Ah-Wichen (Cates Park, Figure 1.2, Image 3), are eroding. This leads to loss of land for the TWN community and impacts structures built along the shorelines. Moreover, the sediment dynamics at intertidal areas and important shellfish beaches are changing, impacting ecosystems for birds and marine life. An example of this is the increasingly coarse sediment composition at Maplewood Mudflats Conservation Area (Figure 1.3).

Currently, there is insufficient knowledge concerning the sediment sources, governing processes for sediment transport, and sediment transport pathways into, within and out of Burrard Inlet. This knowledge is needed to assess potential impacts of current and future land use and infrastructure projects. Moreover, an understanding of the sediment transport patterns is essential to plan and implement shoreline climate adaptation initiatives.



Figure 1.3: Aerial picture of Maplewood Mudflats. In the background, the industrial port in Inner Harbour and the high-rise buildings in the Vancouver city center can be seen (Coastal and Ocean Resources, 2018).

1.3. Research questions

The aim of this research is to estimate the sediment transport pathways through Burrard Inlet and get more insight in the processes responsible for sediment transport there. Understanding the transport patterns is an important step in addressing the shoreline retreat, as this is caused by an exchange between sediment feeding the area and sediment that is withdrawn. As sediment along the shorelines is mobilized, transport processes determine whether this sediment will settle or move away. Moreover, the transport patterns can give insight into which sources of sediment are able to feed the eroding shorelines. Understanding this system enables the Tsleil-Waututh Nation to propose and evaluate effective measures to prevent further erosion.

The transport patterns in Burrard Inlet are the result of an interplay between different forcing mechanisms, such as tidal currents, wind, and wind waves. The role of each of these processes will be assessed to understand their influence on the sediment pathways.

Moreover, human interventions since the first European settlements in 1792 and the industrialization and urbanization that followed might have affected the sediment transport system in the inlet. This study will evaluate to what extent these changes can have affected the transport pathways and equilibria.

To reach this aim, a numerical model of Burrard Inlet will be developed. The model will simulate hydrodynamics in the inlet and give insight into the processes responsible for sediment transport. Special attention will be given to the areas with observed shoreline erosion, including the shoreline in front of the TWN reserve and Cates Park (Figure 1.1 - C).

To achieve this aim, the following research question is formulated:

What are the sediment transport pathways into, within, and out of Burrard Inlet, and what is the role of the different hydrodynamic processes and of human interventions on these patterns?

As a first step, the numerical model will be developed, simulating the hydrodynamics and sediment transport in Burrard Inlet. This model can be used to answer the following sub-questions:

1. *What are the sediment transport pathways under present-day average conditions?*
2. *What are the sources of sediment entering Burrard Inlet and how do they redistribute within the inlet?*
3. *What is the role of tidal currents, wind, and wind waves on the transport pathways?*
4. *What is the effect and sensitivity of the shoreline alterations that have taken place in the past two centuries on the transport patterns?*

1.4. Approach

The research question will be answered by means of numerical modelling. The software Delft3D FM is used to give insight into the governing hydrodynamic processes and residual flow patterns. A detailed model of Burrard Inlet is set up, which is used to resolve the flows and sediment transport in the inlet.

After the model is developed and calibrated, the hydrodynamic behaviour of the inlet is assessed first, as the velocity field forms the basis for sediment transport. Subsequently, the sediment transport vector field is analyzed at different timesteps, to obtain an overview of dominant patterns in the sediment transport.

The transport pathways following from this vector field are visualized using SedTRAILS to answer the first research question. SedTRAILS is a tool to visualize and analyze sediment transport pathways in a Lagrangian framework (Elias and Pearson, 2020). It computes the pathways that sediment particles follow as they travel through a changing velocity field. The pathways computed in SedTRAILS give a comprehensive overview of where the sediment eroding at a certain location is going, or where sediment reaching a specific location comes from.

To answer the second research question, the computed pathways are used to identify how sediment entering the inlet is redistributed by investigating the trajectories originating from sediment sources. This gives insight into the potential of different sources to feed the system.

As a next step, the roles of the different hydrodynamic processes are investigated, addressed in research question 3. This is done by performing several model runs with varying hydrodynamic conditions, as was done by Stevens et al. (2020), to view the influence of the different factors separately. Simulations including wind and waves are compared to the 'baseline scenario' with only tidal forcing, to uncover what influence wind and waves have on the transport patterns.

To answer the fourth research question, the effect of shoreline alterations will be assessed by incorporating reconstructed shorelines from 1792 (before European contact) in the model to see to what extent such changes in the shoreline are able to affect the sediment transport (Tsleil-Waututh Nation, 2021).

TWN has a vast amount of knowledge on the changes that have been observed in the area over the years. Much of this knowledge is captured and documented by Harper (2020), including recollections of Tsleil-Waututh elders and shoreline observations. The results from this research are mapped and compared to the TWN knowledge. Moreover, comparison can be made to the study by McLaren (1994) on the sediment transport pathways. Although this approach has been criticized for being subjective and not picking up smaller scale movements (LeRoux and Rojas, 2007), this is the only comprehensive effort to estimate sediment pathways in Burrard Inlet so far. Therefore, a comparison will be made to these results as well. Figure 1.4 shows a summary of the steps described in this approach.

1.5. Thesis outline

Following the steps in Figure 1.4, this thesis is structured as follows.

In Chapter 2, the literature review, background information on the Tsleil-Waututh Nation and First Nations in Canada is provided. This chapter maps out the physical setting of Burrard Inlet and its characteristics. Moreover, the studies that have been done so far on sediment transport in Burrard Inlet are described.

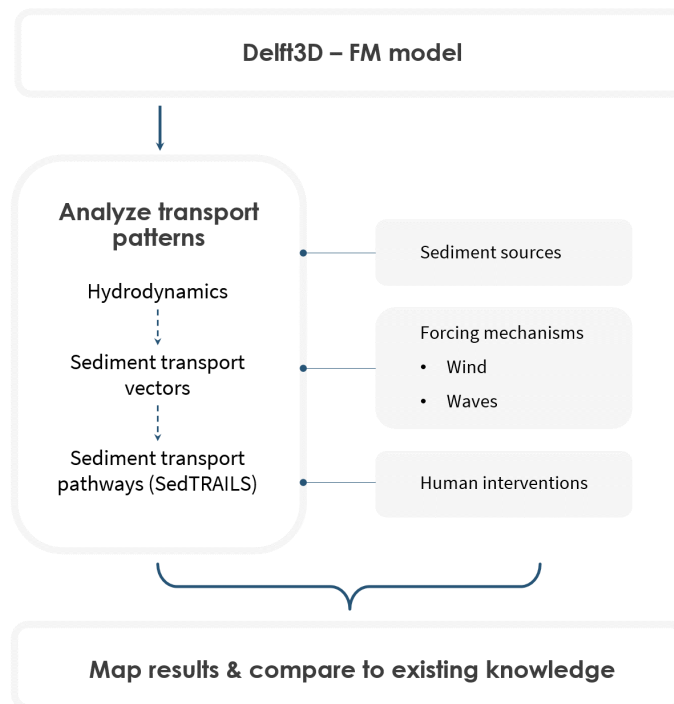


Figure 1.4: Schematic showing the different steps of the research project.

Chapter 3 and Chapter 4 describe the Delft3D FM model that was built. Chapter 3 explains the set-up of the model, elaborating on the grid, boundary conditions and external forcing conditions that were used in the model. Subsequently, Chapter 4 describes how the model was calibrated and validated.

This is followed by Chapter 5, presenting the results. First, the hydrodynamic system of the inlet is described. Then, the sediment transport pathways are mapped out. Pathways from the different potential sediment sources (Capilano River, Seymour River, Lynn Creek and Fraser river) are visualized to see if and how they are able to feed the system with sediment. The contribution of different hydrodynamic processes is assessed by presenting the transport fields including wind and waves and comparing them to the baseline tide-only case. Subsequently, Chapter 6 assesses the effects of human interventions and shoreline changes to Burrard Inlet and Central Harbour specifically.

Finally, Chapter 7 reflects on the obtained results and compares them to the existing knowledge. In Chapter 8, the conclusions are given and recommendations for further research are listed.

Literature Review

2.1. Cultural perspective

2.1.1. First Nations in Canada

First Nations are one of three recognized groups of Aboriginal Peoples in Canada, together with the Inuit and Métis (Wilson and Henderson, 2014). Many groups of First Nations, with a rich variety in culture, language, and history have lived on the land that is now Canada for thousands of years. Traditionally, their societies have been communal and rooted in spiritual ceremonies and values, with culture and knowledge passed on through generations. Many First Nations have strong spiritual ties to the lands and natural resources that they depend on for a living (Morin, 2015).

Since European settlers arrived in Canada, First Nations have lost opportunities to practice many of their rights, such as harvesting traditional food, due to the impacts of colonial development on their territories, lands, and resources. A series of treaties were signed between the Canadian government and Indigenous nations. These gave the Canadian government rights to access lands and natural resources in exchange for many guaranteed rights and services provided to the signing Indigenous peoples (Wilson and Henderson, 2014). However, few historical treaties were signed through British Columbia, including none in present-day Vancouver area. These areas with no treaties remain as completely unceded territories. Despite this lack of treaties in British Columbia, the Canadian government unilaterally assigned and relocated Indigenous communities onto small portions of their traditional territories, known as Reserve Lands, as designated areas for them to live (Wilson, 2018). Most First Nation communities in British Columbia are still primarily based on Reserve Lands today.

The Canadian Government tried to assimilate Aboriginal children into Euro-Canadian culture by establishing residential schools, which were funded by the government and run by Christian churches. Here, they were forbidden to practice their culture and language, or to have contact with their families. As the culture is passed on orally from one generation to the next, many cultural traditions and languages have been lost. In the 1920s, these schools became mandatory and parents faced threat of prison if they failed to comply (Wilson and Henderson, 2014). Many children left the residential schools with traumatic experiences due to the physical, psychological, and sexual abuse they had to undergo. Recently, the discovery of unmarked mass graves at residential school locations has caused worldwide awareness for the dramatic circumstances in these schools (Honderich, 2021).

The last federally funded residential school was closed only in 1996. In 2008, the Prime Minister at the time, Stephen Harper, made an apology on behalf of the federal government, and the Truth and Reconciliation Commission was established (Truth and Reconciliation Commission Canada, 2015).

Many Aboriginal people continue to experience racism and negative stereotypes on a regular basis or are suffering from poverty or traumas. Nowadays, First Nations are focusing on raising awareness on these injustices and on strengthening their local languages, traditions, and communities (Tsleil-Waututh Nation, n.d.-b).

It is in this cultural context that we investigate how the natural dynamics of Burrard Inlet have been affected since European contact.

2.1.2. Tsleil-Waututh Nation

The Tsleil-Waututh Nation (TWN) is a First Nation that has lived along the shores of Burrard Inlet since time out of mind, long before first contact with Europeans. They are one of many groups of Coast Salish peoples living in the Salish Sea bioregion and one of three groups living in the city of Vancouver.

The name Tsleil-Waututh means 'People of the Inlet', and the Nation's cultural and historical identity is strongly connected to Burrard Inlet. Their creation stories are directly connected to the inlet, which has been the center of their traditional territory for thousands of years (Tsleil-Waututh Nation, 2020).

Archaeological findings suggest that there have once been several thousand TWN people, spread out over different villages along the inlet. Their way of life was based on natural food resources and a seasonal cycle of travel and activity. In winter, the community assembled to live from dried foods gathered throughout the year and participated in spiritual ceremonies. In spring and summer, people would spread out and set up camps along numerous beaches and coves. From these base camps, excursions were made to fish, hunt, and collect food. Using a canoe, the whole of Burrard Inlet was within easy daily travel distance from the village sites (Tsleil-Waututh Nation, n.d.-b). At low tide, they would gather at the beach to harvest clams. Nowadays, the shellfish harvest is forbidden due to contamination issues (Tsleil-Waututh Nation, 2019).

The culture of Tsleil-Waututh is strongly based on their ties with the inlet. Having lived in harmony with the lands and waters of Burrard Inlet since time immemorial, they gathered a vast amount of knowledge on the natural systems, passed on by their ancestors. They feel a strong connection to their ancestors, which form the center of many ceremonial activities. There are several archaeological sites, which are important to the community. The archaeological records, spanning over 2500 years of history, confirm the oral histories about the traditional harvest activities (Lilley et al., 2017). TWN has a long-held stewardship obligation towards their ancestors and future generations to protect and care for the water, land, air and resources in the Burrard Inlet.

The first European contact in Burrard Inlet was in 1792. Since then, Tsleil-Waututh's population has been decimated by disease, such as smallpox. Like other First Nations in Canada, the community suffered from residential schools and cultural suppression (Morin, 2015). The land that once was the territory of the Tsleil-Waututh Nation was filled more and more with urban and industrial development as the city of Vancouver was built. Over the last two centuries, the natural resources in the inlet that TWN has always depended on for their living have been depleted. Animal populations have declined and the ecosystem is suffering from pollution and contamination issues (see Section 2.2.7).

Nowadays, the community is small but growing. The Tsleil-Waututh Nation currently consists of over 500 people, most of whom live in TWN's main community (IR#3) on the north shore of Burrard Inlet, as shown in Figure 2.2 (Tsleil-Waututh Nation, n.d.-b). The reserve is governed by an elected Chief, an elected Band Council and a Traditional Council.



Tsleil-Waututh Nation

PEOPLE OF THE INLET

Figure 2.1: The logo of the Tsleil-Waututh Nation

In order to fulfill their stewardship obligation to care for and protect the lands and waters of Burrard Inlet, TWN is actively implementing laws, policies, and actions that aim to ensure a healthy and prosperous future for Burrard Inlet and the Tsleil-Waututh people (Lilley et al., 2017). They commission research projects on the health of Burrard Inlet and make recommendations on how to reduce negative environmental, heritage, and social impacts. Examples of this are the Burrard Inlet Action Plan (Lilley et al., 2017) and the Climate Change Vulnerability Assessment (Tsleil-Waututh Nation, 2019). Moreover, TWN participates actively in several environmental restoration projects, such as fish habitat restoration

projects in Indian River and nature conservation projects. Their goals are to achieve a healthy Burrard Inlet where Tsleil-Waututh people can practice cultural and ceremonial activities in clean water, and to re-establish traditional harvests of wild marine foods in the inlet. (Tsleil-Waututh Nation, n.d.-b).

2.2. Burrard Inlet

2.2.1. Inlet characteristics

Burrard Inlet is an inlet atypical for most west coast fjords. The inlet is relatively shallow, not bounded by steep cliffs and regularly receives freshwater from an external source: the Fraser River.

Burrard Inlet can be divided in several sections, each with different characteristics (Figure 2.2). There is a wide outer basin with sandy beaches and an average depth of 45 m, which is busy with shipping activities. Generally, salinity values are highest here. However, during large freshwater discharge events in the Fraser River, occurring mainly in spring, surface salinity in the Outer Harbour can be lower than in the rest of the inlet, due to the Fraser River influence.

Outer Harbour is separated from Inner Harbour by the First Narrows: a part of the fjord that is relatively narrow and only 18 meters deep. This sill prevents the salty and dense deep waters from penetrating further into the inlet (Lilley et al., 2017). The Port of Vancouver is located in Inner Harbour; a large industrial port with deep-sea vessels entering and leaving on a daily basis. The basin is well-circulated and flushed regularly by tides and currents. It is one of the most industrialized parts of Burrard Inlet, as 80% of the shoreline in Inner Harbour is altered by human interventions.

Further inland, Second Narrows forms the barrier between the Inner Harbour and Central Harbour, where there are more natural shorelines. TWN's main community is located on the north shore of Central Harbour (Figure 2.2). The extension further eastwards is called Port Moody Arm, a shallow arm with slow circulation and little freshwater input.

At the connection between the Central Harbour and Port Moody Arm, Indian Arm stretches northwards. Contrary to Burrard Inlet itself, Indian Arm is long and narrow, characterized by deep waters, steep cliffs and a fjordlike appearance. It is separated from Central Harbour by a 27m deep sill at the entrance, limiting water exchange. Indian Arm is the most untouched of the basins. It has very little developed coastline and only limited pollution issues. The average depth in Indian Arm is 120 m and depths can locally reach up to 245 m (Thomson, 1981).

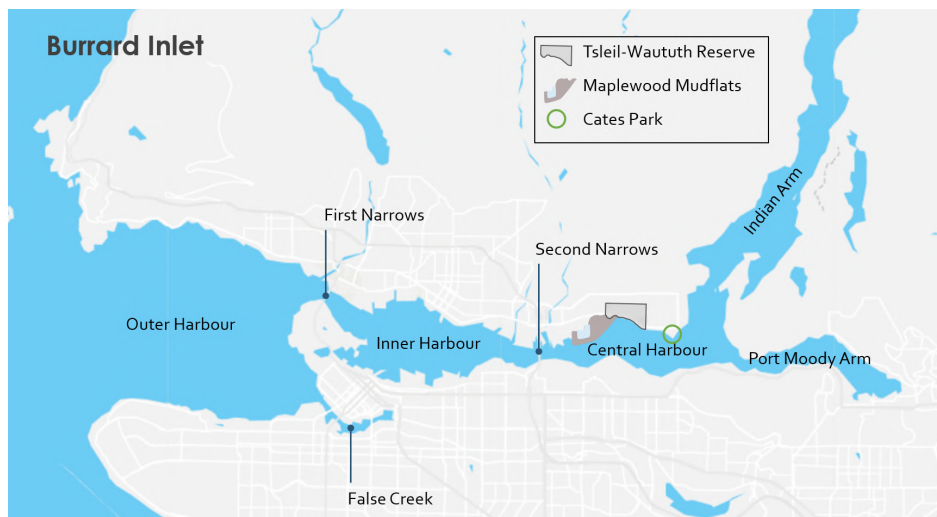


Figure 2.2: Map showing the different sections of Burrard Inlet and the location of the TWN reserve, Maplewood Mudflats and Cates Park.

2.2.2. Hydrodynamics

The flow in the basin is dominated by the tides. The contributions of wind forcing and freshwater discharge are relatively weak. The tides are mixed, mainly semidiurnal and dominated by the semidiurnal M2 component and the diurnal K1 and O1 components (Wu et al., 2019). Due to the interplay of these constituents, the daily inequality varies strongly, ranging from almost diurnal to almost semidiurnal tides

over the spring-neap tidal cycle. The mean tidal range is 3.3 m up to a maximum tidal range of 5.0 m. This tidal range slightly increases when propagating deeper into the inlet, with a maximum in Port Moody Arm.

The tidal currents show a strong spatial pattern associated with local coastlines and topography. Tidal flows are strongest in the First and Second Narrows, where they can reach velocities up to 3 m/s (Thomson, 1981). After the Narrows, the flow decelerates in the Harbours. The tidal currents form eddies which reverse in circulation with the turning of the tide. The tides are asymmetric (overall flood-dominated but ebb-dominated at some locations), causing significant residual flows, which could play a role in the sediment transport (Wu et al., 2019).

In the Narrows, the momentum balance is dominated by the advection and pressure gradient term. In the Inner and Central Harbour, the pressure gradient is mainly balanced by the advection and Coriolis term, which are equally important here (Wu et al., 2019).

2.2.3. Salinity

Due to the presence of the Fraser river, the salinity field is strongly variable in space and time, both in the Strait of Georgia and in Burrard Inlet (SalishSeaCast, 2021). The Fraser river causes a strong fluvial freshwater input, which meets saline waters coming from the ocean.

Inside Burrard Inlet, a weak 2-layer structure can be found. Freshwater runoff occurs along the surface while saline water enters at the bottom. The sills at the Narrows and at the entrance to Indian Arm prevent the entering of saline water from the lowest layers. Past First Narrows, the maximum salinity is ca 26 PSU (Thomson, 1981, SalishSeaCast, 2021). As flow through the Narrows is highly turbulent, water entering the Inner Harbour and Central Harbour is well-mixed (Baines, 1957) There is a strong seasonal variation. In spring, when Fraser river discharges are high and the freshwater plume reaches Burrard Inlet, the outer part of the inlet is relatively fresh.

In the Indian Arm, a more pronounced estuarine circulation is set up. There is a strong surface outflow of freshwater with saltier water flowing in underneath and a halocline at 3-5 m depth. The surface currents are almost always directed southwards but can vary in strength depending on the tidal stage and wind direction. Due to the sill separating Indian Arm from Burrard Inlet, the water exchange is limited. Full replacement of the deep waters in Indian Arm takes 7-10 years and happens in so-called 'exchange events' when the waters in front of the sill have sufficient density and kinetic energy to flow into Indian Arm and displace some of the deep water. Those deep water renewals mainly occur in winter and during neap tide, as under these conditions waters of highest density can reach the entrance of Indian Arm (deYoung and Pond, 1988, Stacey et al., 2002).

2.2.4. Wind and waves

Due to the presence of the mountains north of Vancouver, the area is relatively sheltered. Winds in the area are not very strong and predominantly east-west directed (Figure 2.3), because of funneling effects of the mountains north of Burrard Inlet.

A seasonal effect can be distinguished in the wind directions: in winter, cold continental winds from the east blow towards the sea. In summer, when the land mass heats up and the sea remains relatively cool, westerlies are more frequent (Thomson, 1981). Extreme winds can occur in case of strong windstorms on the ocean and are therefore generally associated with westerly winds.

Because the fetch within Burrard Inlet is limited, it is impossible for winds to generate high waves. The largest wave heights are found in Outer Harbour when the wind in the Strait of Georgia is strong. Deeper into the inlet, average significant wave heights range between 5 and 10 cm (Beatty, 2021). Depending on the wind direction, low swell-like waves can propagate into the inlet but rapidly decrease in strength. Because wind-generated wave heights inside the inlet are so low, vessel-generated waves have a significant effect when it comes to disturbing the shoreline (Beatty, 2021, Thomson, 1981).

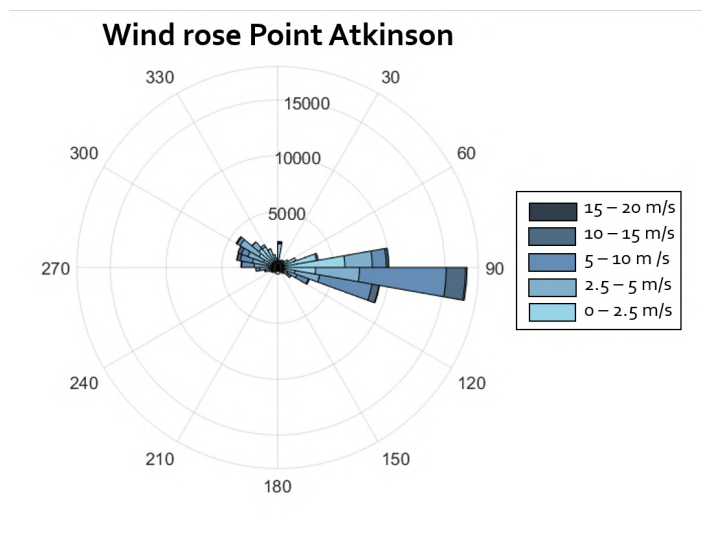


Figure 2.3: Wind rose for Point Atkinson, located at the entrance of Burrard Inlet. It shows how winds are predominantly east-west directed, where easterlies occur more frequently but winds from both directions can be equally strong. (Government of Canada, 2021b)

2.2.5. River discharge

The major rivers flowing out into Burrard Inlet and Indian Arm are depicted in Figure 2.4. Indian River supplies Indian Arm with water and sediment. Moreover, water flows into the Indian Arm via the powerhouse at Buntzen Lake. In Burrard Inlet, Capilano River, Seymour River and Lynn Creek are the major rivers. It is still visible how the Second Narrows are the historical delta of Seymour River and Lynn Creek (Figure 2.5). In earlier times, Seymour River and Lynn Creek would fan out and discharge at several locations in the Second Narrows and Maplewood Mudflats. Nowadays, their outflow location has been fixed. Until the building of Cleveland Dam in the 1950s, the Capilano River deposited large amounts of sediment in the First Narrows and regular dredging was needed to keep the channel open for ship traffic (Armstrong, 1990, Baines, 1957, Armitage, 2001). Seymour River has been dammed upstream as well, reducing its sediment discharge.



Figure 2.4: The main rivers flowing out into Burrard Inlet and Indian Arm.



Figure 2.5: The delta of Seymour River and Lynn Creek in the 1940's (right image) and 2021 (left image). Much of the natural delta has been replaced by hard shorelines and intertidal area is lost.

2.2.6. Strait of Georgia and Fraser River

Burrard Inlet flows out into the Strait of Georgia. Thus, conditions in the Strait of Georgia determine the boundary conditions for Burrard Inlet.

Flow in the Strait of Georgia is predominantly determined by the tide. The ocean tide enters via the Juan de Fuca Strait at the south side and is reflected at the constricted northern end of the channel (Figure 2.6). The combination of the northward advancing wave and the reflected wave moving southward causes a standing wave character. The incoming wave has a larger influence due to the effect of friction on the reflected wave. Due to this standing wave character, the entire water level along the Strait of Georgia moves up and down in unison (Thomson, 1981). The tidal range increases from circa 2 m at the southern entrance to 3.35 m at the northern end where reflection occurs. The tide consists of a combination of the M2 and K1 constituents and is mostly semi-diurnal with a strong daily inequality.

The part of the Strait where Burrard Inlet and Fraser River are located is called the Central Strait. It is characterized by moderately strong tidal streams and the influence of Fraser River discharge. Due to the proximity to Vancouver, this is the most used marine passageway in British Columbia.

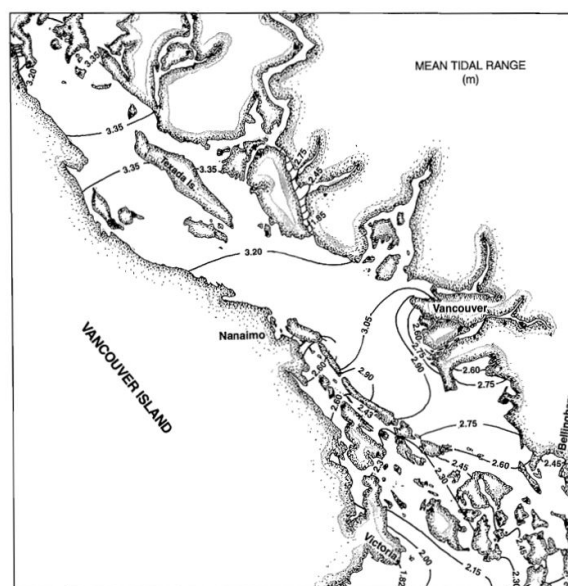


Figure 2.6: The topography and tidal range in the Strait of Georgia. The map shows the proximity of Fraser River delta to Burrard Inlet (From Thomson, 1981)

The Fraser River is the biggest estuary on the Canadian west coast. It drains an area of 230,000 km², which is about 1/4th of the area of British Columbia. The discharge is highly variable and peaks in spring (late May to early June), as two thirds of the runoff consist of snow melt. In periods with high discharge, the freshwater plume reaches Burrard Inlet, which is located just north of the Fraser River mouth. Moreover, sediment loads are highest during this period (Attard et al., 2014).

Moreover, Fraser River transports large amounts of sediment. The delta has been adding sediments at a rate of 12 million m³/year since the last ice age 8000 years ago (Thomson, 1981). The Fraser river delta is very wide and shallow and ends with a steep dropoff into the Strait of Georgia. About 70% of the sediment load transport is silt- and clay-sized material (Attard et al., 2014).

2.2.7. Environment

Since the first European contact, the shores and ecosystems in Burrard Inlet have changed drastically. Populations of salmon, forage fish, shellfish, birds, and marine mammals have declined from historic levels. Some salmon and bird species show signs of recovery but other species are still declining. The main threats for the species living in Burrard Inlet are loss of habitat, disease, human disturbance, pollution, and climate change (Lilley et al., 2017).

Loss of Habitat

The reasons for loss of habitat are twofold. To begin with, much of the shoreline has been altered due to development. Of the total shoreline of 190 km, 53 km of natural shoreline habitat such as eelgrass and kelp beds is lost.

Moreover, according to the TWN Action Plan, "shoreline hardening, construction of overwater structures, and dredging appears to have changed circulation and sediment transport patterns and rates of deposition and erosion in some parts of Burrard Inlet, e.g. Central Harbour" (Lilley et al., 2017). Due to shoreline erosion and changing sediment composition, intertidal areas are lost, which serve as a habitat for many species, such as shellfish. Moreover, this impacts species that forage food in the intertidal areas, such as marine birds and salmon.

In addition to current developments, climate change has the potential to further contribute to loss of habitat in the future. Higher water levels in combination with more severe storms can potentially increase coastal erosion. Moreover, the rising sea level leads to a phenomenon called coastal squeeze: as the sea level rises, the intertidal area will shift landwards. However, in many parts of Burrard Inlet, the intertidal zone cannot move inland due to development. Hence, even more intertidal area is lost (Tsleil-Waututh Nation, 2019).

Climate change is expected to impact the inlet in several ways. Sea level rise, precipitation changes and stronger storms have the potential to cause more severe flooding and increase (coastal and river) erosion, damaging property, cultural areas, and natural habitat.

Contamination

Polluted water and contaminated sediments affect the environmental quality, limiting human uses of Burrard Inlet, such as fishing and shellfish harvesting. At some locations, the levels of contaminants are unsafe and the shellfish harvest in Burrard Inlet has been closed due to contamination issues. Many of the long term changes in important water quality parameters such as temperature, dissolved oxygen and acidity are of concern.

The sources of contamination are diverse and not well characterized. Industrial discharges, sewer outflows, stormwater runoffs, and spills of oil or other hazardous substances are expected to contribute to the pollution issues (Tsleil-Waututh Nation, n.d.-a).

In 1994, McLaren did a study on the sediment transport patterns in Burrard Inlet with the goal of predicting the fate of contaminated sediments and found that contaminants can accumulate at certain locations where much deposition takes place. Port Moody and Indian Arm have quiet waters which are especially susceptible to deposition. Moreover, it was found that contaminants have a greater association with fine sediments such as silt and clay than with coarser sediments (McLaren, 1994).

2.3. Sediment availability

In this section, the nature of the sediments currently present in Burrard Inlet is analyzed. Sediment sizes in the inlet are highly variable, ranging from very fine silt to gravel and cobblestones (McLaren, 1994). On many places, the sediment composition shows a bimodal distribution with peaks for $10\ \mu\text{m}$ (fine silt) and $250\ \mu\text{m}$ (medium sand) (Alden, 2020). Based on classification of the sediment samples taken by McLaren (1994), a map of the composition of bottom sediments in Burrard Inlet has been made (Figure 2.12 - A). It shows that the Narrows are relatively sandy, which can be expected due to the higher flow velocities there. Port Moody, where flow velocities are low, has a muddy bed. Moreover, the bottom sediment composition of Central Harbour is coarser than that of Inner Harbour, which may indicate erosion or more energetic flows.

Figure 2.7 shows the shoreline characteristics along Burrard Inlet (Tsileil-Waututh Nation, n.d.-a). The Outer Harbour shorelines are a mix of rocks, gravel beaches, gravel flats and sand beaches. It is clearly visible that Inner Harbour and False Creek consist almost entirely of altered shorelines. In Central Harbour, sand and gravel beaches and flats can be found, consisting of a combination of glacial till and alluvial deposits (Baines, 1957). The majority of the shorelines at Indian Arm are rocky, or combined rocks with gravel beaches. In Port Moody Arm, several sand- and mudflats can be found.

The ShoreZone project (Coastal and Ocean Resources, 2018) provided extensive mapping of the different shoreline types by photos and videos of the whole Burrard Inlet shoreline taken from a helicopter. Images of the characteristic shorelines at different locations can be found in Figure 2.8.

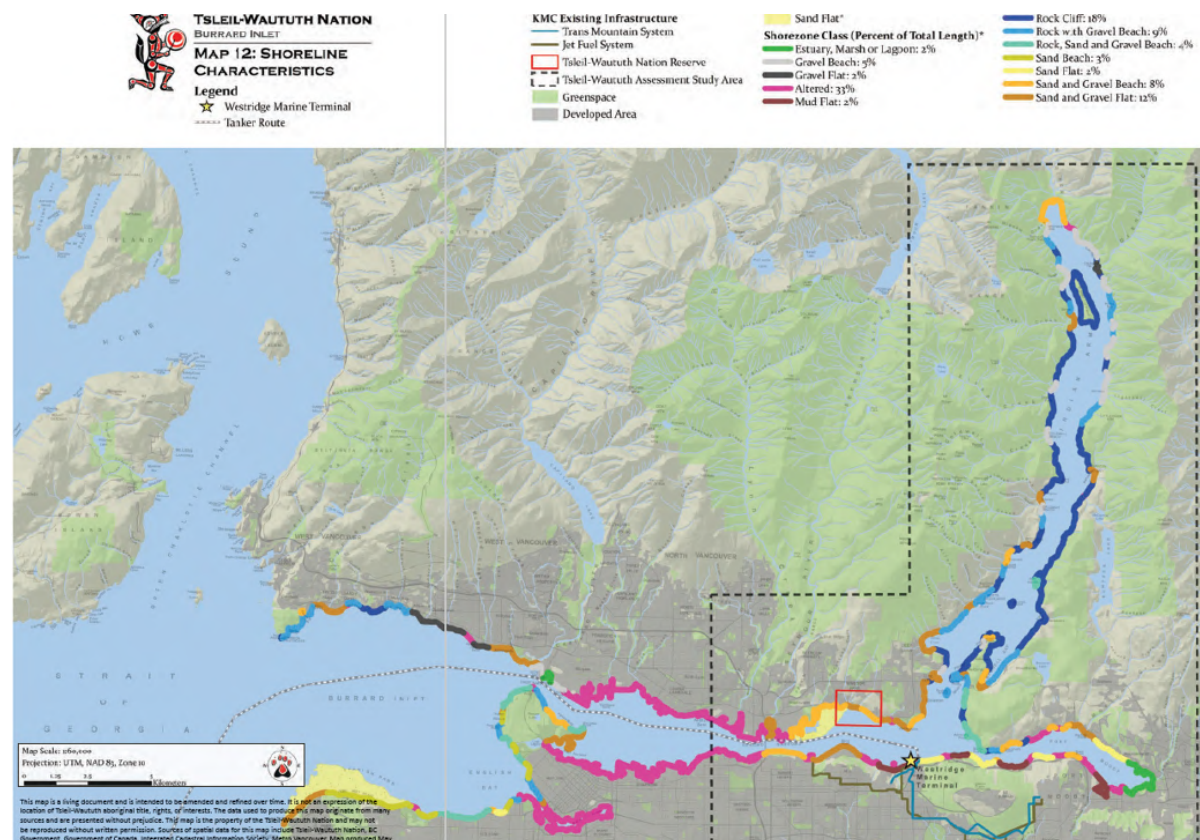


Figure 2.7: Shoreline characteristics along Burrard Inlet. Map obtained from Tsileil-Waututh Nation, n.d.-a.

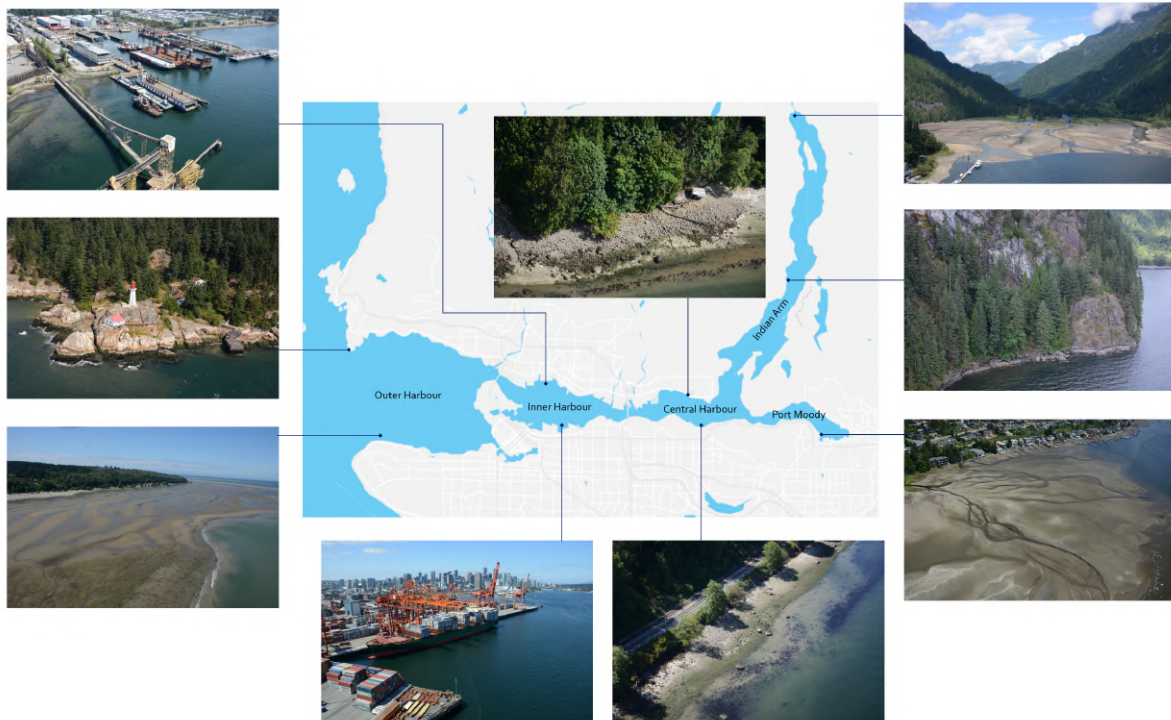


Figure 2.8: Map of Burrard Inlet with images of the shoreline at various locations. Pictures taken as part of the ShoreZone project (Coastal and Ocean Resources, 2018)

2.4. Sediment transport patterns

The circulation patterns of sediment transport are predominantly controlled by the tides. The geometry of the inlet, with its sills and constrictions between basins, affects transport and deposition patterns. As a result, transport pathways in Burrard Inlet are complex and spatially strongly varying, forced by topographical features.

This section describes the studies that have investigated the circulation and transport patterns in Burrard Inlet and lists their results, in order to obtain a comprehensive overview of what is known about these patterns.

2.4.1. Large scale transport patterns

Sediment transport study by Mc Laren

Sediment transport pathways as well as erosion and deposition patterns have been computed by McLaren (1994), based on over 500 bottom sediment samples taken from the inlet in a grid of 500 by 200 m. The differences in grain-size distribution between different sediment samples were used to indicate the direction of transport and identify whether erosion or deposition had taken place. This grain trend analysis is based on the idea that sediment sorting improves in the downstream direction. In case the sediment composition got finer in the transport direction, the researchers concluded that deposition had taken place. A coarsening sediment composition indicates erosion (McLaren, 1994). The results found in the study by McLaren, 1994 are depicted in Figure 2.12 - B. The certainty of the results differs per location.

The sediment transport directions found in Inner Harbour coincide with residual tidal currents. Moreover, sedimentation patterns found on a shipwreck in Inner Harbour have confirmed both the direction of transport and the statement that there is net sedimentation (McLaren, 1994).

The sediment transport northwards into the Indian Arm is also found to be plausible. The northwards tidal current will probably be along the bottom, counteracting the freshwater outflow at the surface.

The results found in Central Harbour, however, are less certain. Correlations in the grain size trends along these transport lines are weak and the net accretion trend is uncertain. Furthermore, no information could be found by Mc Laren to either support or contradict the derived patterns. It

is interesting to see that the study by McLaren predicts net accretion at the north shore of Central Harbour, where the TWN reserve is located. TWN observations, which speak of ongoing erosion along these same shores, seem to contradict these findings (Burrard Inlet Science Symposium, 2017, Tsleil-Waututh Nation Climate Summit, 2018).

Oil spill model

In 2019, a modelling study was carried out to predict the consequences of a possible oil spill in Burrard Inlet (Genwest Systems Inc., 2019). Two models (model A and B) with different forcing conditions are deployed. Model A used tidal forcing and included river discharges but no wind forcing. The tidal forcing covered a 10-year period (2004 - 2014) obtained from a tidal station at First Narrows. Model B was based on tidal data for one year only (2005) and included wind forcing using wind data from the same year, but did not include river discharges. The fate of oil particles released from a spill was modeled using Lagrangian particle tracking.

Results from the study show that the tracked particles spread quickly in the confined geophysical setting of Burrard Inlet. Material released in the First Narrows is transported through the complete inlet and has the possibility to end up in Port Moody or Indian Arm. Within one tidal cycle, tracked oil particles are able to move across the entire inlet.

2.4.2. Central Harbour

A study focusing specifically on the sediment transport directions in Central Harbour was performed by Harper (2020). A conceptual model of the sediment transport system is developed by assembling existing data such as historical maps and aerial photos, bathymetric survey data and side-scan sonar imagery, the seabed sediment samples collected by McLaren (1994), and conversations with elders from the TWN community.

The composition of sediment samples collected by McLaren (1994) in Central Harbour are analyzed to map high-energy and low-energy areas (Harper, 2020). Areas with high gravel content indicate a high-energy regime with strong currents where usually erosion takes place. Contrarily, high mud content can be found in areas with relatively weak currents that can be classified as low-energy (Figure 2.9).

High-resolution imagery of the seabed, obtained using multibeam bathymetry and side-scan sonar imagery, is used to deduce sediment transport directions based on present bedforms and 'current shadows' behind hard points (eg. a shipwreck). The results show a motion directed to the southwest along Maplewood Mudflats (Figure 2.9).

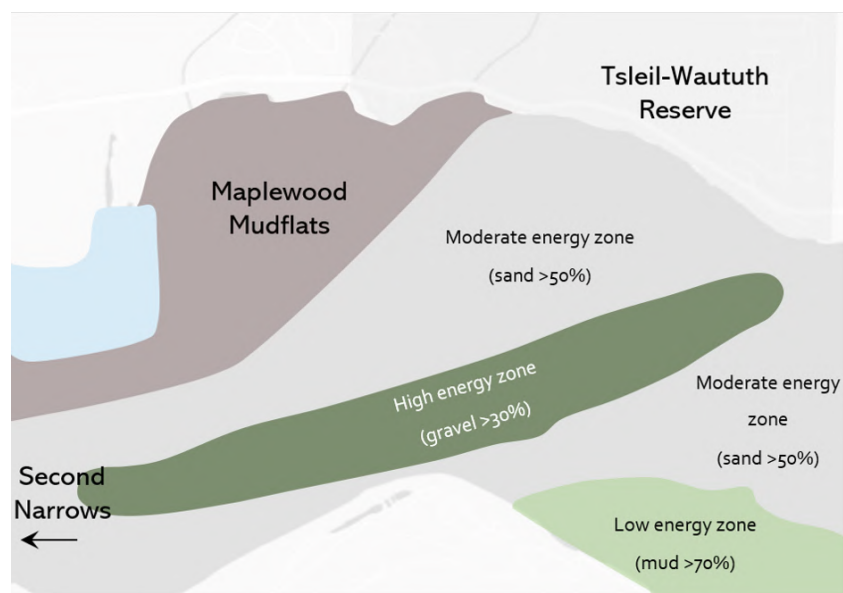


Figure 2.9: Map showing the high- and low-energy zones in Central Harbour. This map has been constructed using the data and maps from Harper (2020) and McLaren (1994)

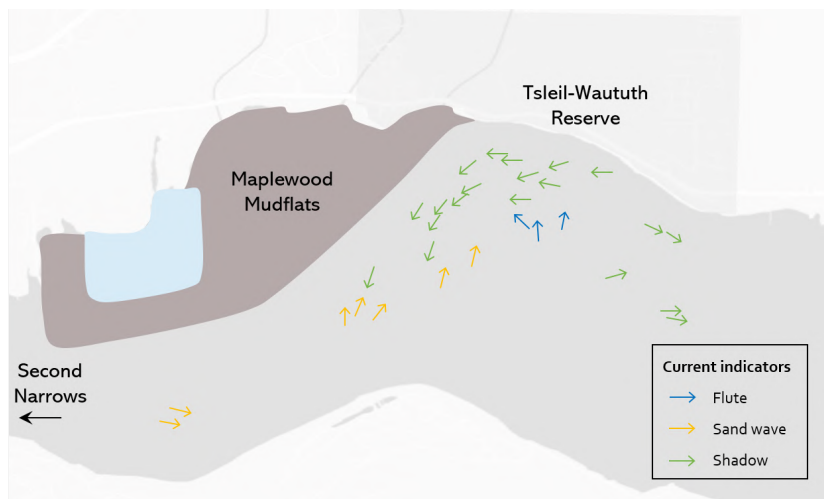


Figure 2.10: Map showing the sediment transport directions along the bed as established by Harper (2020). The colors indicate what bedform was used to determine the transport direction at that location. With 'shadow', local sedimentation due to current shadow behind a fixed object is meant.

Shoreline evolution

Historical maps show that the shoreline has been retreating at the northern shore of the Second Narrows and Maplewood Mudflats, from the 1920s until present (Harper, 2020). A map of erosion and sedimentation locations is constructed based on observations from the TWN community (Figure 2.11). Elders from the TWN community consistently recollect that the high water line in front of the reserve has retreated 5 to 10 m over the past 50 years, which would amount to a retreat of 10-20 cm per year. For these recollections, the location of the shoreline was related to the position of fixed objects such as specific trees in the backshore or large boulders in the intertidal zone (Harper, 2020). The shoreline at Cates Park is retreating as well, and archaeological sites at Cates Park are eroding. During assessments between April and September 2018, several areas along the shore at Cates Park were identified as showing signs of erosion (TWN Communication, 2018).

The sediment composition of Maplewood Mudflats and the beaches in front of the TWN reserve is coarsening (Figure 2.11). Nowadays, the mudflats consist mostly of gravel and cobblestones (Burrard Inlet Science Symposium, 2017). Elders remember that the beaches used to have more sand, whereas they are more rocky in recent years (Harper, 2020).



Figure 2.11: An overview of the areas where erosion or sediment coarsening takes place, according to TWN records (Burrard Inlet Science Symposium, 2017, Harper, 2020). The strongest erosion takes place along the reserve shoreline and the shores of Cates Park. At Maplewood Mudflats, the sediment composition is coarsening.

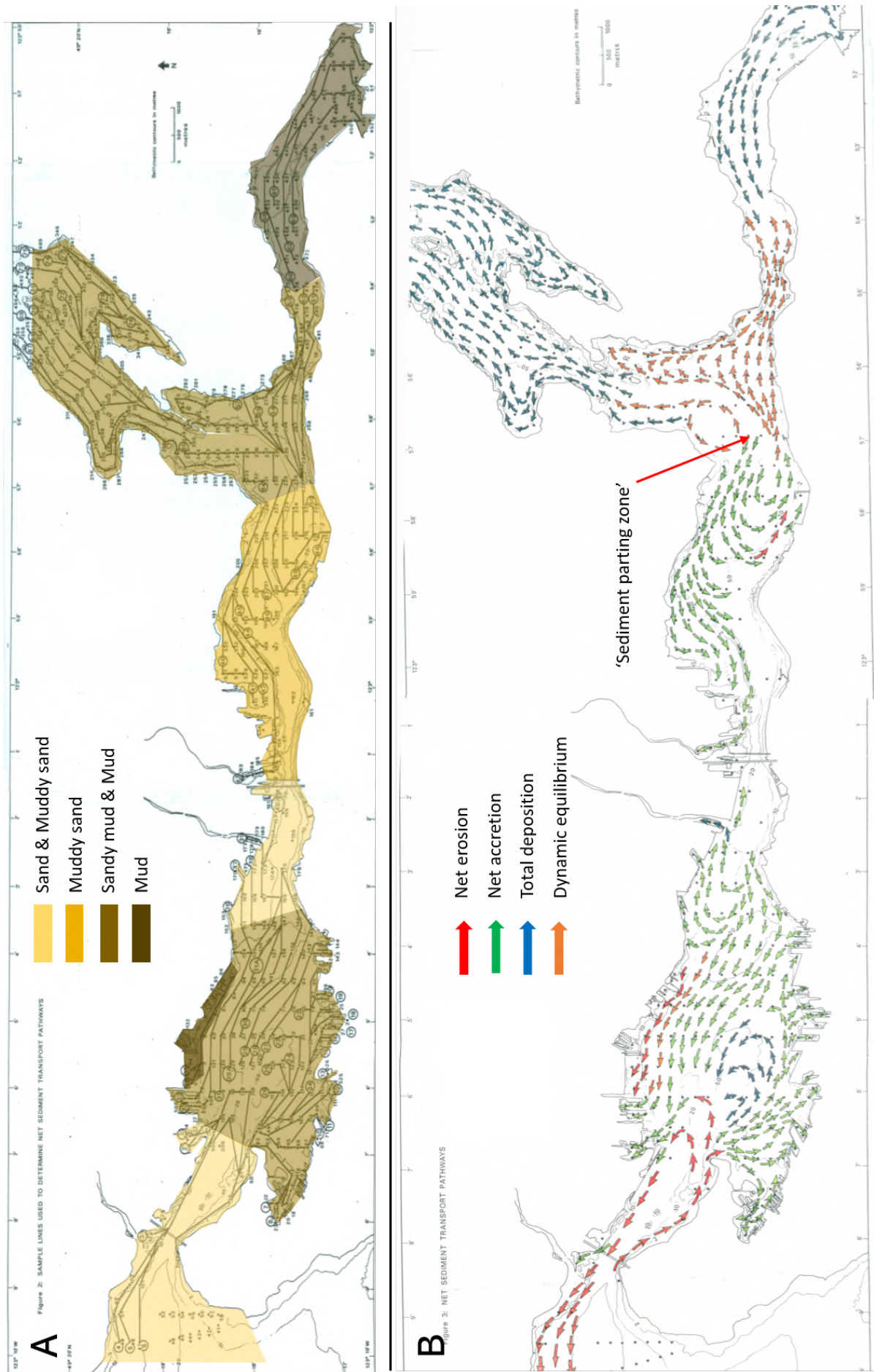


Figure 2.12: A: The bottom sediment composition in Burrard Inlet (image constructed based on the classification of the sediment samples taken by McLaren (1994)). B: Sediment transport pathways and areas of erosion or deposition as found by McLaren, 1994.

Model Set-up

3.1. Model Set-up

This section describes the set-up and calibration of the hydrodynamic model. A Delft3D Flow Flexible Mesh model is used (Deltares, 2021). This hydrodynamic model simulates the water motion by solving the unsteady shallow-water equations in an unstructured mesh. At each timestep, flow velocities and sediment transport rates are resolved by the model. The model is depth-averaged and thus does not compute flow gradients over the water depth.

3.1.1. Model domain

The model domain extends beyond the shallow Fraser river delta into the deeper parts of the Strait of Georgia (Figure 3.1a). This is done to be able to include the sediment plume supplied by Fraser river to see whether these sediments are able to reach Burrard Inlet.

The model is nested into a larger model of the complete Puget Sound area. This larger model is used to obtain the boundary conditions for the model of Burrard Inlet, as no measuring data at the model boundaries is available. The Puget Sound model was developed by Deltares and USGS and covers the complete Salish Sea (Figure 3.1b). Its resolution ranges from 1600 m in the ocean to 400 m in the more shallow and complex areas.

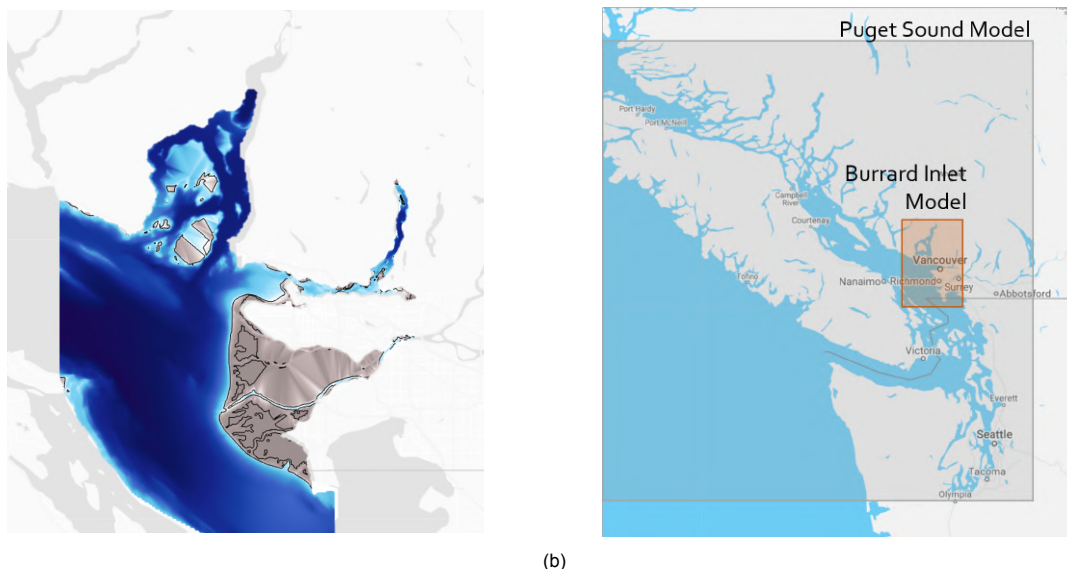


Figure 3.1: a) Map showing the model domain of the Burrard Inlet model with the bathymetry in the Strait of Georgia. b) The model domain of the Puget Sound model and the Burrard Inlet model, which is nested inside the larger Puget Sound model.

3.1.2. Grid

The model domain is divided into several areas with varying grid resolutions (Figure 3.2). The resolution in the Strait of Georgia ranges from 400 m in the deeper parts to 200 m in the shallower Fraser river

delta and the area in front of Burrard Inlet. The inlet itself consists of a detailed curvilinear grid with a resolution as fine as 30m in the focus area (Central Harbour, including Maplewood Mudflats, the TWN reserve and Cates Park). In the deeper waters of Indian Arm, the resolution is somewhat lower (40-70 m) to reduce the runtime.

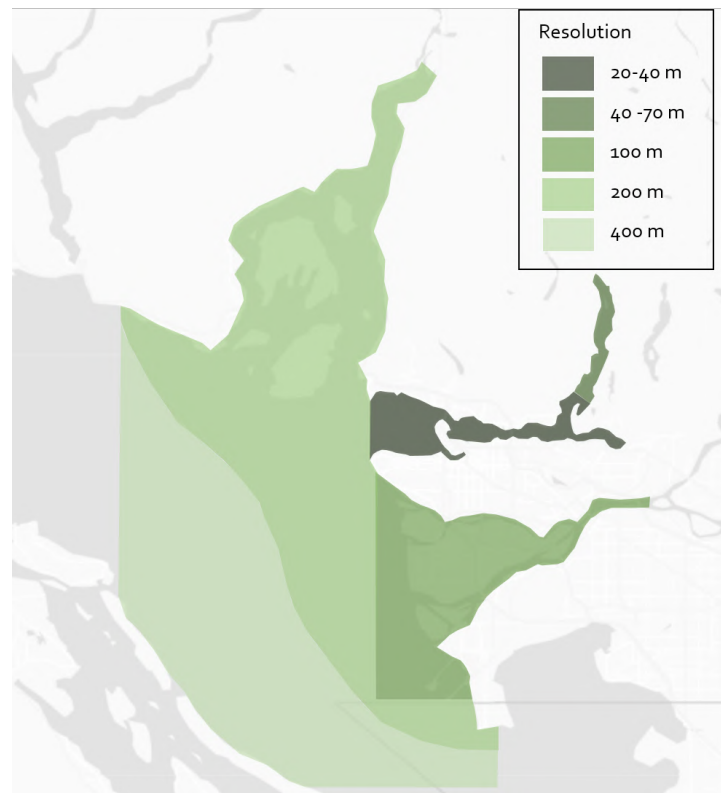


Figure 3.2: Map showing the different grid resolutions in the model.

In Burrard Inlet, the grid extends landwards from the land boundaries. This gives some extra space, in case the model is used for other purposes, such as to assess flooding. Moreover, the old shoreline can thus be imposed on the same grid in order to compare the present situation with the past.

The southwestern border of the model domain consists of a row of islands: Gabriola Island, Valdes Island and Galiano Island. Flow between those islands will not influence the area of interest but might increase the runtime of the model or cause potential errors. To reduce unnecessary complexity, those islands are replaced by a continuous land boundary.

Finally, some breakwaters with lengths up to several kilometers are present in the Fraser river delta, which have been included in the model as thin dams.

3.1.3. Bed level

The bathymetry of Burrard Inlet is provided by Matias Bofarull Oddo, a PhD student from the University of British Columbia. He constructed a very detailed bathymetry dataset of Burrard Inlet by combining data from the Canadian Hydrographic Service (CHS), the SalishSeaCast model and the Canadian Federal Elevation Model. As this bathymetry has an extremely high resolution, the bathymetry data is resampled to the grid resolution to reduce the file size. For the bathymetry outside Burrard Inlet, the CHS NONNA (Non-Navigational) dataset is used (Fisheries and Oceans Canada, 2020). The vertical datums of the different bathymetry datasets are matched to prevent a 'jump' where the different datasets come together. Gaps in the data and discontinuities within a dataset are solved using triangular interpolation.

The sediment transport module is activated using the van Rijn 2007 transport equations, which separate the sediment transport into suspended and bed load transport (vanRijn, 2007). The simulation is carried out morphostatically, which means the bed level is kept constant over the entire simulation. This prevents the changing bed level from influencing the modelled flow and enables us to isolate the

role of the flows on the sediment transport patterns. Sediment sizes in the inlet are highly variable, ranging from very fine silt to gravel and cobblestones (McLaren, 1994). A single sediment fraction of 70 μm (very fine sand) was used for the complete model domain, which is a major simplification (see Section 3.4 - Grain size schematization).

3.1.4. Rivers

The four major rivers flowing out into Burrard Inlet are included in the model: Capilano River, Seymour River, Lynn Creek and Indian River (indicated in Figure 2.4). Moreover, water entering the inlet from lake Buntzen via the Buntzen powerhouse is included. Monthly discharge data is obtained from the Canadian Wateroffice for Seymour River and from the FlowWorks platform for Lynn Creek (Water Office Canada, 2021). For Capilano River and Indian River, monthly monitoring data was not available. For these rivers, mean annual discharge values are obtained from literature (deYoung and Pond, 1988). The distribution of the discharge over the year for both rivers is assumed to be similar to Seymour River, since the climatic and topographic conditions are similar. Hence, a monthly distribution is obtained for Capilano River and Indian River based on their mean annual discharges and the monthly discharge distribution of Seymour River (Table 3.1).

The inflow from lake Buntzen is not determined by meteorological events but by the production of the powerhouse and could thus not be assumed based on other rivers. Therefore, the mean annual discharge found in literature ($23\text{m}^3/\text{s}$, deYoung and Pond, 1988) is assumed to be constant over the year.

Table 3.1: Monthly discharges for the four major rivers flowing out into Burrard Inlet. *The monthly distributions for Capilano River and Indian River are based on the monthly distribution of Seymour River and their mean annual discharges as obtained from literature (deYoung and Pond, 1988).

	Seymour River	Lynn Creek	Capilano River*	Indian River*
January	17.7 m^3/s	9.9 m^3/s	25.0 m^3/s	15.0 m^3/s
February	14.9 m^3/s	6.5 m^3/s	21.1 m^3/s	12.7 m^3/s
March	13.8 m^3/s	8.9 m^3/s	19.5 m^3/s	11.7 m^3/s
April	15.6 m^3/s	8.7 m^3/s	22.0 m^3/s	13.2 m^3/s
May	20.3 m^3/s	6.8 m^3/s	28.7 m^3/s	17.2 m^3/s
June	16.8 m^3/s	4.3 m^3/s	23.7 m^3/s	14.2 m^3/s
July	8.0 m^3/s	2.1 m^3/s	11.3 m^3/s	6.8 m^3/s
August	3.3 m^3/s	0.7 m^3/s	4.7 m^3/s	2.8 m^3/s
September	5.6 m^3/s	4.3 m^3/s	7.9 m^3/s	4.8 m^3/s
October	16.4 m^3/s	6.7 m^3/s	23.1 m^3/s	13.9 m^3/s
November	16.4 m^3/s	12.1 m^3/s	23.1 m^3/s	13.9 m^3/s
December	21.1 m^3/s	8.7 m^3/s	29.8 m^3/s	17.9 m^3/s
Yearly Average	14.2 m^3/s	6.6 m^3/s	20.0 m^3/s	12.0 m^3/s

With its mean annual discharge of ca $3500\text{m}^3/\text{s}$, which is two orders of magnitude larger than the local rivers, Fraser river is assumed to heavily affect hydrodynamics, sediment, and salinity in the inlet. In spring, when Fraser river discharges are high, the plume of fresh and sediment rich water reaches the mouth of Burrard Inlet (Thomson, 1981). To be able to include this effect in the model, Fraser river is modeled using a discharge boundary condition close to the Port Mann bridge.

3.1.5. Boundary conditions

At the Southern and Western end of the model domain, water level boundaries are applied. These water levels are taken from observation points in the Puget Sound model (Figure 3.1b) and converted to boundary conditions using the nesthd toolbox from Deltares' OpenEarthTools. Before starting the nesting procedure, the bathymetry in the Puget Sound model is replaced by the CHS NONNA bathymetry that is used in the detailed model to ensure that both models have identical topographical features along the boundaries.

Because the bathymetry describes a steep drop-off along the western boundary (with depths of up to 400 m in the deepest parts), imposing correct boundaries provided a challenge. The large depth variations between the boundary support points can make the system prone to numerical errors, leading to unrealistically high velocities and water levels. To prevent those numerical errors from occurring, the

boundaries are strongly simplified and reduced to only three support points on each side. Moreover, the velocity along the boundaries is set to zero.

3.1.6. Wind

The wind climate in Burrard Inlet is dominated by the so-called Easterlies and Westerlies due to the funneling effect of the mountains (Thomson, 1981, see Section 2.2.4). TWN has deployed a wave buoy in front of the shores of the TWN reserve from August 2019 to September 2020, reporting wind and wave data every hour (Beatty, 2021). Wave motion was sampled at 5 Hz and wind data at 2 Hz. Additionally, a wind record from Point Atkinson, spanning over several decades, is available.

Because available information on the wind field is rather limited and winds in the area are complex and unpredictable (due to topographic steering by the mountains and local wind effects in the city), creating and verifying a schematization of the spatial wind field in the inlet is complicated. Therefore, a uniform spatial wind field is assumed, where wind data measured by the TWN wave buoy is used for the complete modelling area (see Section 3.4 - Input reduction techniques).

The wave buoy has been measuring wind data for only a year, which is too short to gather relevant statistics on the long-term wind characteristics. Additionally, a wind record spanning over several decades is available from the measuring station at Point Atkinson. The data from Point Atkinson is used to get long-term representative values for the TWN location. The wind data obtained from Point Atkinson is compared to the wind data by the wave buoy for the period over which the wave buoy has been deployed (08-2019 to 09-2020). For this period, the ratio between the wind speed measured at Point Atkinson and at TWN is found, which is equal to 1.792. In this way, statistical wind data can be obtained from Point Atkinson and subsequently modified using the found ratio to represent the circumstances at the TWN shoreline.

This modification is based on the assumption that the wind behaviour at both locations is similar due to their close proximity. For example, if there is a storm at Point Atkinson, there will also be a storm at the TWN shorelines, only the wind speed at TWN will be lower due to its sheltered location.

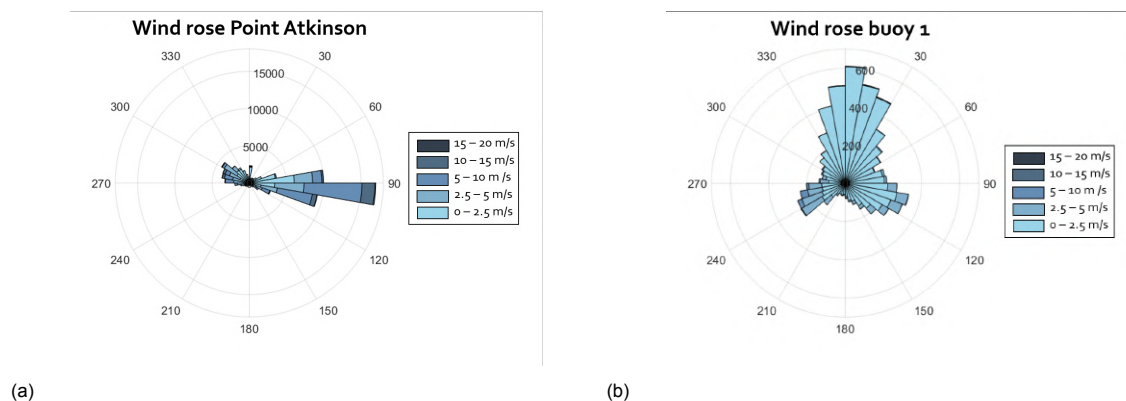


Figure 3.3: a) Wind rose showing wind speed and velocity at Point Atkinson for a 10-year period (2010 to 2020, Government of Canada, 2021b). b) Wind rose showing wind speed and velocity measured by the wave buoy in front of the TWN shoreline from 08-2019 to 09-2020 (Beatty, 2021).

In order to reduce runtime and complexity, it is not possible to run the full wind climate. Therefore, five different wind scenarios are chosen. As Figure 3.3a shows, the dominant wind directions are East and West. The wave buoy at TWN also measures some weaker winds from the North, which is a local effect that can be attributed to the close proximity to Indian Arm.

The first two scenarios use the yearly average wind speed coming from respectively the East and the West to give an illustration of the behaviour under regular conditions. The third and fourth scenario consider the transport pathways under strong winds. Strong winds are here defined as the mean of the highest 1% of wind speeds measured during the 10-year period from 2010 to 2020. An overview of the scenarios can be found in Table 3.2. Each of these scenarios is a simplified representation of reality. However, the combined information from these scenarios gives valuable information on the response of the system under various conditions.

The fifth scenario considers extremely strong wind. This scenario is used as a sensitivity check to investigate how large the influence of winds on sediment transport can theoretically be, using the

Table 3.2: Overview of the wind speed at Point Atkinson and TWN for each scenario. The modification factor that is used to translate the Point Atkinson data to values representative for the TWN shoreline is 1.792. Data retrieved from Beatty, 2021 and Government of Canada, 2021b

	Point Atkinson	TWN Reserve Shoreline
Scenario 1: Average wind - East (90°)	3.41 m/s	1.90 m/s
Scenario 2: Average wind - West (270°)	3.41 m/s	1.90 m/s
Scenario 3: Strong wind - East (90°)	15.57 m/s	8.69 m/s
Scenario 4: Strong wind - West (270°)	15.57 m/s	8.69 m/s
Scenario 5: Extreme wind - West (270°)	24.2 m/s	-

strongest possible winds occurring in the area. To find the largest occurring wind speed, the strongest wind storms in the past two decades are examined. In 2006, a devastating windstorm hit Vancouver and heavily damaged the Stanley Park seawall (City of Vancouver, 2006). Sustained wind speeds (not including wind gusts) during this storm reached up to 87 km/h (Government of Canada, 2021b), translating to 24.2 m/s. In December 2018, a windstorm that was described by BC Hydro as "the most damaging storm in BC Hydro's history" caused power outages for over 750,000 people in Vancouver. During this storm, the highest measured sustained wind speed in Vancouver was again 87 km/h (BC Hydro, 2019). Hence, 24.2 m/s is used for the 'extreme wind' scenario. Because this is a sensitivity case, no modification factor is applied to this wind speed.

3.2. Waves

Waves are able to influence sediment transport in several ways. Apart from mobilizing sediment and increasing erosion rates, waves have the potential to affect transport patterns due to wave-induced currents. The effect of these wave-induced currents on the sediment transport patterns is investigated by including waves in the model.

Waves are simulated using the spectral wave model SWAN, which simulates wave evolution using the wave action balance equation (Booij et al., 1999). SWAN is coupled with Delft3D-FM, enabling an exchange between the models to obtain a realistic interaction between flow and waves. Every 60 minutes, flow results such as water depths and velocities are communicated to SWAN, which computes the corresponding wave field.

The SWAN wave model uses a regular grid covering Burrard Inlet as well as the Fraser River delta. The boundaries are located in deep water to simulate the wave evolution as waves enter the shallower waters of the inlet and the Fraser delta. A detailed grid with a resolution of 60x90 m covering Burrard Inlet is nested inside the larger grid.

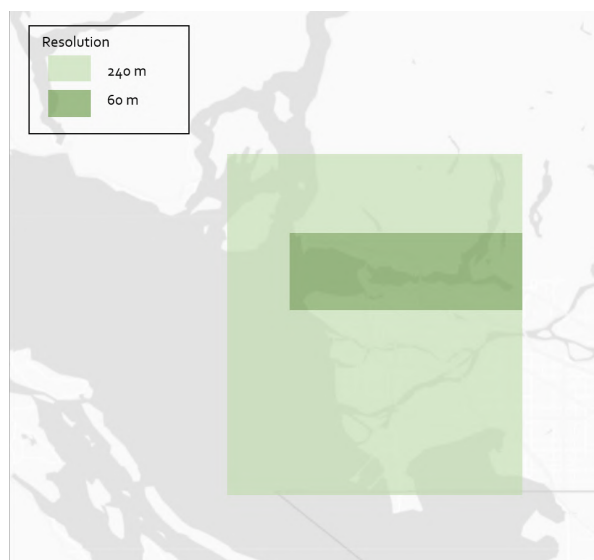


Figure 3.4: Map showing the grid resolutions of the wave model grid. The finer grid is nested inside the coarse grid.

3.2.1. Wave input

Wave data for the boundaries is obtained from the Halibut Bank Buoy, located in the Salish Sea, west of Burrard Inlet (Government of Canada, 2021a, Figure 3.5). The data contains 29 years of measurements (1992 - 2021) on wave and wind data.

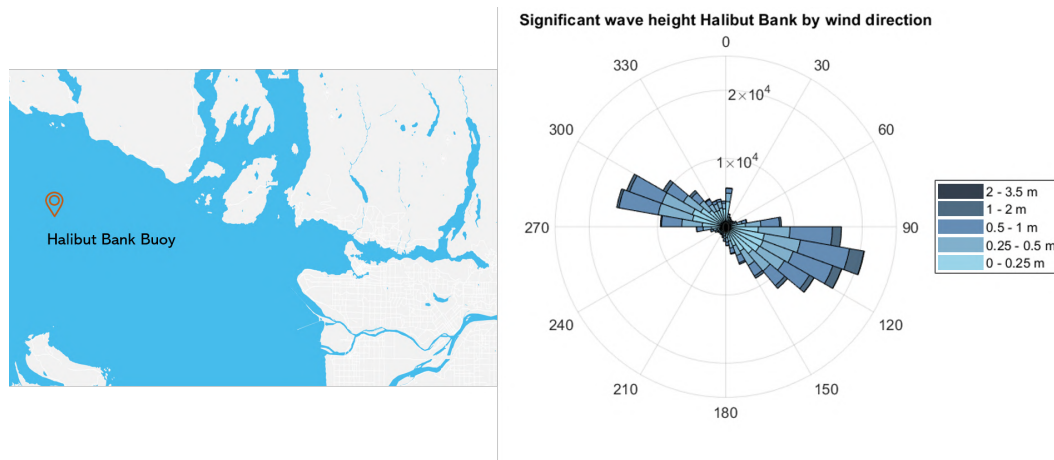


Figure 3.5: Left: location of Halibut Bank wave buoy. Right: wind rose showing wave heights measured at Halibut Bank. Note: because wave directional information is lacking, the wave heights are plotted for wind direction. (Government of Canada, 2021a).

The same approach as for the wind data is used: several scenarios are established with accompanying wave height, period and direction. Table 3.3 lists the different scenarios. For waves, scenarios with waves from the south are added for average and high waves. These scenarios are added for two reasons: as the vulnerable areas (TWN shoreline and Cates Park) are located on the northern shores, southerly waves may have a larger impact on these shores. Moreover, southerly waves could potentially be relevant in transporting sediment from the Fraser river delta northwards into Burrard Inlet.

The average scenario contains the average significant wave height over the entire measurement period after filtering outliers from the dataset. Scenarios 4, 5, and 6 - high waves - are created by taking the mean of the 1% highest significant wave heights. Scenario 7 has the purpose of investigating the limits of the wave-driven contribution to the transport patterns. For this, the highest measured significant wave height from the measurement period is taken. This wave height ($H_s = 3.5$ m) was measured during a windstorm in April 2010 (Armstrong, 2010). After establishing the boundary conditions and running the model, modeled wave heights at the TWN shorelines are compared to the wave heights measured by the wave buoy for each scenario (Beatty, 2021). For average waves, the wind speed is increased from 1.8 m/s to 4 m/s in order to obtain representative average wave heights ($H_s = 5$ cm) for this location, as a wind speed of 1.8 m/s generated wave heights in the order of millimeters.

Table 3.3: Overview of the significant wave height and peak period for each scenario. Data retrieved from Government of Canada, 2021a.

	H_s boundary	H_s TWN	Peak period	Wind speed
Scenario 1: Average waves - East (90°)	0.38 m	~ 0.05 m	3.56 s	4 m/s
Scenario 2: Average waves - West (270°)	0.38 m	~ 0.05 m	3.56 s	4 m/s
Scenario 3: Average waves - South (180°)	0.38 m	~ 0.05 m	3.56 s	4 m/s
Scenario 4: High waves - East (90°)	1.64 m	~ 0.30 m	5.12 s	8.69 m/s
Scenario 5: High waves - West (270°)	1.64 m	~ 0.30 m	5.12 s	8.69 m/s
Scenario 6: High waves - South (180°)	1.64 m	~ 0.30 m	5.12 s	8.69 m/s
Scenario 7: Extreme waves - West (270°)	3.5 m	~ 0.70 m	6.9 s	24.2 m/s

3.3. Representative tidal cycle

Most data for calibration and verification is available for the years 2019 and 2020. The data obtained at the tidal gauge at Point Atkinson is analyzed for the years 2019 and 2020 to find which month in this period is most representative for the long term behaviour. Choosing a representative month

ensures that the model behaviour is representative for the long-term flows and not only reflects some meteorological event during the modelling period.

The representative month is chosen by performing harmonic analysis on the water level timeseries using T-TIDE to identify the tidal components (Pawlowicz et al., 2002). Gaps in the tidal signal are filled using linear interpolation. The major 10 components for the complete period 2019-2020 (see Table 3.5) are compared to the major 10 components of each separate month within this timespan. The components for August 2019 prove to be most similar (lowest root mean squared error, see Table 3.4) to the longer term behaviour. Hence, the model is further calibrated for August 2019.

The location of Point Atkinson is used for this purpose because this measurement station is located at the entrance of the inlet. At locations deeper inside the inlet, there will be more interference and reflection in the tidal signal caused by the topography, which lowers the accuracy of the T-TIDE analysis.

Table 3.4: Root mean squared error and T-TIDE match. The root mean squared error quantifies the difference between the major 10 tidal constituents of each respective month and the full measurement period (April 2019 - July 2020). The T-TIDE match gives an indication of the accuracy of the T-TIDE computation.

2019									
Month	April	May	June	July	Aug	Sept	Oct	Nov	Dec
RMSE [m]	0.0254	0.0084	0.0511	0.0405	0.0017	0.0707	0.0407	0.0065	0.0741
T-Tide match	98.0%	99.0%	99.4%	99.5%	99.5%	99.3%	98.6%	99.3%	98.9%
2020									
Month	Jan	Feb	March	April	May	June	July		
RMSE [m]	0.0703	0.0023	0.0571	0.0230	0.0060	0.0408	0.0320		
T-Tide match	98.5%	98.3%	98.7%	99.2%	99.0%	99.7%	99.6%		

Table 3.5: Amplitude of the 10 major tidal constituents for the period 2019-2020 measured at Point Atkinson.

Constituent	Amplitude [m]
M2	0.920
K1	0.867
O1	0.480
P1	0.273
S2	0.236
N2	0.196
Q1	0.078
K2	0.065
J1	0.046
S1	0.042

The SedTRAILS analysis is usually performed for one tidal cycle that is representative for the long-term transports. This tidal cycle is then repeated over and over to obtain the transport pathways. To capture the strong daily inequality in the tidal signal, two consecutive tidal cycles (covering a period of 24 hours and 50 minutes) are taken for this research. The month that is used to calibrate the model (August 2019) contains a full spring-neap tidal cycle. From this month, the tidal cycle that generates transports most representative for the long-term transports is taken, which is the morphological tide.

To run SedTRAILS, it is important that the velocities at the beginning and end of the morphological tide are identical for the area of interest. Because this tide is repeated many times, a discrepancy between the velocities at the start and end of the timeseries will cause SedTRAILS to compute a net transport at the beginning of each cycle that does not occur in reality. The time series is chosen such that it begins and ends at zero velocity in the area of interest, to ensure that a small discrepancy between start and end velocity will not lead to a large error.

The area of interest is located next to and strongly influenced by Second Narrows. In Second Narrows, the highest velocities of the model domain can be found. Hence, it is important to minimize the error here. The morphological tide for SedTRAILS is selected such that it starts and ends at zero velocity in Second Narrows. This moment of zero velocity is determined by investigating the discharge time series at a cross section taken over Second Narrows. As the flow in the Narrows is spatially very

variable, the discharge over the full cross section gives a better image of when the average velocity over the full cross section approaches zero.

The net sediment transport vectors for the full spring-neap tidal cycle are plotted (see Figure B.2 in Appendix B). Subsequently, the net transports for each tidal cycle within this month are plotted with the aim to select the tidal cycle of which the net transport patterns are most similar to the long term net transport patterns. Following from this, the tidal cycle starting 14-08 at 12.10 and ending 15-08 at 12.50 was selected (Figure 3.6).

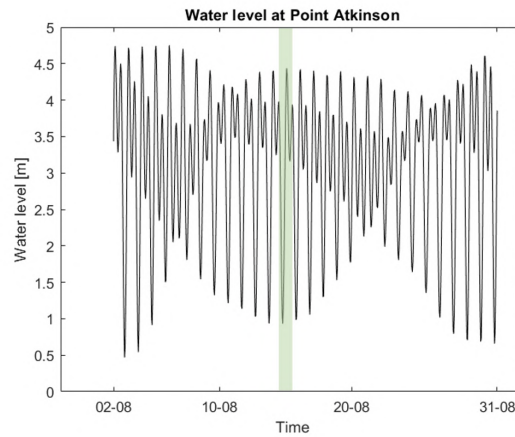


Figure 3.6: The spring-neap tidal cycle of August 2019. The selected tidal cycle is highlighted in green (14-08 12.10 to 15-08 12.50).

3.4. Limitations

Several assumptions have been made in the model set-up to reduce model complexity or due to missing data. The limitations of the model that result from these assumptions are listed in this section. These limitations should be kept in mind when interpreting the model results in Chapter 5.

Depth-averaged flows

The Delft3D FM model of Burrard Inlet is depth-averaged and thus does not resolve flow gradients over the water depth. The weak estuarine circulation as described in Section 2.2.3 cannot be accounted for because a depth-averaged model is used. However, previous studies (Wu et al., 2019, deYoung and Pond, 1989) suggest that the currents, especially in the Narrows where the highest currents occur, are tidally dominated and the contributions of wind forcing and freshwater are relatively weak. The total discharges of all the rivers rarely exceed one percent of the maximum flood discharge through the First Narrows (Baines, 1957). Because the flow through the First and Second Narrows is highly turbulent, water in the Inner and Central Harbour is generally well-mixed (Baines, 1957). Additionally, no information on the vertical distribution of velocities is available. Hence, inclusion and verification of the vertical dimension into the model would be very difficult. It must be noted that Indian Arm is more stratified, as little mixing takes place there. The penetration of saline water into Indian Arm is driven by renewal events which are still poorly understood (deYoung and Pond, 1988, Stacey et al., 2002). However, flows in Indian Arm are not expected to strongly influence the rest of the inlet. Velocities in Indian Arm are low, the arm is separated from the rest of the inlet by a sill and exchange between the two is limited (deYoung and Pond, 1988).

Apart from this, 3D effects could play a role in possible transport of sediments from Fraser river delta into Burrard Inlet. Fraser river has a high freshwater discharge (two magnitudes higher than the discharges of the local rivers in Burrard Inlet) and transports significant amounts of fine sediments into the Strait of Georgia (Attard et al., 2014, Thomson, 1981). Buoyancy effects could affect the dynamics of the freshwater plume.

Grain size schematization

A variety of grain sizes is present in Burrard Inlet, ranging from very fine mud to coarse gravel and cobblestones (McLaren, 1994, McLaren, 1995). A single sediment fraction of 70 μm (very fine sand),

which is the finest available non-cohesive sediment fraction, was used for the complete model domain, which is a major simplification. Coarser sediment fractions are less mobile, so the transport patterns shown by those fractions are likely less widespread and more poorly connected. Additionally, the full behaviour of finer mud and clay fractions, which can be transported by lower flow velocities, might not be captured. To obtain a first estimate on the behaviour of these sediment fractions, hydrodynamic particle tracking can be used as a proxy for fine suspended sediments.

Moreover, spatial availability of sediment can affect transport patterns. The patterns found in this research can be interpreted as the maximum potential transports based on the hydrodynamic forcing. For the actual transport, supply limitations play an important role while in the model, an infinite sediment supply was assumed.

Input reduction techniques

To prevent a computationally expensive simulation over a long time period, a morphological tide is selected as described in Section 3.3. This morphological tide is selected to be representative for the long-term transports. To account for the strong daily inequality, a period of 24 hours and 50 minutes (two tidal cycles) is selected.

The sensitivity to the chosen representative tidal cycle has been tested by running the model for two other periods in different phases of the spring-neap tidal cycle (Appendix B.2). The patterns found in Central Harbour for these two sensitivity runs correspond to the patterns found for the representative tidal cycle. At neap tide, the transport is weaker but shows the same pattern nonetheless. In Inner Harbour, choosing a different tidal cycle changes the observed transport patterns. Thus, the transports found in this study are considered representative for Central Harbour, but not necessarily for Inner Harbour. This was foreseen, as the representative tidal cycle was selected based on the long-term net transport behaviour in Second Narrows and Central Harbour, which is the area of interest. In order to obtain transports for Inner Harbour, another tidal cycle might be more representative.

For wind and waves, input reduction has been applied by the use of scenarios. Both average and storm conditions are covered in the scenarios. The combined information from these scenarios gives valuable information on the response of the system under various conditions and gives an indication of the sensitivity of the sediment transport behaviour to wind and waves. With this comes the limitation that behaviour that might occur under a sequence or combination of different wind/wave directions and strengths cannot be captured, which could be considered by combining several scenarios in future research.

Creating and verifying a schematization of the spatial wind field in the inlet is complicated, considering the large influence of topographic steering by the mountains and local wind effects due to the city, while the available information on the topographic wind field is rather limited. Hence, a uniform spatial wind distribution throughout the full inlet is assumed. The wind data measured by the TWN is used for the complete modelling area. It should be noted that this data is, in fact, not representative for the full inlet as it is gathered in a relatively sheltered area. However, it is representative for the Central Harbour and TWN shorelines, which is the area of interest in this project.

Representativeness outside of Burrard Inlet

To prevent numerical errors, the boundaries have been simplified to only three support points per boundary. Subsequently, the boundaries have been adapted to generate correct water levels at the mouth of Burrard Inlet (Point Atkinson). Moreover, the model is calibrated using a uniform initial salinity and roughness coefficient to match water levels and velocities at different measuring stations inside Burrard Inlet (Point Atkinson, Vancouver, AmpleSide, Kitsilano, Port Moody, and Indian Arm for the water levels, and First and Second Narrows for the velocities, see Chapter 4 and Figure 4.1).

As a result of these measures, the flows and water levels generated by the model hold only for Burrard Inlet and are not necessarily representative for the rest of the Strait of Georgia.

Set-up effects

Wind and waves can lead to a water level set-up, increasing the water level beyond the tidal forcing. Local wave set-up effects are not included in the model. As a result, submergence of intertidal areas during storm conditions and resulting sediment transport there is not captured in the model. This can lead to an underestimation of transports on intertidal areas such as Maplewood Mudflats under storm conditions.

Nearshore erosional processes

The model resolution is too coarse to resolve nearshore erosional processes. This means that for example increased erosion of the shoreline due to wave action is not included in the model. It is known that wave breaking exerts a force on the shoreline and can thus increase erosion rates. Moreover, the orbital motion in the water column caused by waves enhances shear stresses on the bed and stirs up sediment (Bosboom and Stive, 2015). However, this mobilization of sediment by wave action is not resolved by the model.

As soon as sediment is mobilized, it can be transported by currents. The interpretation of model results focuses on identifying transport directions and resulting sediment pathways. These pathways are related to the observed shoreline retreat problems by investigating supply of sediment to, and withdrawal from, the eroding shorelines.

Vessel waves

The Tsleil-Waututh Nation has a specific interest in the effects of vessel waves, which increase the overall wave energy in Central Harbour beyond that of the natural wind-generated wave environment (Beatty, 2021). As the area is sheltered and wind-generated wave heights are very low, vessel waves potentially have a significant impact on erosion rates. The wave height statistics used in this study are based on wave buoy measurements in Central Harbour and include the combined vessel and wind wave field (Beatty, 2021). The formulations of the SWAN wave model that is used describe wind waves. Thus, specific characteristics of vessel waves, such as a different wave skewness or changes in orbital velocities, are not included in the formulations. Hence, the model uses wave statistics from combined vessel and wind waves and but simulates them as if they are wind waves (with the same height as the vessel and wind waves in Central Harbour combined). This might cause a difference in the resulting transport patterns.

3.5. Post-processing of the results using SedTRAILS

In order to get an insight in the trajectories and transport pathways of the sediment system, SedTRAILS is used (Sediment TRANsport visualization & Lagrangian Simulator). SedTRAILS is a tool to visualize and analyze sediment transport pathways in a Lagrangian framework (Elias and Pearson, 2020). It is not a separate model simulation but a post-processing tool for the Delft3D-FM results.

3.5.1. Description of the method

The sediment transport vector fields computed by Delft3D-FM can be analyzed to assess the transport on the time scale of a single timestep or tidal cycle. SedTRAILS visualizes the results of these transport vectors on larger spatial and time scales. It is a helpful tool to understand sediment transports in complex morphodynamic systems such as tidal inlets and estuaries, without the need for computationally expensive long-term morphodynamic simulations. From the sediment transport fields at each timestep as computed by Delft3D-FM, SedTRAILS computes the pathways that sediment particles follow as they travel through a changing velocity field. In this way, the erosion problems can be analyzed by investigating along which trajectories eroding sediment can travel and at which locations it is likely to end up.

The end result is a map (Figure 3.7) showing the source points as circles and the particle trajectory from a given source point as a line originating in the respective circle. The result of the SedTRAILS model can give a comprehensive overview of where the sediment eroding at a certain location is going, or where sediment reaching a specific location comes from.

3.5.2. Limitations of the approach

Even though the output of SedTRAILS is a sediment pathway, SedTRAILS does not explicitly track individual sand particles, but only visualizes possible pathways based on the transport vectors in each timestep using the morphological tide. Because of the acceleration factor that is used, the transport pathways visualized using SedTRAILS represent the net motion. In order to assess gross particle movements, instantaneous velocity and transport fields must be analyzed.

Pathways visualized using SedTRAILS should be interpreted with caution. The pathway of each particle is dependent on its initial position. Shifting a source point only a short distance can result in a completely different trajectory. As there is only a finite amount of source points, some information is lost.

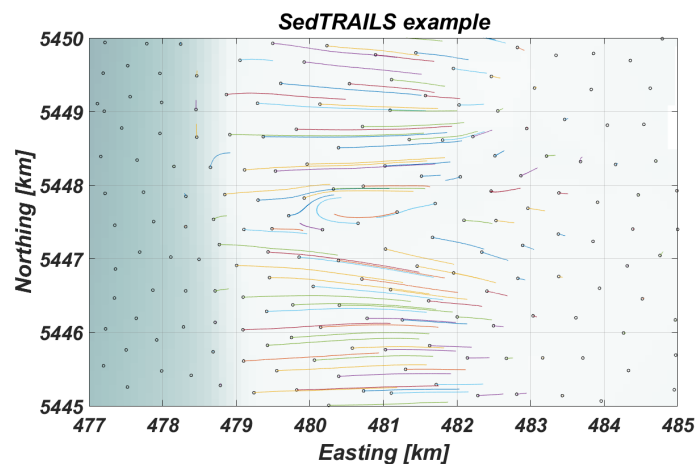


Figure 3.7: Example of sediment pathways visualized using SedTRAILS. The black circles show the starting points and the coloured lines originating from the respective circles are the trajectories as computed by SedTRAILS. Colours are assigned random to be able to distinguish the separate trajectories. Longer pathways indicate more mobile sediment: in this example, the sediment is most mobile in the middle of the plot (between $x = 479$ and 482 km). With a few exceptions, most trajectories in this plot are directed eastwards.

Hence, it is important to always compare the SedTRAILS results to the net transport vectors. As the SedTRAILS results only cover pathways for the selected source points, they cannot give information on whether there is a net import or export, and whether a certain scenario leads to more mass transport or less. To answer these questions, the vector fields must be analyzed.

Moreover, SedTRAILS only visualizes idealized pathways and does not account for effects as particle settlement or resuspension. The tool does not give any information on the sediment availability. It shows the trajectories from any given source point if there would be sediment available at this location. This makes it a useful tool for assessing the impact of interventions, as it can answer the question: 'If there would be sediment added or taken away at this location, where would it go?'

3.5.3. Application

In this study, SedTRAILS is applied in several ways, as described in this section.

Visualize particle trajectories

As a first step, the transport patterns that result from the vectors on larger time scales are visualized. This is done by equally distributing source points throughout the inlet to generate a comprehensive overview plot of where sediment originating from different areas will go. Source points can also be concentrated in specific areas (eg. in the Narrows or a specific basin) to target the distribution of sediment originating from that area.

Hydrodynamic particle trajectories

The visualization of transport pathways can be done for hydrodynamics, as well as sediment. When performing a SedTRAILS run for hydrodynamics, flow velocities are used instead of sediment velocities, to be able to predict the movement and trajectory of water particles. Due to the relatively high flow velocities (as compared to sediment transport velocities) this is generally done for a single tidal cycle, and the acceleration factor is set to 1. This application of SedTRAILS is used to obtain an overview of the possible connections within Burrard Inlet and can show how water moves through the inlet within a tidal cycle.

Predict the fate of eroding particles

By placing source points along the retreating shorelines, the fate of eroding particles can be predicted using SedTRAILS. The trajectories show where material that is mobilized along the shorelines moves, e.g. whether it tends to stick to the shoreline or moves further away. In this study, these trajectories are used to compare transport patterns for 1792 and 2019. For this purpose, comparing transport vectors is

the first step and already gives valuable information. SedTRAILS can then visualize the consequences of these changed transport vector fields for the eroding shorelines.

Reversed particle trajectories

To get an insight in the origin of sediment that reaches vulnerable shorelines, and thus can possibly feed these shorelines, SedTRAILS is run backwards in time. The direction of the transport vectors, as well as the timesteps, are reversed. In doing this, the consequent trajectory describes where sediment that ends up in this area can possibly come from.

Sources

The visualization of sediment pathways is used to identify how sediment reaching the inlet is redistributed. The trajectories of particles originating from sediment sources are investigated. For each source, this shows which areas of the inlet can be supplied with sediment by this source

Model calibration and validation

The model is calibrated using water level and velocity data from measuring stations inside the inlet. For the calibration, the month of August 2019 is used, as described in Section 3.3. Water level data is obtained from the department Fisheries and Oceans at the Canadian Government (Fisheries and Oceans Canada, 2021). Velocity data in First and Second Narrows is obtained via the measurement stations used in the SalishSeaCast model (SalishSeaCast, 2021). The measurement stations and their locations are shown in Figure 4.1.

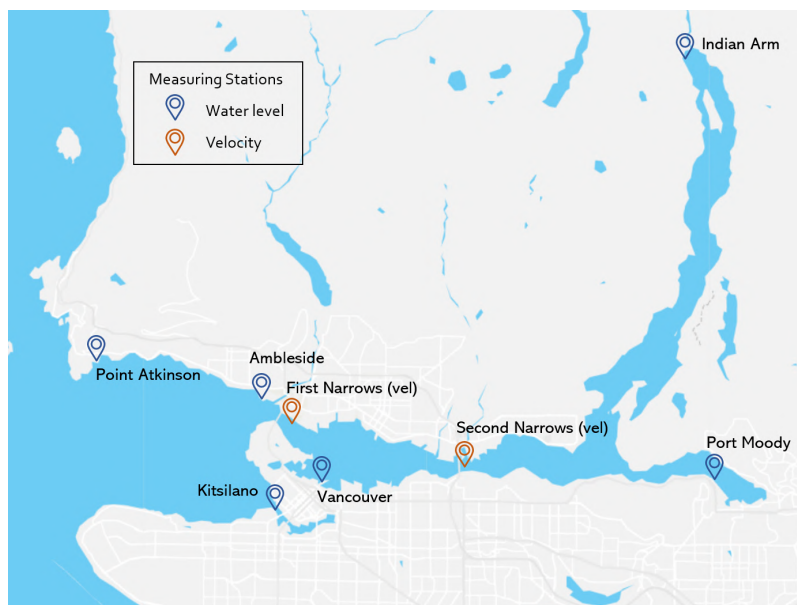


Figure 4.1: The locations of the measuring stations providing the data used for calibration and validation of the model. Blue markers represent water level measurements, orange markers show velocity measurements.

As a first step, the results of the Burrard Inlet model are compared to results of the Puget Sound model to check whether the nesting procedure has been executed correctly. This is done for selected observation points that are present in both models on the exact same location.

By nesting inside the Puget Sound model, tidal propagation through the model domain and the subsequent phase difference between the southern and western boundary has been accounted for and is implemented in the model. Subsequently, non-tidal contributions such as meteorological events in the modelling period are added, using measurement data.

To do this, the boundary forcing is adapted to ensure the amplitude, phase and shape of the tidal wave reaching Burrard Inlet are correct. The measuring station at the mouth of the inlet, Point Atkinson, is used for this purpose. The difference between the modeled and measured water level at Point Atkinson is taken at each timestep and added to the boundary forcing time series. This is repeated for several iterations until the water levels generated by the model match the measured water levels at Point Atkinson.

The calibration focuses on resolving the flows correctly inside and at the mouth of Burrard Inlet in order to obtain representative sediment transport patterns here. Hence, the boundaries are adapted to generate realistic flows in Burrard Inlet. It is important to notice that the model results are thus not necessarily valid in the rest of the Strait of Georgia.

4.1. Salinity

In order to include 2D salinity in the model, a spin-up time of a month is assigned, to ensure a realistic salinity distribution throughout the model. However, in some parts of the inlet such as Indian Arm, 3D processes such as density stratification are important and mixing is very limited. Therefore, the initial salinity partly defines the salinity gradient over the inlet and thus the tidal propagation.

Model runs for several initial salinity values (0, 10, 15, 20, 25 and 30 PSU) are compared. These model runs prove that the initial salinity can significantly influence the evolution of water levels throughout the inlet. An initial salinity of 10 PSU gives the best results (Figure 4.2).

At the ocean boundaries, a salinity of 30 PSU is prescribed. The Fraser river discharge boundary and the rivers flowing into Burrard Inlet are fresh (0 PSU).

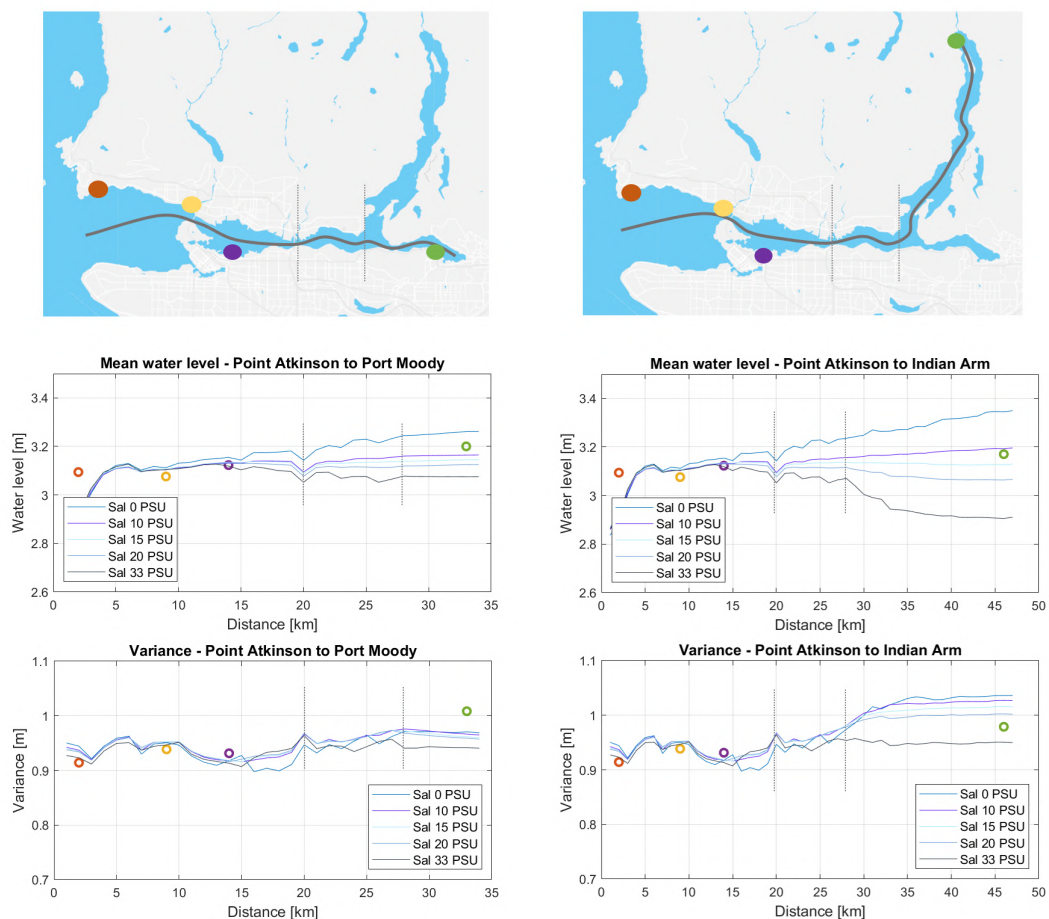


Figure 4.2: Plot showing the evolution of the water level (upper graph) and variance (lower graph) throughout the inlet, starting at the entrance and reaching to Port Moody (left panels) and Indian Arm (right panels) respectively. The lines show the model results comparing a range of initial salinities. The coloured dots are the values measured at the respective measuring stations. The grey dotted lines indicate the locations of Second Narrows and Roche Point, where Burrard Inlet splits into Port Moody and Indian Arm.

4.2. Roughness coefficient

The model is calibrated using a range of Manning coefficients ($0.02 - 0.05 \text{ s/m}^{\frac{1}{3}}$), looking at water levels and velocities at measurement locations shown in Figure 4.1. The Manning coefficient is a depth-dependent roughness parameter, where a higher value indicates a rougher bed. The default Manning coefficient used in Delft3D FM is $0.023 \text{ s/m}^{\frac{1}{3}}$. An optimal Manning coefficient of $0.040 \text{ s/m}^{\frac{1}{3}}$ is found (Figure 4.3a). This value is typically associated with mountain creeks or other channels with rough, rocky beds (USDA Forest Service, 2004). This can be explained by the high roughness of Burrard Inlet. Many bedforms and irregularities from glacial deposits are present in the inlet, causing a rough and turbulent surface flow. It should be noted explicitly that although this value is applied for the full model domain, it does not hold for the Strait of Georgia, since the calibration focuses on obtaining correct flows inside the inlet. Additional calibration could consider spatially varying roughness, which is not done in this research for simplicity and time reasons.

After calibration, velocity deviations are in the order of 5% in the Narrows (Appendix A). Water levels show a root mean squared error lower than 10 cm at all measuring stations (Figure 4.3a). The simulated and measured mean water level and variance deviate less than 5 cm at all measurement stations, which demonstrates that the propagation of the tidal wave through the inlet is simulated correctly (Figure 4.2).

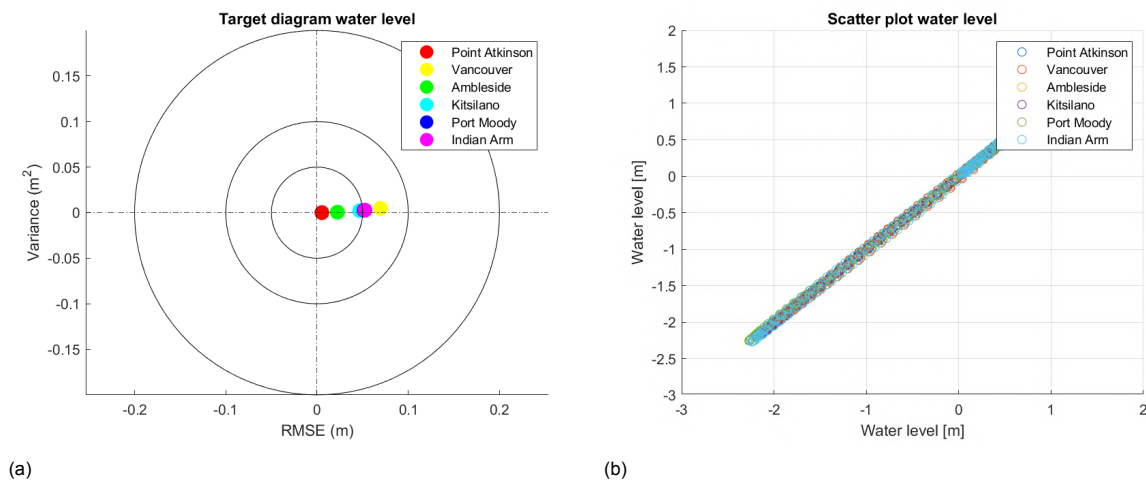


Figure 4.3: a) Target diagram showing the root mean squared error (RMSE) and variance for the water levels at several locations (see Figure 4.1 for the locations). Manning Coefficient is $0.040 \text{ s/m}^{\frac{1}{3}}$ and initial salinity is 10 PSU. Points located closer to the centre indicate a lower error, i.e. a better model performance. b) Scatter plot of the observed and modeled water levels at various measuring station. The measured water level is given on the x axis and the modeled water level on the y-axis.

5

Results

Based on the Delft3D FM model results, the sediment transport patterns in the inlet are investigated and presented in this chapter. As a first step towards understanding the system, the hydrodynamics are analyzed, identifying the dominant flow and velocity patterns. Next, sediment transport patterns are investigated using a tide-only forcing. In a later stage, the effects of wind and wave forcing are added to the simulation, to be able to isolate their influence on the sediment pathways.

5.1. Hydrodynamics

The selected representative period covers 24 hours and 40 minutes and thus 2 tidal cycles, including 2 flood periods and 2 ebb periods. These can be divided into a strong ebb and a strong flood (ebb 1 and flood 1 in Figure 5.1), followed by a weaker ebb and a weaker flood (ebb 2 and flood 2). In this section, the flows in Burrard Inlet during the dominant ebb 1 and flood 1 are analyzed. The velocities for the weaker ebb and flood events are found not to differ significantly from these trends and can be found in Appendix C, where also the velocity maps zooming in at Central Harbour can be found.

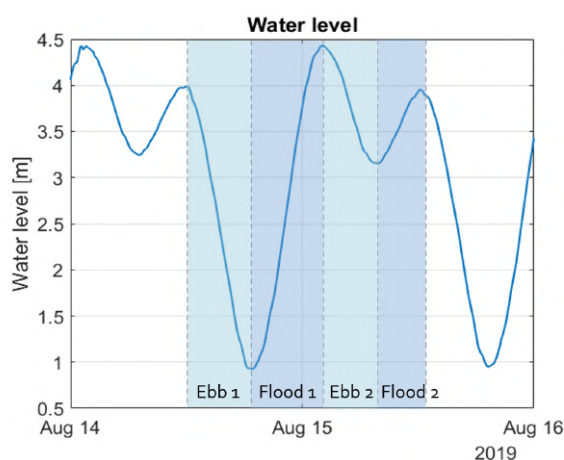


Figure 5.1: The selected representative period can be divided into two ebb periods (ebb 1 and ebb 2, indicated green) and two flood periods (flood 1 and flood 2, indicated blue).

During ebb, water motion is directed out of Burrard Inlet (Figure 5.2). In large parts of the inlet, flow velocities are low (<0.5 m/s) but in First and Second Narrows, velocities increase significantly where mean velocities over the full ebb period reach 1.8 m/s and peak velocities up to 2.5 m/s. In the wider basins, the flow decelerates and forms eddies.

During flood, water enters the inlet via Outer Harbour and First Narrows. Again, a strong acceleration in First and Second Narrows can be observed (Figure 5.3).

Zooming in on Central Harbour, the main flood flow describes a meandering motion, first moving along the southern shores and further eastwards attaching to the shorelines on the north side close to Cates Park (Figure 5.4). At Cates Park, the main flow moves northwards into Indian Arm. A weaker flow also moves into Port Moody. Three eddies form in Central Harbour during flood: a counterclockwise

eddy in front of the Tsleil-Waututh reserve and Maplewood Mudflats (eddy I), a counterclockwise eddy east of Cates Park (eddy II), and a clockwise eddy in the south (eddy III, Figure 5.4).

For a weaker flood event, the eddy in front of the TWN reserve is smaller and shifts westwards (see Figure C.2 in Appendix C). This specific eddy has been observed regularly by Tsleil Waututh (Tsleil-Waututh Nation Climate Summit, 2018). Observations from the community confirm that the eddy shifts from West to East with a bigger flood event, which corresponds well with the model predictions.

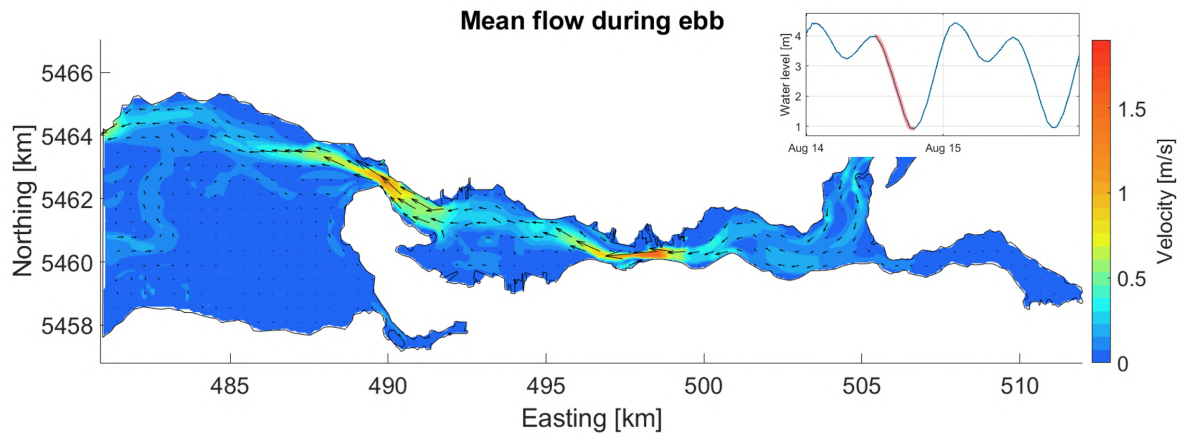


Figure 5.2: Map showing the velocities in Burrard Inlet averaged over the full ebb period. The ebb period is defined here as the time that the water moves westwards (x -velocities are negative).

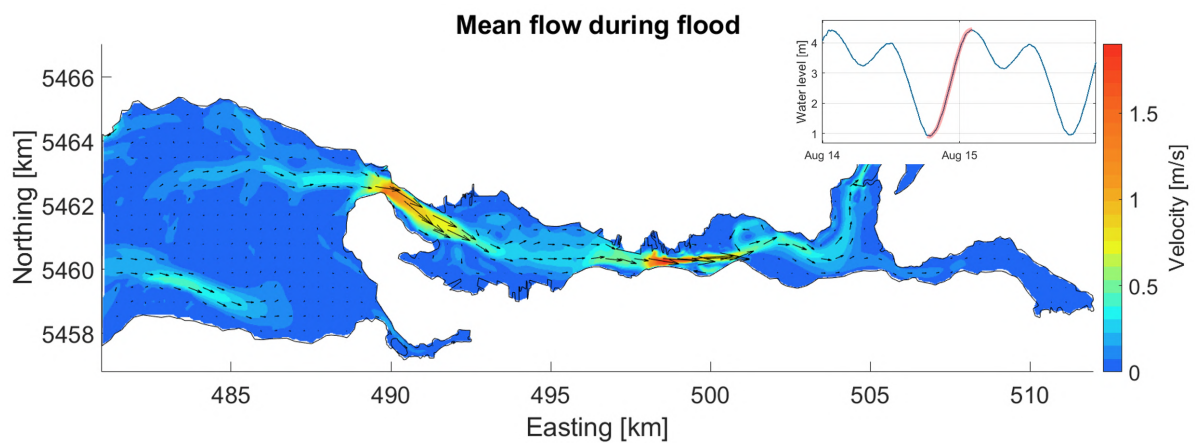


Figure 5.3: Maps showing the velocities in Burrard Inlet averaged over the full flood period. The flood period is defined here as the time that the water moves eastwards (x -velocities are positive).

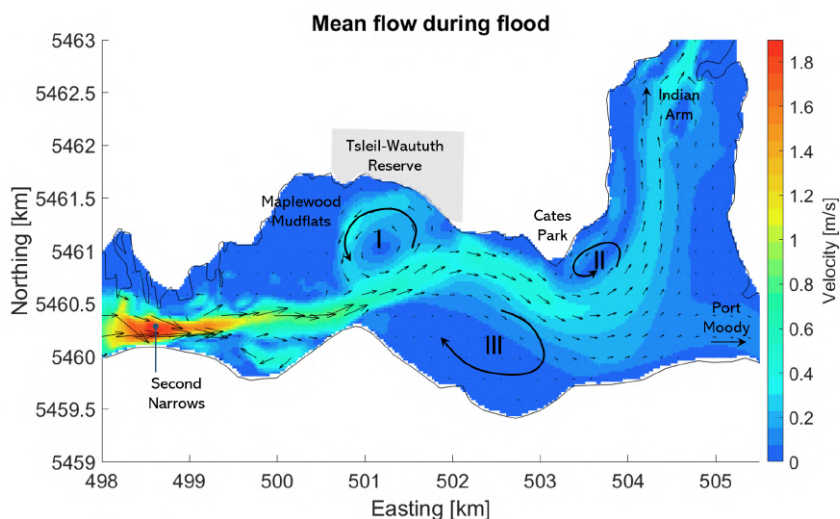


Figure 5.4: Maps showing the velocities in Central Harbour averaged over the full flood period. The main flood flow meanders through the basin and moves into Indian Arm. Around this main flow, three eddies form.

5.1.1. Hydrodynamic particle trajectories

In addition to the velocity maps, a SedTRAILS analysis is performed for the hydrodynamics (see Section 3.5.3). In this way, the patterns of water motion and connections between different basins can be visualized. These patterns are interpreted as the maximum potential sediment behaviour, if sediment would be floating freely and there would be no limitations due to deposition.

Because simulating the water motion from particles all over the inlet at once results in a chaotic figure that is difficult to interpret (see Figure D.1), the different basins are isolated to be able to distinguish patterns in the water motion. A separate SedTRAILS run has been done for each section of the inlet, containing source points only in this section (Figure 5.5). As such, the simulation gives an overview of the potential pathways for particles originating from this basin.

When performing SedTRAILS for hydrodynamics, the starting time of the simulation can strongly impact the trajectories, due to the relatively high velocities compared to sediment transport. To include all possible trajectories, all simulations are performed for two release moments: high water slack (just before ebb) and low water slack (just before flood). A complete overview of all simulations can be found in Appendix D.

The results of the SedTRAILS runs for the various source locations are presented below.

Outer Harbour

The northern shore of Outer Harbour is the main passageway for water to leave the inlet (Figure 5.5 A and E). Short trajectories, indicating limited movement are found in the central parts of Outer Harbour (Figure 5.5 D). Most pathways move towards First Narrows, except for the single strong outflow along the north shore into the Strait of Georgia.

First Narrows, Inner Harbour and Second Narrows

In both First and Second Narrows, strong acceleration of the flow leads to straight, jetlike pathways (Figure 5.5 A and B). Further away from the Narrows, the flow decelerates and pathways tend to become more variable and chaotic. Ebb flow through Inner Harbour is concentrated along the Northern Shore (Figure 5.5 B and C), as was already indicated in the velocity maps (Figure 5.2).

Central Harbour

Water moving from Second Narrows into Central Harbour moves into the three eddies already observed in Figure 5.4 (Figure 5.5 B and E). Port Moody seems rather detached from the rest of the inlet: the majority of the trajectories reaching Roche Point flows northwards into Indian Arm.

Placing source points along the shoreline in front of the TWN reserve (Figure 5.5 F) shows that water originating from these shores has the potential to move all the way into Indian Arm or Outer Harbour. As these pathways are regarded as the upper limit for sediment transport, they are expected to be longer and more dispersive than sediment pathways.

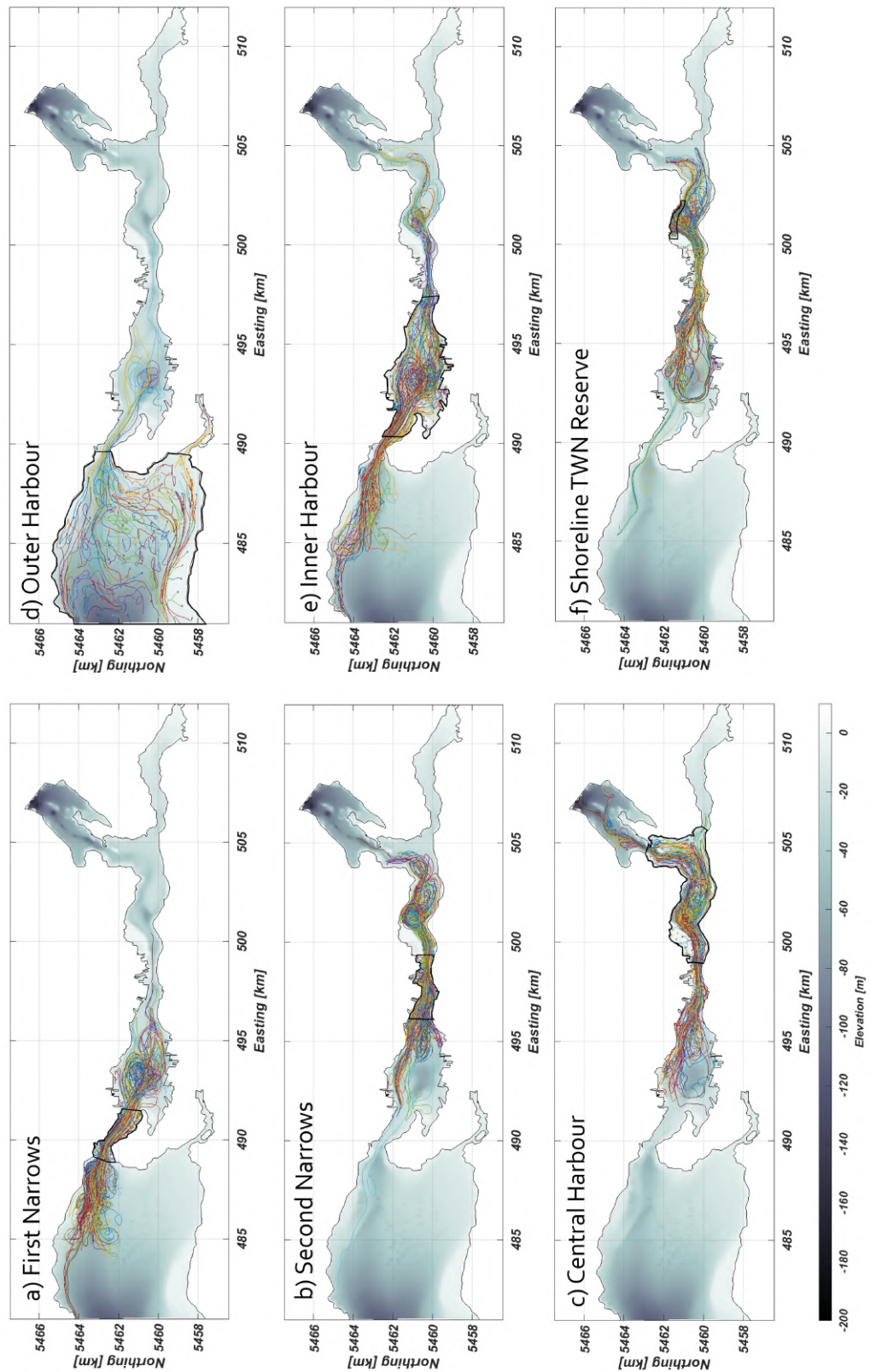


Figure 5.5: SedTRAILS runs for hydrodynamics. Each plot shows a SedTRAILS run with source points in a different section of the inlet, released at high water slack.

5.2. Sediment transport vectors

Moving from the velocity patterns analyzed in the previous sections towards sediment transport, the dominance of First and Second Narrows in the transport is revealed.

During ebb and low tide, sediment transport is strong in Inner and Outer Harbour (Figure 5.6). Sediment is moved out into Outer Harbour, again remaining largely in the northern part of the basin. No sediment transports of any significance can be found in Central Harbour under ebb currents.

During flood, sediment is transported into Inner Harbour and Central Harbour (Figure 5.7).

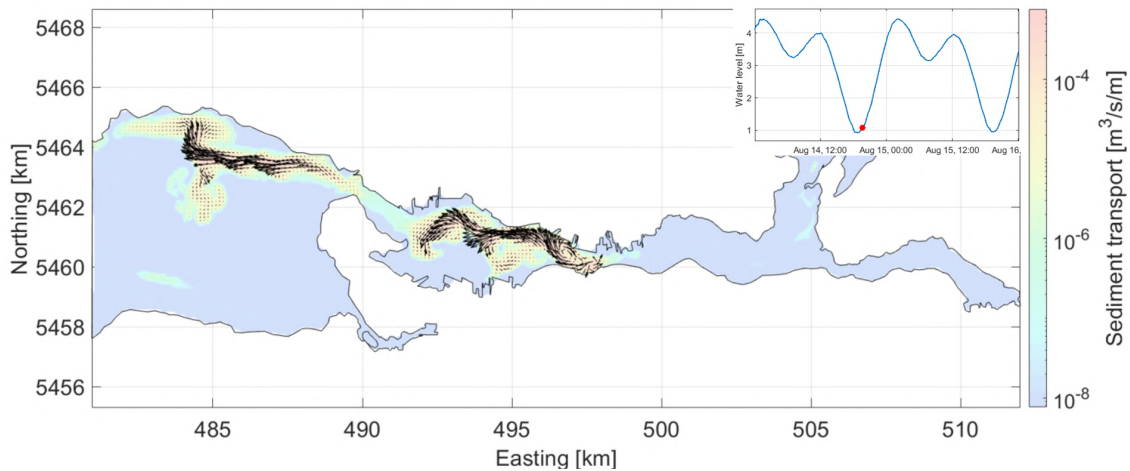


Figure 5.6: Sediment transport vectors in Burrard Inlet for low water. Transports are concentrated to Inner Harbour and sections of Outer Harbour. There is no transport in Central Harbour. Note that the color scale, indicating the strength of the sediment transport capacity is logarithmic.

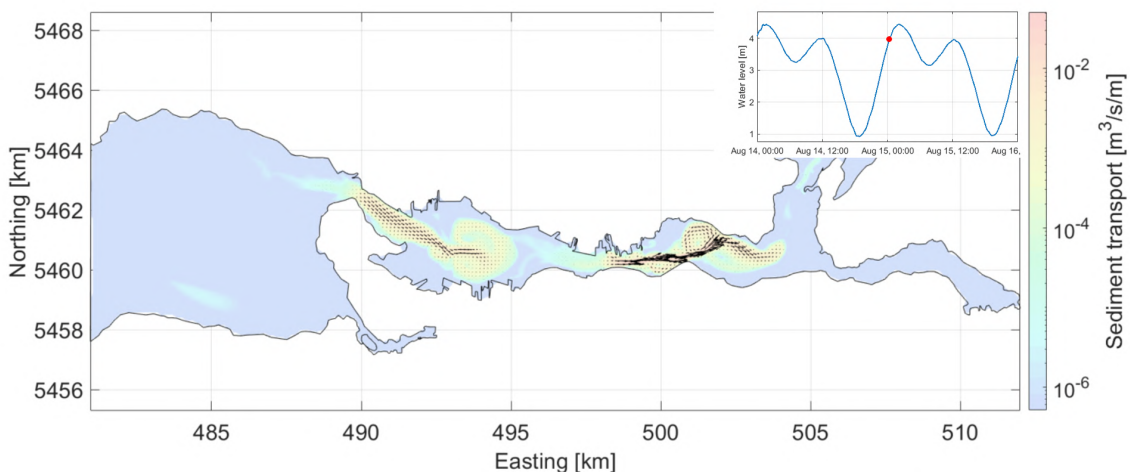


Figure 5.7: Sediment transport vectors in Burrard Inlet during flood. The highest transports can be found in Inner and Central Harbour. Note that the color scale, indicating the strength of the sediment transport capacity is logarithmic.

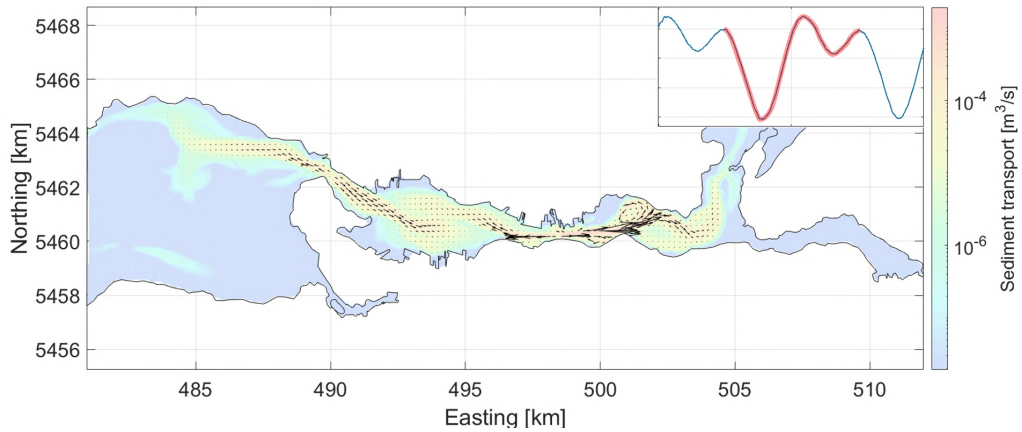


Figure 5.8: Net transport over the full tidal period. Sediment transport moves away from First and Second Narrows in both directions. Note that the color scale, indicating the strength of the transport capacity, is logarithmic.

Analyzing the net transport over the full morphological tide shows that net transport moves away from First and Second Narrows in both directions (Figure 5.8). This pattern can be explained by the strong flow acceleration in the Narrows.

There is a large spatial variation in the flow as velocities increase rapidly in the constriction. As a result of the rise in velocity, the sediment concentration increases and sediment transport starts picking up, directed away from the Narrows, as illustrated in Figure 5.9 for Second Narrows. First Narrows shows the same behaviour (see Figure C.3 in Appendix C). This pattern holds true for both ebb and flood flow. Flow moving into the Narrows is too weak to generate significant sediment transport, whereas there is considerable transport away from the constriction. This leads to the pattern of net sediment transport as observed in Figure 5.8.

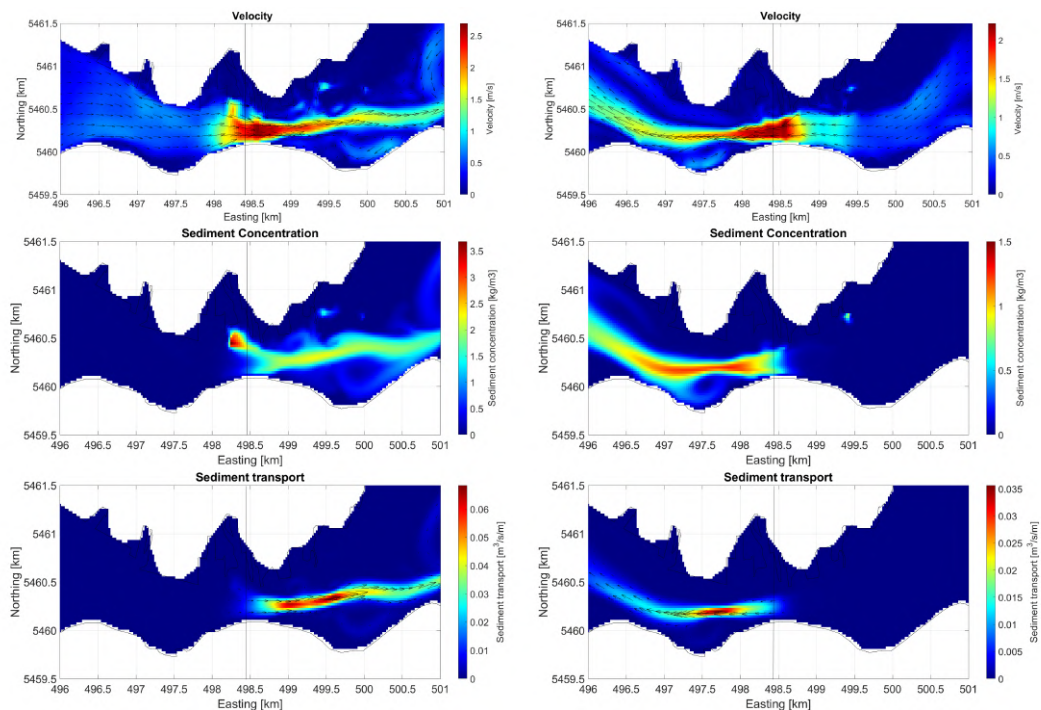


Figure 5.9: Left panels: Velocity, sediment concentration and sediment transport in Second Narrows during peak flood. Right panels: velocity, sediment concentration and sediment transport in Second Narrows during peak ebb. Net transport moves away from the Narrows in both directions. At the location of the black line, the center of the constriction, sediment transport is limited.

5.2.1. Sediment transport in Central Harbour

The strongest net transports in Burrard Inlet can be found in Central Harbour, which is the area of interest. As no transport takes place in Central Harbour during ebb, the net transport here is dominated by the flood transport (Figure 5.10). The same patterns that have been found for the flood flow velocities (Figure 5.4) arise here for sediment transport. The presence of Second Narrows dominates the transports in the basin. The largest transport vectors are concentrated in a narrow band leading eastwards from Second Narrows into the basin. This transport diverges as soon as it reaches the northern shores of Central Harbour. Sediment then either moves west along the TWN shoreline and Maplewood Mudflats into eddy I or east towards Cates Park, where it then moves northwards into Indian Arm. Eddies I, II and III that were observed in the flood flows are distinguished for sediment transport as well.

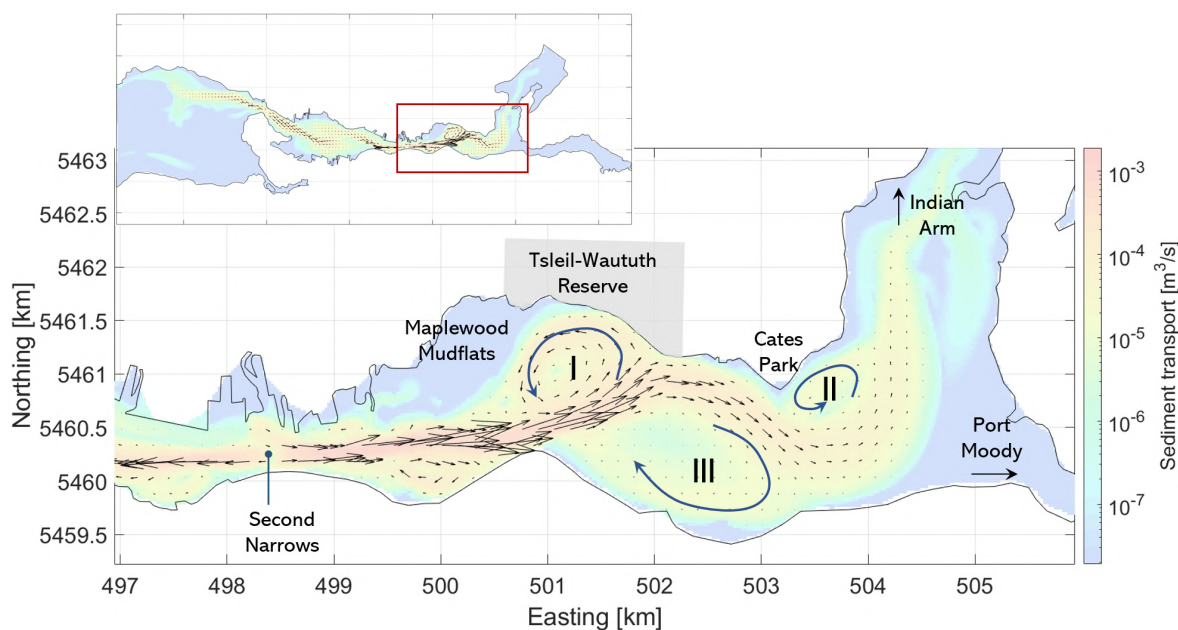


Figure 5.10: Net transport over the full tidal period in Central Harbour. The three eddies observed in the flood velocities arise for sediment transport as well. Note that the color scale, indicating the strength of the sediment transport capacity is logarithmic.

5.3. Sediment transport pathways using SedTRAILS

SedTRAILS is used to visualize the transport pathways that emerge from the net sediment transports in Burrard Inlet, depicted in Figure 5.10. The sediment pathways (Figure 5.11) are computed for tide-only forcing with a sediment size of 70 micron (very fine sand), a runtime of 20 days and an acceleration factor of 20.

In Outer Harbour, very little transport is observed. There is export from First Narrows through the Northern part of the basin. This outward flow corresponds to the trend observed for the hydrodynamics (Figure 5.5).

Sediment originating from both First and Second Narrows has the potential to reach Inner Harbour. In Inner and Central Harbour, there is significant movement and dispersal within the basins. Many sediment pathways in these basins end up in an eddy (Figure 5.12 and Figure E.3 in Appendix E).

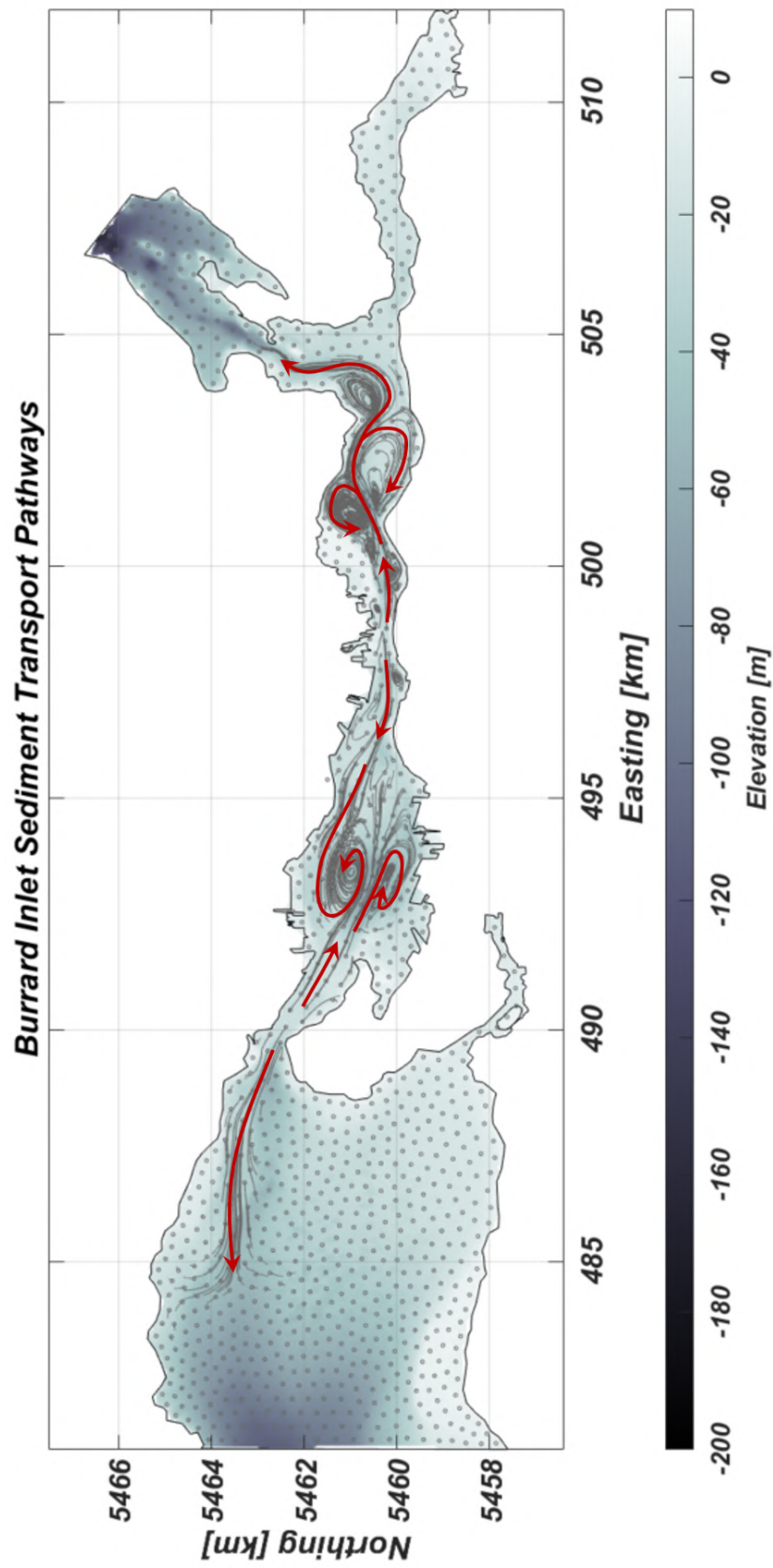


Figure 5.11: SedTRAILS run for Burrard Inlet, with 1000 source points distributed over the inlet, a runtime of 20 days and an acceleration factor of 20.

5.3.1. Central Harbour

Zooming in on Central Harbour, the eddy in front of the TWN shoreline observed in the sediment transport vectors translates into a spiralling sediment pathway. The transport patterns in Central Harbour can be described by a main flow from Second Narrows driving a net transport into Indian Arm (Figure 5.12). This main transport line meanders around three large eddies: one in front of the TWN shoreline and Maplewood Mudflats, one in the south and one east of Cates Park.

Plotting the pathways of particles originating from the TWN shorelines and Cates Park gives an indication of the fate of sediment eroding along these shores (Figure 5.13). Considering source points along the TWN shoreline (trajectories indicated in blue), there is a clear divergence point at the eastern end of the reserve. To the west of this point, sediment moves west along the shoreline and bends south as it reaches Maplewood Mudflats. From here, the sediment is either trapped inside the eddy or moves eastwards and finally into Indian Arm. Sediment moving east at the divergence point ends up either in the eddy east of Cates Park or is transported northward into Indian Arm (Figure 5.13).

Sediment particles at the shorelines of Cates Park (trajectories indicated in black) move south and away from the shore, both on the eastern and western side of Cates Park. Practically all pathways end up in the eddy east of Cates Park.

Both the pathways for the TWN shoreline and Cates Park show a clear trend: as soon as shoreline sediment is mobilized, it tends to move away from the shorelines, with an end destination either in one of the eddies or in Indian Arm.

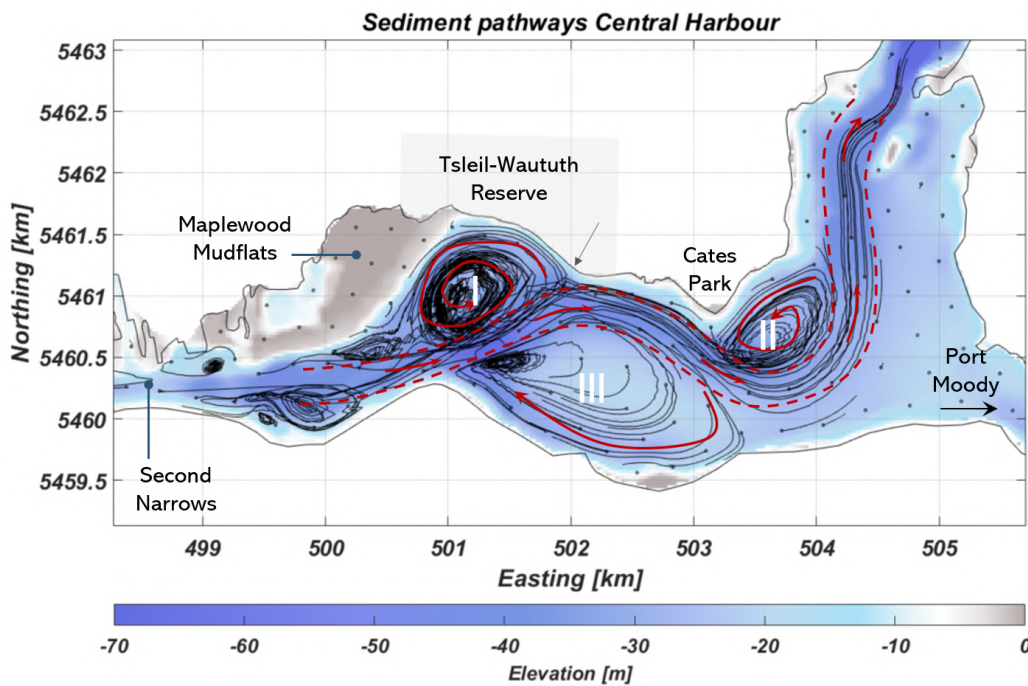


Figure 5.12: Sediment pathways in Central Harbour, computed using SedTRAILS with a runtime of 20 days and an acceleration factor of 20. The bathymetry has been plotted in blue to show the relation between the transport pathways and depth contours more clearly. The main patterns are indicated by the red arrows. The 'sediment divergence point' at the eastern end of the TWN reserve is indicated by the grey arrow.

To get insight in the origin of sediment that reaches the vulnerable shorelines at TWN and Cates Park, SedTRAILS is run backwards in time. This visualizes where sediment that ends up at these shorelines comes from.

Virtually all pathways reaching the TWN shoreline and Cates Park are provided by transport resulting from Second Narrows (Figure 5.14). Second Narrows drives a strong sediment transport into Central Harbour, opening up pathways that reach the northern shorelines.

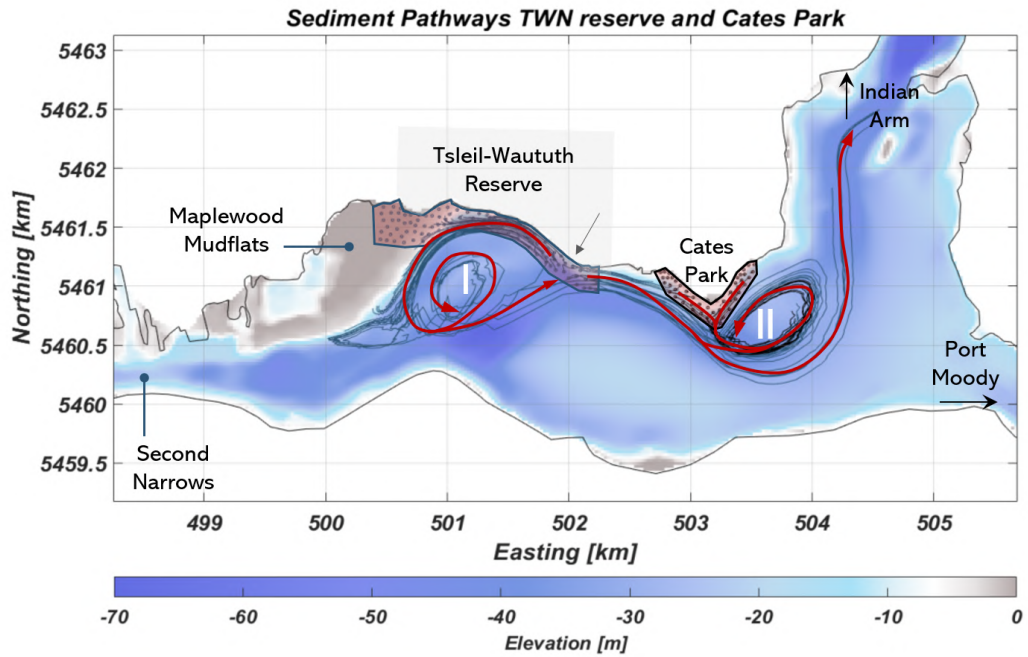


Figure 5.13: Sediment pathways originating from source points along the shores of TWN (blue) and Cates Park (black), using SedTRAILS with a runtime of 20 days and an acceleration factor of 20. The main patterns are indicated by the red arrows. The 'sediment divergence point' at the eastern end of the TWN reserve is indicated by the grey arrow.

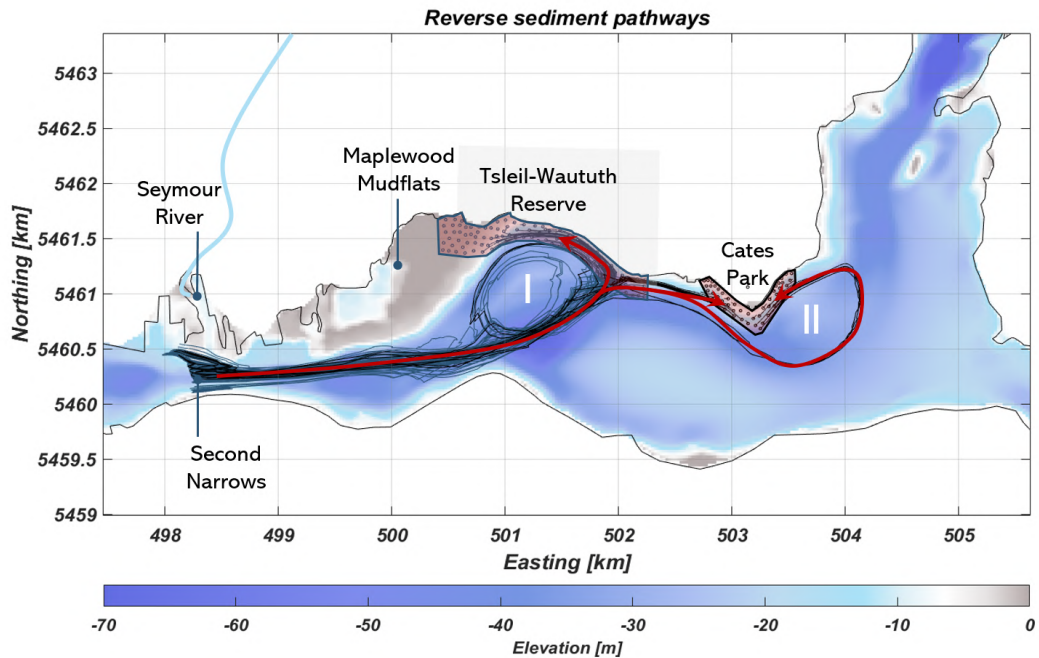


Figure 5.14: Reversed sediment pathways in Central Harbour, computed by running SedTRAILS backwards in time with a runtime of 20 days and an acceleration factor of 20. The plot shows the possible pathways of sediment reaching the TWN shorelines and Cates Park.

5.4. Sediment sources

The visualization of sediment pathways using SedTRAILS can be used to identify how sediment reaching the inlet is redistributed, by investigating the trajectories of particles originating from sediment sources. In this section, the fate of sediment from the rivers discharging into Burrard Inlet (Capilano River, Seymour River and Lynn Creek) and Fraser river is analyzed using SedTRAILS.

5.4.1. Rivers in Burrard Inlet

Three main rivers flow out directly into Burrard Inlet: Capilano River in First Narrows, Lynn Creek and Seymour River in Second Narrows. All three of them have the potential to feed the basins with sediment (Figure 5.15). Material from Capilano River moves westwards into Outer Harbour. Sediment brought in by Lynn Creek moves around in Second Narrows and will likely settle on the northeastern shores of Inner Harbour. Seymour River sediments have the possibility to either settle on the southeastern tip of Maplewood Mudflats or move further eastwards into Central Harbour and sometimes even Indian Arm.

For all three rivers, the outflow locations of the river itself are rather sheltered. In the SedTRAILS run, many of the source points located very close to the river mouth show little to no movement. Hence, it is possible that the rivers feed Burrard Inlet with sediment on a longer timescale: material might first accumulate at the sheltered river mouth and form a delta, as can be seen for Capilano River. As soon as sediment from the rivers moves out of the sheltered zone, it is hit by the strong currents in the Narrows and transported into the basins.

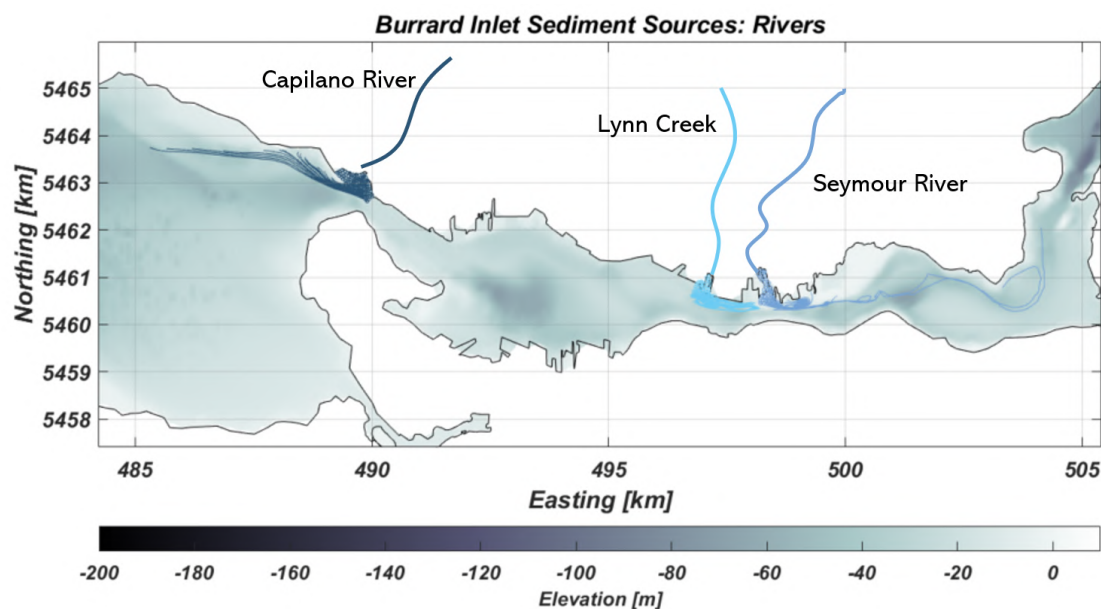


Figure 5.15: The three main rivers flowing out in Burrard Inlet: Capilano River, Lynn Creek and Seymour River. The results of three consecutive SedTRAILS runs with source points at the mouth of each respective river have been combined into one figure.

5.4.2. Fraser River

Fraser river, which flows out into the Strait of Georgia just south of Burrard Inlet, has been identified as a major potential source of sediment. The river has been adding sediments at a rate of 12 million m³/year and the northern delta is advancing seaward at 2.3 m/year (Thomson, 1981).

The domain for which the results are visualized is expanded to include the Fraser river delta to see whether sediments from Fraser river are able to reach Burrard Inlet. The model run for tide-only forcing shows very little movement at Point Grey, which separates the Fraser delta from Burrard Inlet (Figure 5.16a). Sensitivity testing reveals that waves play an important role in the sediment transport in the Fraser delta (Figure 5.16b).

The results show a potential for transport, since there is activity in the northern delta and around Point Grey for southerly and westerly waves. For high westerly waves, transport pathways directed into the inlet open up along the shorelines (Figure 5.16b, for more wave runs, see Appendix F). However, the results do not show a clear connection between the Fraser delta and Burrard Inlet and are not conclusive about whether Fraser river sediments can reach the inlet. A SedTRAILS run for hydrodynamics reveals that water from Fraser river is able to flow into the inlet, which is a promising indication for fine suspended sediments (Figure F.1).

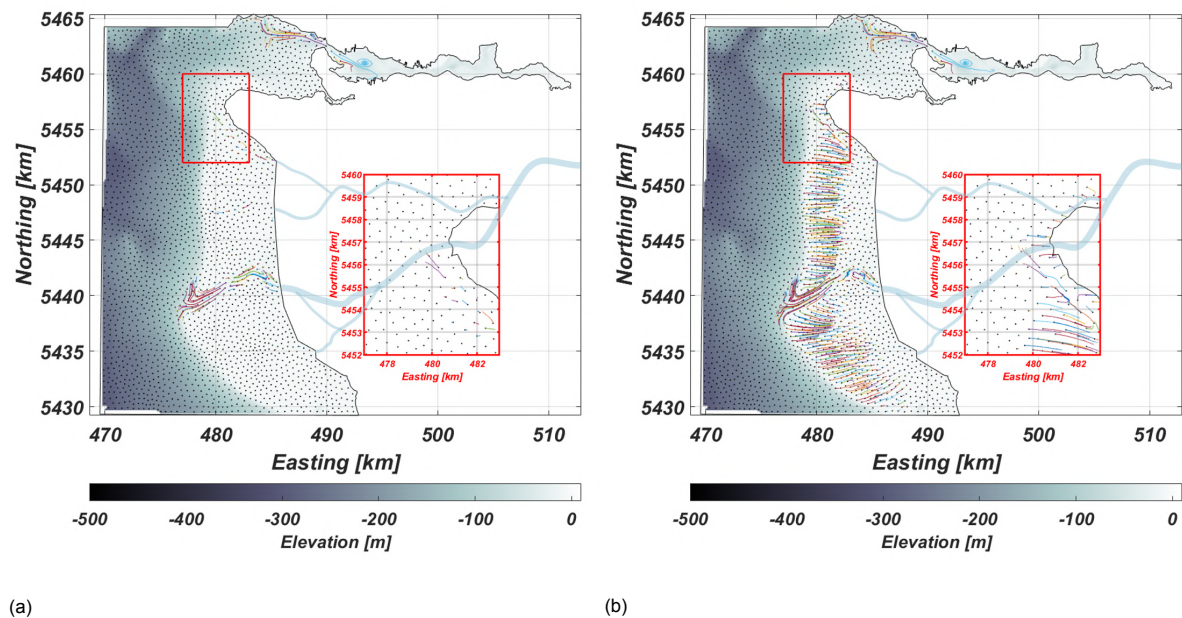


Figure 5.16: a) SedTRAILS run including the Fraser river delta: tide only. Runtime is 50 days and an acceleration factor of 30 is used. The zoomed inset box shows Point Grey, which separates the Fraser delta from Burrard Inlet. b) SedTRAILS run including the Fraser river delta with high waves ($H_s = 1.64$ m) from the West.

5.5. Influence of wind and waves

In the previous sections, the sediment transport patterns are analyzed for a simplified situation where only tidal forcing is considered. However, wind-generated currents and waves can affect both the direction and magnitude of the sediment transport.

The importance of these factors on the velocity patterns and sediment transport is assessed in this section. The results show that wind and waves can lead to minor local effects in the flow and sediment transport. However, the main tidal transport patterns are robust and do not change much, even under more extreme conditions.

5.5.1. Wind

The velocity patterns and sediment transports are investigated for the five wind scenarios presented in Section 3.1.6. Average winds (with a wind speed of 1.90 m/s) have a minimal effect on the velocity field, with deviations in the order of 0.01 m/s. The influence of strong winds (8.69 m/s) is slightly larger

with velocity differences of 0.3 to 0.5 m/s. Flow directions remain largely the same. For an extreme storm (24.2 m/s), the circulation in Central Harbour is significantly changed at low water (Figure 5.17a). However, at high water, when tidal velocities in Central Harbour are larger, the flow again follows the patterns for tide-only circulation (Figure 5.17b). During flood, a northeast directed flow over Maplewood Mudflats towards the northern shoreline is found. This motion is however not seen in the sediment transports.

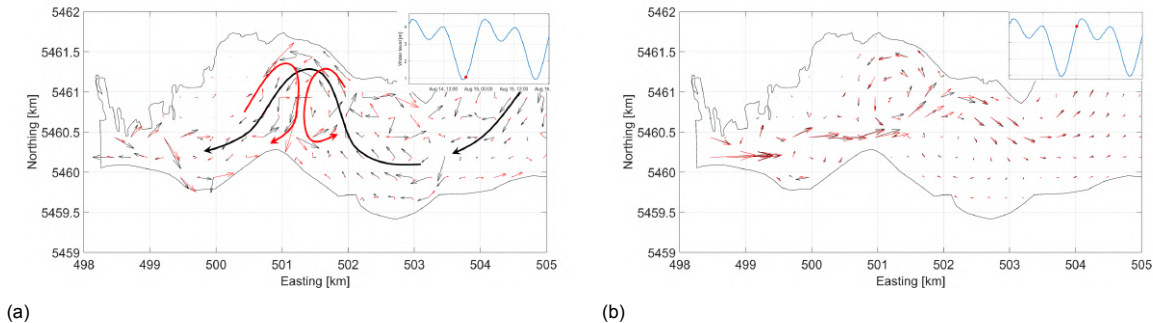


Figure 5.17: Map showing the velocity vectors for extreme winds (24.2 m/s) from the west. Velocity vectors for tide-only forcing are plotted in black, the velocity field including wind is plotted in red. a) Flows during low water: circulation patterns changed significantly from the patterns without wind. b) Flows during high water: there are no deviations from the regular flow patterns anymore.

Equal to the hydrodynamics, the influence of wind on the sediment transport is rather limited. While it should be noted that the general patterns remain the same and changes are only very subtle, some trends can be observed.

Strong easterly winds tend to reinforce the net sediment transport (over the full tidal cycle) in all three eddies in Central Harbour (Figure 5.18a and 5.18b). Westerly winds, on the other hand, weaken the transport vectors of the eddies.

The 'main line of transport' from Second Narrows to the east end of Central Harbour seems to shift depending on the wind direction. For easterly winds, the curvature of this line increases, bending further northwards just west of Cates Park, and further southwards at Westridge compared to the tide-only forcing (Figure 5.18a). Westerly winds tend to decrease this curvature and cause the main line of sediment transport to move more to the center of the basin (Figure 5.18b).

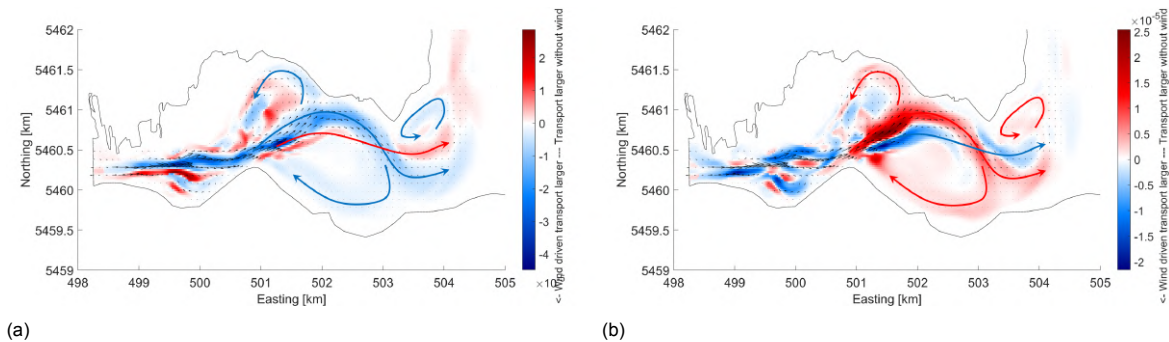


Figure 5.18: Maps showing net transport over the full tidal period for wind. In areas highlighted in blue, transport vectors have increased due to the presence of wind. In red areas, the vectors were larger without wind. a) Strong wind (8.69 m/s) from the east. Transport in the eddies is reinforced, as indicated by the blue arrows. The main line of transport has obtained a stronger curvature. b) Strong wind (8.69 m/s) from the west. Transport in the eddies is weakened (red arrows). The curvature of the main line of transport has decreased.

5.5.2. Waves

Wave heights are simulated for seven scenarios presented in Section 3.2, including three different wave heights: average, high and extreme. Wave heights simulated in front of the TWN shorelines are compared to data measured by the wave buoy at this location (Beatty, 2021). Average waves lead to significant wave heights of ~ 0.05 m (Table 3.3), which corresponds to average wave heights

measured at this location, including both wind and vessel waves. For the 'high waves' scenario (1 % largest significant wave heights from the dataset), wave heights at TWN are ~ 0.30 m (Figure 5.19), roughly equivalent to the highest significant wave heights measured at this location in the year the wave buoy has been deployed. Simulating extreme waves gives a $H_{sig} \sim 0.70$ m, which is unrealistically high for this location and is used more as a sensitivity case.

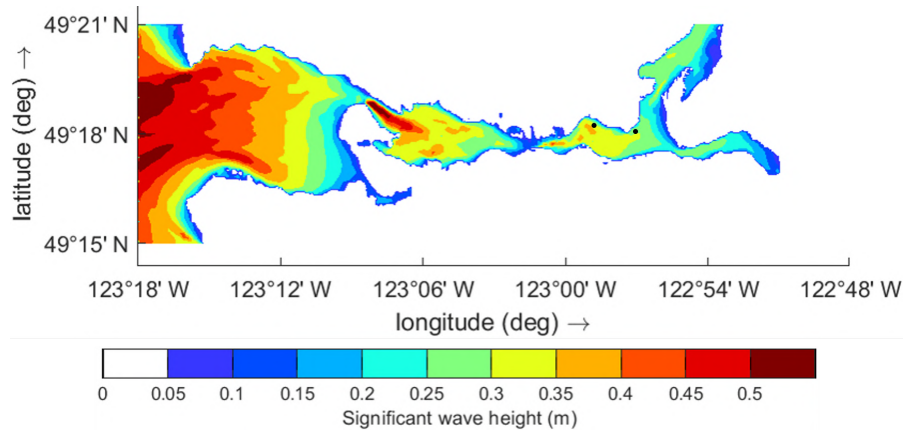


Figure 5.19: Significant wave heights in Burrard Inlet for strong winds and high waves from the east (the wave heights in Central Harbour for strong winds from the south and west are comparable, see Appendix G). The locations of the wave buoys are indicated using black dots.

Wave-driven currents are able to cause deviations from the tide-only flow vectors in the order of 0.3 - 0.5 m/s. There is no strong difference between the magnitude of the change between average and strong waves. Concerning the patterns that are found, no clear distinctions could be found between the different wave directions. In Second Narrows, at the location where the strongest acceleration takes place, no notable differences in velocity can be found.

Some very strong (0.5 m/s stronger than for tide-only) local offshore directed currents can be found at the edge of Maplewood Mudflats during ebb and low water (Figure G.15). This effect did not take place for wind, suggesting that it is a wave-driven phenomenon. This local offshore current increases for higher waves.

Concerning the net transport rates, high waves tend to increase sediment transport along the shorelines and along Maplewood Mudflats compared to the tide-only situation (Figure 5.20). Moreover, for high waves, the main line of transport shifts slightly southwards.

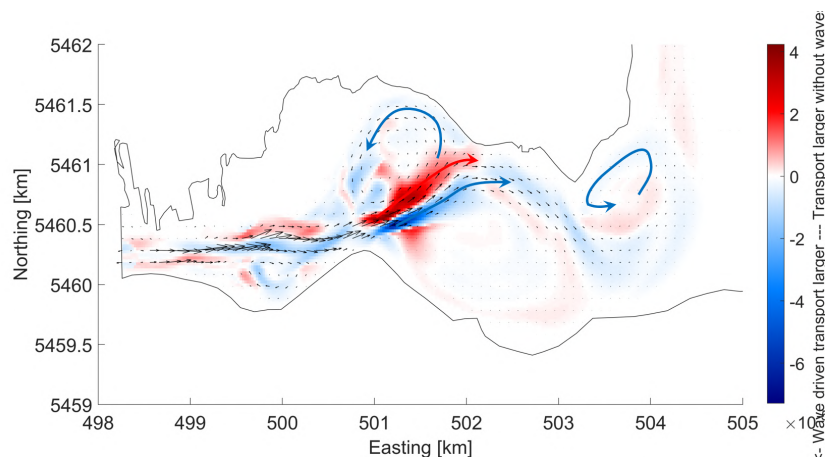


Figure 5.20: Net transports over the full period for high waves from the east. Results for high waves from the south and west are similar (see Appendix G.2). Sediment transports along the shoreline and along Maplewood Mudflats have increased compared to the tide-only situation, indicated by blue arrows. The main line of transport has shifted southwards.

Human interventions

Industrial and urban developments in the city of Vancouver have taken place since the first European settlements in 1792 and have altered the shorelines of Burrard Inlet. Examples of these interventions to the shoreline are changes in the shoreline location and loss of intertidal area. Shorelines have hardened, due to quay walls in the harbour and city center, and the placement of rip-rap armouring on beaches. Other human activities potentially influencing the sediment availability in the inlet are the upstream damming of Seymour and Capilano river, and dredging activities.

6.1. Implementation of shoreline changes in the model

The Tsleil-Waututh Nation has made an effort to reconstruct the historic shorelines from 1792, before European contact (Figure 6.1, Tsleil-Waututh Nation, 2021). These shorelines are incorporated in the model to assess the sensitivity of the sediment transport system to the changes in the shoreline that have taken place in the past two centuries.

A low-tide line and a high-tide line are available. The intertidal area (defined as the area located between the low-tide and the high-tide line) is given a fixed depth. Tidal elevations vary between 0.80 and 4.45 m. Two model runs are performed, giving intertidal areas a height of respectively 1 and 2 m above chart datum.

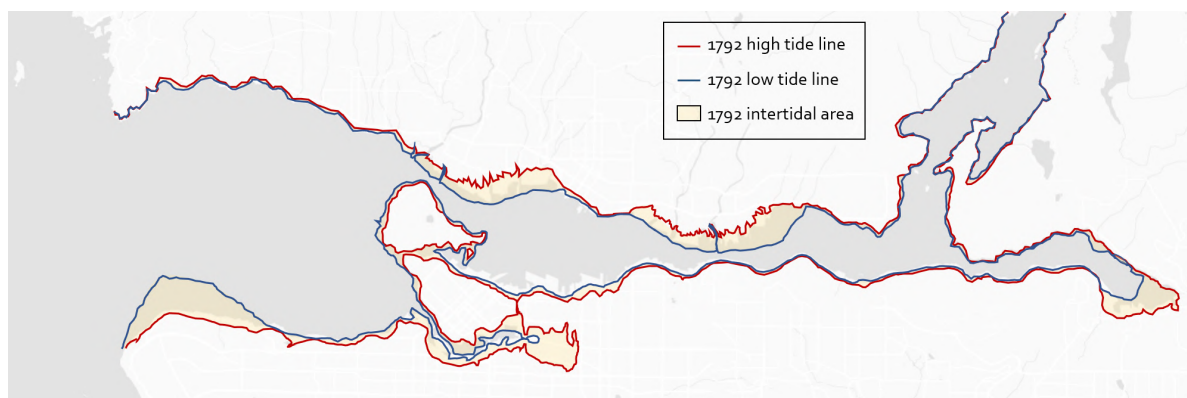


Figure 6.1: The reconstructed high-tide line and low-tide line from 1792, reconstructed by TWN (Tsleil-Waututh Nation, 2021), imposed on a present-day map of Burrard Inlet

No information about the 1792 bathymetry is available. The only historic bathymetric information is a map dating from 1893 (Stewart and Boulton, 1893). Using information from this map, it is concluded that there have been little significant depth changes between 1893 and the present. To limit unsupported speculations, the present bathymetry is used. This bathymetry is only altered in the intertidal areas: as they are located between the low tide and high tide mark, it is known that their height must be within the tidal range.

Due to restrictions imposed by the model grid, the intertidal area at the eastern end of False Creek and its historic connection to Inner Harbour is not included in the model (see Figure H.1 in Appendix H).

Tidal boundary forcing is kept constant, as no information on changes in tidal amplitude and tidal components is available. Moreover, the water level is assumed to remain unchanged. This assumption has been made to be able to isolate the effect of the shifting shoreline, without confusing these effects with effects of sea level rise. This assumption is considered valid as the relative sea level has risen in Vancouver at a rate of only 3.7 cm/century, based on records from 1910-2014 (British Columbia Ministry of Environment, 2016). This relatively low rate of sea level rise can be explained by local uplift due to eg. post-glacial rebound (Mazzotti et al., 2008).

Moreover, the river discharges are not changed in this model run. Both Capilano River and Seymour River have been dammed in the 1950s and 1960s (Armstrong, 1990, Metro Vancouver, n.d.). Accordingly, river discharges in 1792 are likely to be larger and show a stronger seasonality compared to 2019. However, discharge values of these rivers before damming are unknown.

To conclude, implementing the 1792 shorelines into the model enables us to assess the sensitivity of the hydrodynamic and sedimentary system to the shoreline changes that have taken place in the past two centuries. The results should however be treated with caution and be interpreted only as a sensitivity study, as many important factors are unknown. It is emphasized that this model isolates the effect of the shifted shorelines and increased intertidal area, and that other factors such as bathymetric changes, river discharges, tidal boundary forcing, and sea level rise are not included.

6.2. Hydrodynamic changes

This section assesses the changes in several important parameters (tidal prism, velocity, water level and sediment flux) in both First and Second Narrows in order to characterize the changes between the 1792 and the 2019 scenarios. The 1792 scenario has been modeled with intertidal area heights of both 1 m and 2 m above chart datum. Both are compared to the 2019 scenario.

Compared to 2019, the tidal prism in First Narrows is 6 to 7 % larger with the historic shorelines. In Second Narrows, the tidal prism increases by 3 to 4 %. The tidal prism is defined as the amount of water entering the inlet with the flood and ebb of the tide, which is an important metric for an estuary (Hume, 2005).

The cross-sectional area of First Narrows at present is much larger than in 1792, as dredging activities in the early 1900s have deepened and widened the channel. Due to the combination of a larger tidal prism and smaller cross-sectional area, the peak flow velocity for 1792 in First Narrows almost doubles from 1.5 to 3 m/s (an increase of 96 - 98% during flood and an increase of 79% during ebb, Figure 6.2a). In Second Narrows, this change in flow velocity is less pronounced. During ebb, peak flow velocities are 4 - 7% lower for 1792 compared to 2019. During flood, they are 5 - 6% higher (Figure 6.2b). This can partly be explained by the fact that ebb duration in Second Narrows was larger for 1792.

In First Narrows, the tidal range has remained relatively constant. However, the deeper the tide propagates through the inlet, the larger the differences become, showing a smaller tidal range for 1792. Compared to 2019, the tidal range in Second Narrows is 7.5 - 8.5 % (30 cm) smaller for the historic shorelines (Figure 6.3b).

Table 6.1: Overview of the change in tidal prism and peak velocity in First and Second Narrows, comparing the results from the 2019 model to two variants of the 1792 model, assigning a height of respectively 2 m and 1 m above chart datum to the intertidal area.

	Tidal Prism		Peak velocity			
	First Narrows	Second Narrows	First Ebb	Flood	Second Ebb	Flood
Value 1792 - 2m	372568 m ³	267820 m ³	3.11 m/s	3.10 m/s	1.96 m/s	1.86 m/s
Value 1792 - 1m	376767 m ³	270083 m ³	3.10 m/s	3.08 m/s	1.89 m/s	1.88 m/s
Value 2019	350505 m ³	259626 m ³	1.57 m/s	1.73 m/s	2.05 m/s	1.77 m/s
Difference - 2m	22063 m ³	8194 m ³	1.54 m/s	1.37 m/s	- 0.09 m/s	0.09 m/s
Difference - 1m	26262 m ³	10457 m ³	1.50 m/s	1.36 m/s	- 0.15 m/s	0.11 m/s
Difference % - 2m	6.3 %	3.2 %	98 %	79 %	-4.3 %	5.1 %
Difference % - 1m	7.5%	4.0 %	96%	79 %	-7.4 %	6.1 %

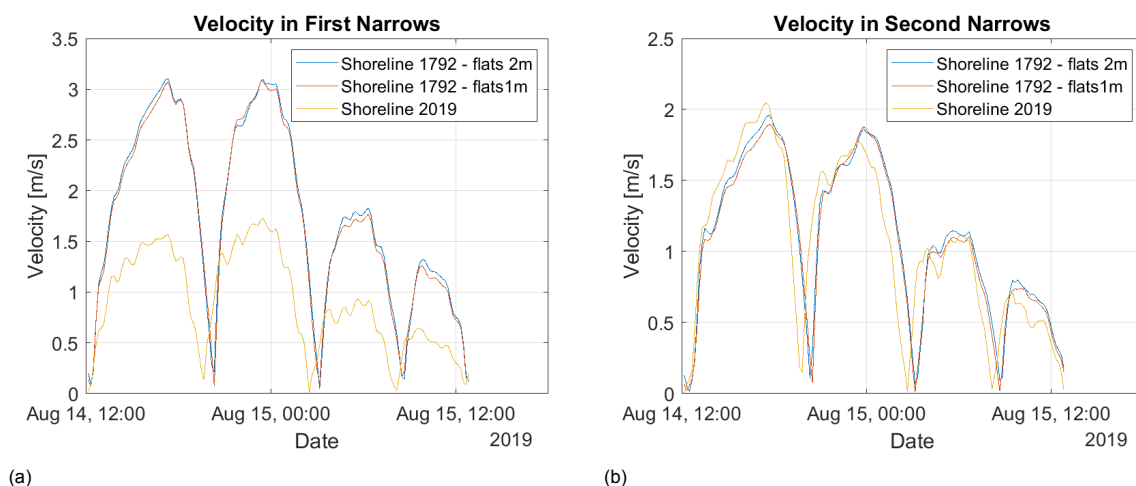


Figure 6.2: a) The velocity magnitude in First Narrows. For the 1792 shorelines, velocities in First Narrows almost double. b) Velocity magnitude in Second Narrows. Velocity changes here are less pronounced than in First Narrows

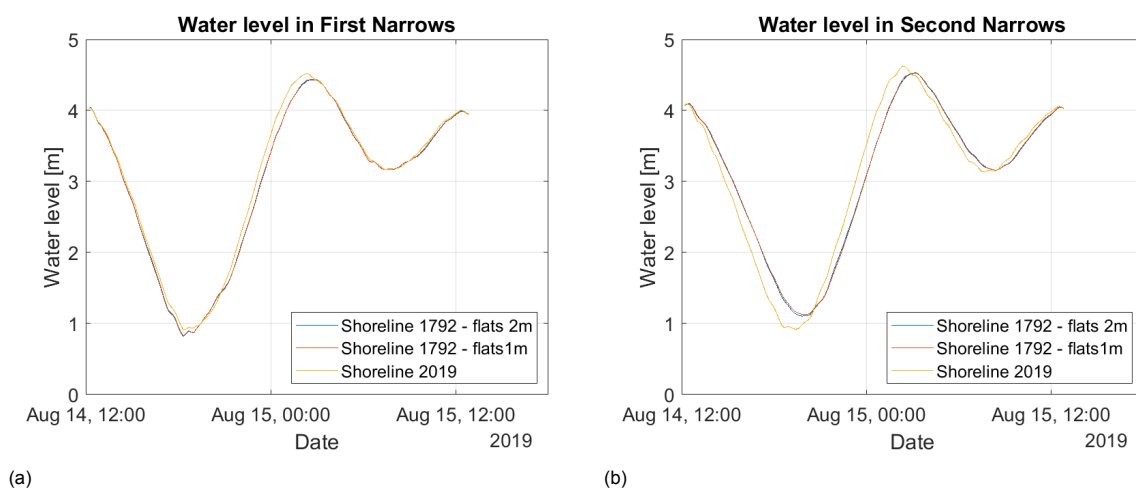


Figure 6.3: a) The water levels in First Narrows. b) Water levels in Second Narrows. For the 1792 model, the tidal range has decreased.

6.3. Changes in sediment transport

Implementing the 1792 shorelines, the sediment flux through First Narrows increases massively, by 435 to 456 % (Figure 6.4a). During ebb, the sediment flux through Second Narrows for the 1792 model is 19 - 28 % smaller than for 2019. During flood, no clear trend can be distinguished, as both 1792 scenarios differ stronger from each other than from the 2019 scenario (Figure 6.4b and Table 6.2).

In terms of transport maps, the 1792 models show similar results for the tidal flats heights of respectively 1 and 2 meters. Hence, only the results for the scenario using 1m high flats will be presented. An overview of the transport patterns for both scenarios can be found in Appendix H.

A remark should be made here that the velocity and sediment transport in the Narrows is spatially highly variable. The graphs in Figure 6.4a and 6.4b display the sediment flux at a single cross-section and are not necessarily representative for the complete behaviour of the Narrows. Viewing the changes in transport on a map (Figure 6.5) shows how the net sediment transport capacity in both First and Second Narrows has decreased since 1792 in both directions.

As a result, the main transport channel through Central Harbour and transport in front of the TWN reserve was stronger with the 1792 shorelines compared to the current shorelines. Additionally, transport directions are affected: in eddy I (Figure 6.5), the eddy curvature was less strong in 1792 and transport vectors were directed more towards the shore. On Maplewood Mudflats, transport vectors for 1792 were directed consistently towards the shore, while they are scattered into seemingly random

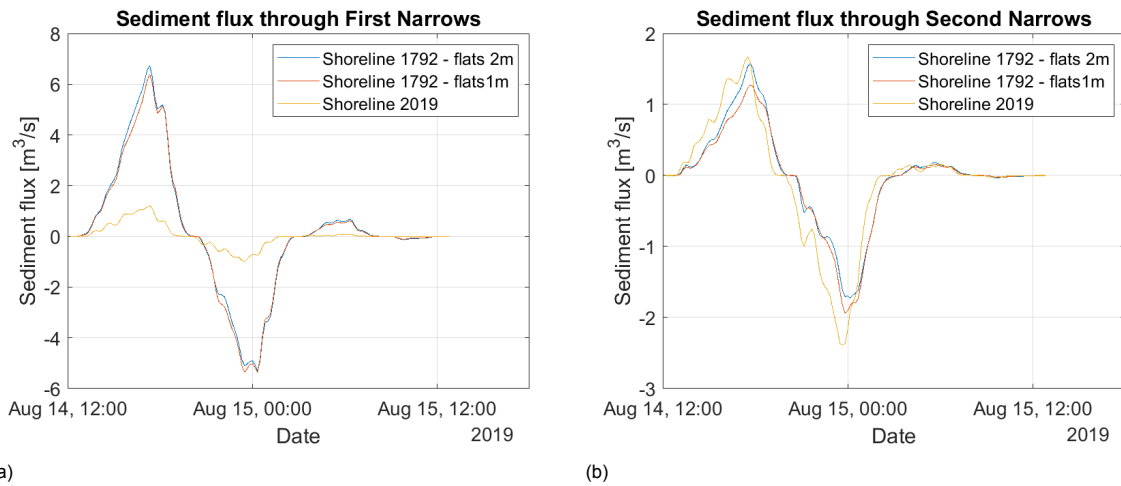


Figure 6.4: a) The sediment transport flux through First Narrows. The sediment flux in 1792 is significantly stronger than for 2019. b) Sediment transport through Second Narrows. The sediment fluxes in 1792 and 2019 do not differ significantly.

Table 6.2: Overview of the change in sediment flux and tidal range in First and Second Narrows, comparing the results from the 2019 model to two variants of the 1792 model, assigning a height of respectively 2 m and 1 m above chart datum to the intertidal area.

	Sediment flux				Tidal range	
	First <i>Ebb</i>	<i>Flood</i>	Second <i>Ebb</i>	<i>Flood</i>	First Narrows	Second Narrows
Value 1792 - 2m	6.73 m ³ /s	5.37 m ³ /s	1.58 m ³ /s	1.72 m ³ /s	3.61 m	3.42 m
Value 1792 - 1m	6.39 m ³ /s	5.31 m ³ /s	1.27 m ³ /s	1.94 m ³ /s	3.61 m	3.41 m
Value 2019	1.21 m ³ /s	0.99 m ³ /s	1.67 m ³ /s	2.39 m ³ /s	3.62 m	3.70 m
Difference - 2m	5.52 m ³ /s	4.38 m ³ /s	- 0.09 m ³ /s	- 0.67 m ³ /s	- 0.004 m	- 0.28 m
Difference - 1m	5.18 m ³ /s	4.31 m ³ /s	- 0.40 m ³ /s	- 0.45 m ³ /s	- 0.009 m	- 0.30 m
Difference % - 2m	456%	427%	- 5.4 %	- 28 %	- 0.1%	- 7.6 %
Difference % - 1m	441%	435%	- 24 %	- 19 %	- 0.2%	- 8.1%

directions in 2019.

At the eastern end of Central Harbour, transports are stronger for the 2019 scenario. Transport vectors along the eastern and western shores of Cates Park, in eddy II and northwards into Indian Arm are stronger for 2019.

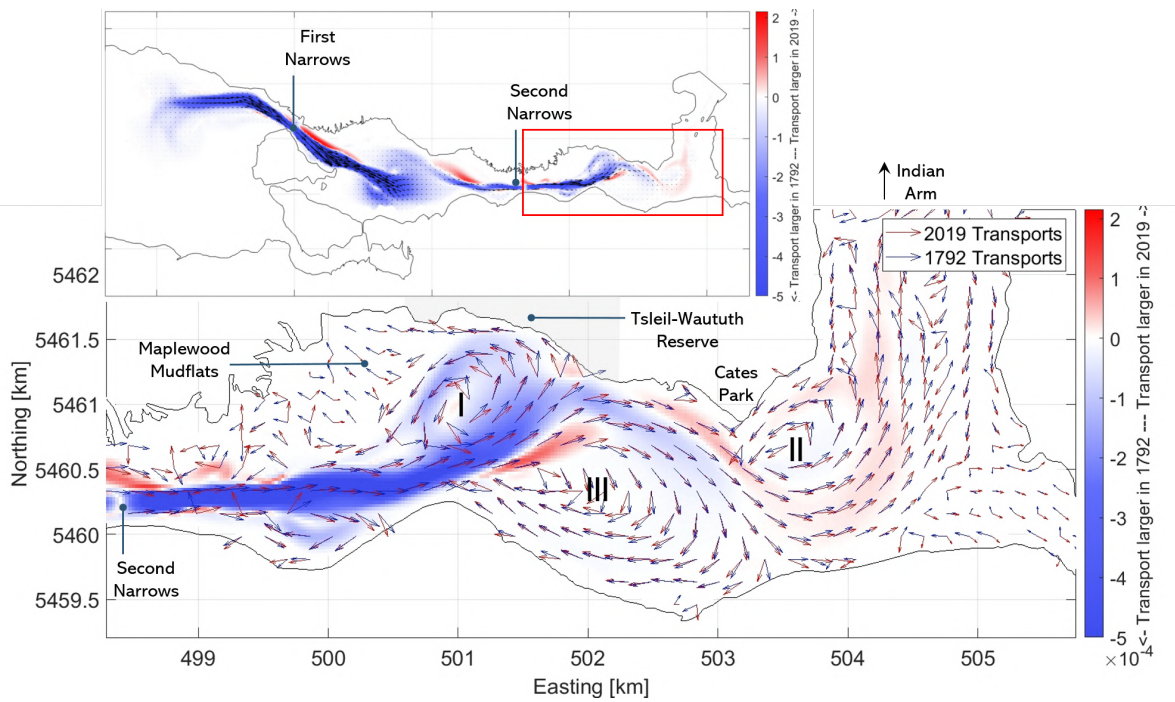


Figure 6.5: Comparison of the net transports over the full simulation period for the 1792 and 2019 shorelines. In blue areas, transport vectors were stronger in 1792. In red areas, transport vectors are stronger in 2019. Transport in First and Second Narrows has decreased in both directions. Zooming in on Central Harbour reveals the following: 1. Transports along Cates Park, in eddy II and up to Indian Arm are stronger in 2019. 2. In eddy I, in front of the TWN reserve and Maplewood Mudflats, the eddy curvature was less strong in 1792 and transport vectors in 1792 were directed more towards the shore. 3. On Maplewood Mudflats, transport vectors for 1792 were consistently directed towards the shore.

6.4. Changes in transport pathways

SedTRAILS is used to visualize the effect of these changing transport vector fields on the possible sediment pathways. The general patterns when assessing the full inlet are similar on a large scale: the basins are rather separated and net transport is directed away from the Narrows (see Section 5.2 for the explanation of this behaviour). The trajectories inside Inner and Outer Harbour show significant changes (Figure 6.6) compared to the SedTRAILS for 2019 shorelines (Figure 5.11). In Outer Harbour, a recirculation towards First Narrows opens up.

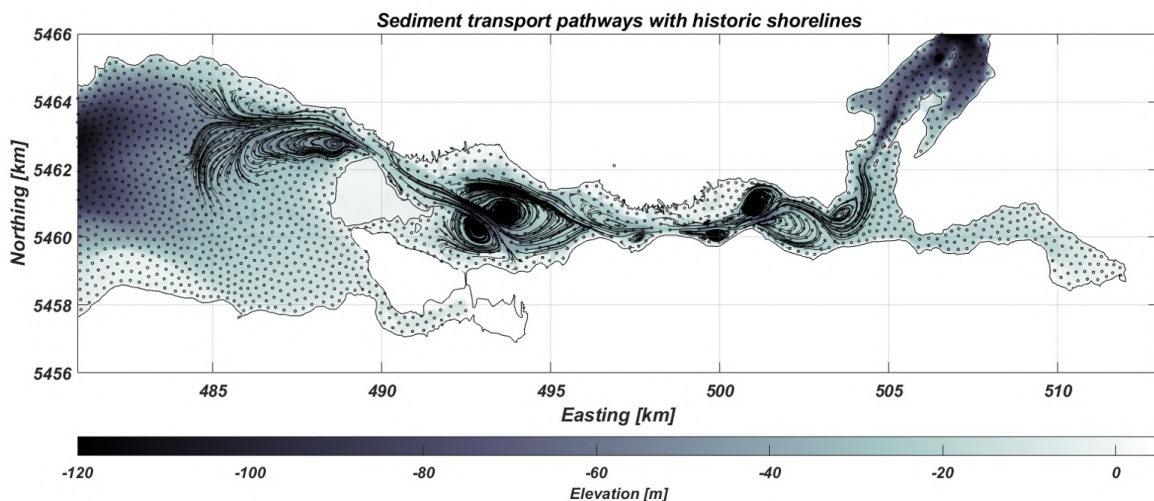


Figure 6.6: Transport pathways computed using SedTRAILS in Burrard Inlet using the 1792 shorelines.

In general, pathways located on the intertidal areas show a flood-dominated motion, directed deeper

into the inlet. This pattern is seen both in First and Second Narrows.

Zooming in on Central Harbour reveals that the changing shorelines affect the trajectories here as well. Source points were applied along the shoreline in front of the Tsleil-Waututh reserve and Cates Park, in order to predict the fate of sediment eroding from these shores. Model runs for the 1792 and 2019 shorelines are compared. To facilitate equal comparison, the source points used for both runs are identical. Other parameters affecting trajectory length, such as runtime, acceleration factor and grain size are kept constant as well. In this way, the only factor causing differences in the length and directions of the pathways is the imposed shoreline change.

Comparing the results shows that, with the 1792 shorelines, sediment is much more retained towards the shore (Figure 6.8a and 6.8b). All of the pathways initially moving to the west end either along the shoreline or at Maplewood Mudflats. By contrast, using the 2019 shorelines, much more trajectories move further away from the shores, ending up in the eddies or Indian Arm. This can be explained by the directions of the transport vectors: the curvature of eddy I is stronger for the 2019 model (Figure 6.5). After being released, sediment pathways in the 2019 model instantly move further offshore (Figure 6.7 - 1). As the trajectories move southwards, pathways for 1792 remain close to the shorelines, while 2019 pathways show a stronger curvature and bend more and more offshore (Figure 6.7 - 2). This makes them more likely to be drawn into the eddy (Figure 6.7 - 3 and 4).

A similar trend occurs for Cates Park. Applying source points to the shores of Cates Park shows that for the same conditions, more trajectories move away from the shore in the 2019 scenario (Figure 6.9a and 6.9b). Transport vectors are directed away from the shores in both the 1792 and 2019 scenario. The 2019 model run however shows stronger transports in this area, leading to more mobile pathways and more particles being moved offshore. Once particles are drawn away from the shore, they become trapped in the eddies or move towards Indian Arm. In either case, they do not return to the shore.

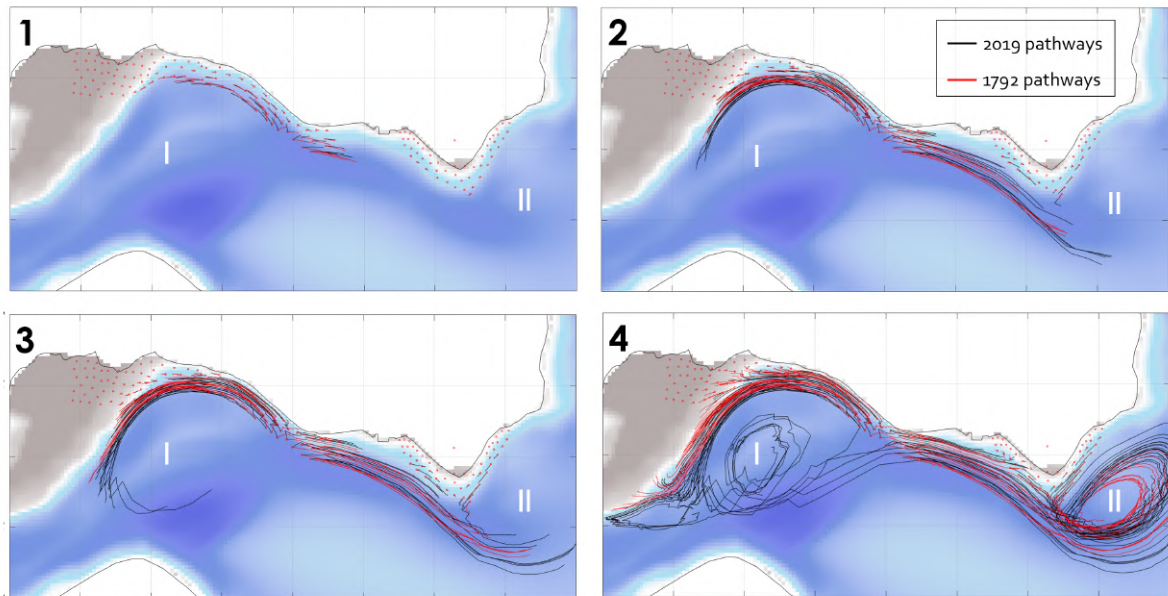


Figure 6.7: Step by step sequence showing the evolution of the sediment trajectories for the 1792 and 2019 shorelines. Pathways for the 1792 scenario are given in red, 2019 in black. 1: At the start of the trajectory, there is a slight difference in curvature, due to the different directions of the transport vectors (Figure 6.5). 2: Due to this difference in curvature, 2019 pathways bend further offshore and move faster southwards. 3: As the 2019 pathways have moved further offshore, they have a larger possibility to be drawn into the eddy. 4: The end result is that pathways for 2019 move much further offshore, while the 1792 pathways stick to the shorelines and Maplewood Mudflats.

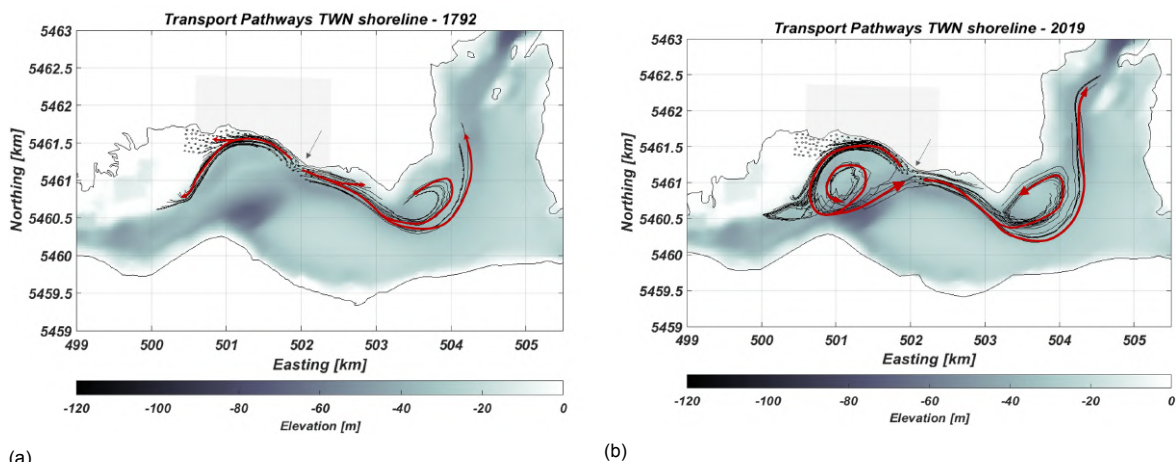


Figure 6.8: a) Trajectories originating from the TWN shoreline, 1792. b) Trajectories originating from the TWN shoreline, 2019. Trajectories tend to move further away from the shoreline. The source points, runtime, acceleration and grain size are identical for both runs.

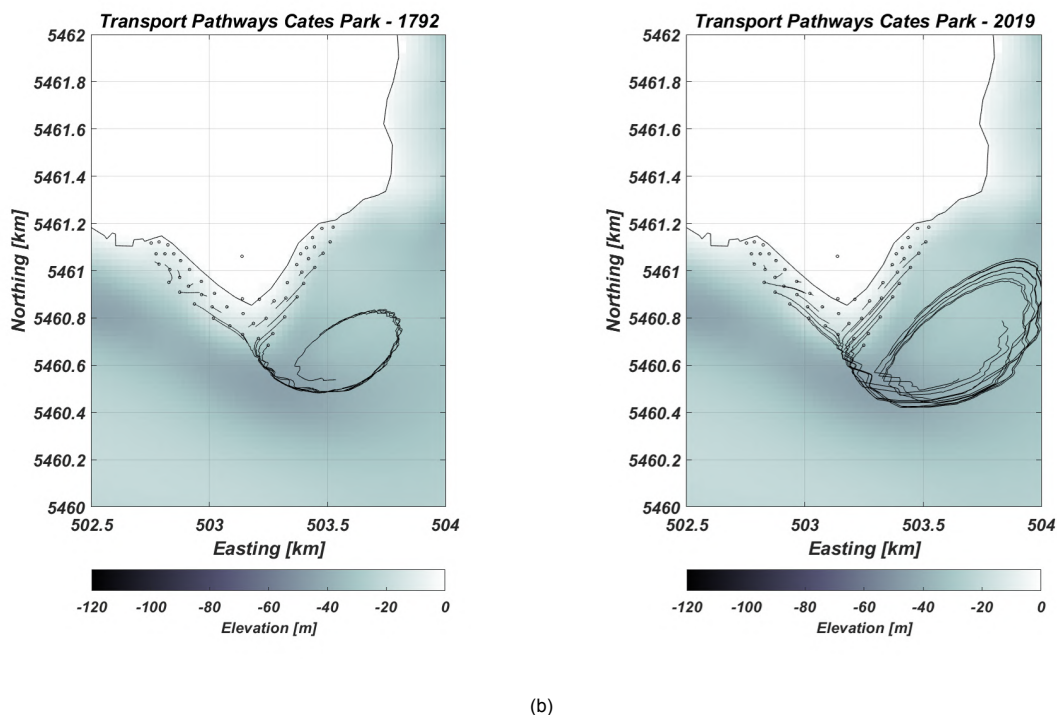


Figure 6.9: a) Trajectories originating from Cates Park, 1792. b) Trajectories originating from Cates Park, 2019. The source points, runtime, acceleration and grain size are identical for both runs. For the same source points, more trajectories move away from the shores and into the eddy for the 2019 shorelines.

Discussion

7.1. Interpretation of the results

Transport patterns in Burrard Inlet

In this research, the sediment transport was investigated using the flow field as a basis for understanding the system behaviour. It must be noted that the velocity differences in Burrard Inlet are relatively large. This causes the stronger flows to be very dominant in sediment transport. Since the velocities in most of Burrard Inlet are small (generally <0.5 m/s except in the First and Second Narrows), only the peak velocities generate sediment transport for fine sand-sized particles ($70 \mu\text{m}$).

The topography and bathymetry of Burrard Inlet, specifically the presence of the First and Second Narrows, is governing for the system behaviour. Because of the substantial flow acceleration in the Narrows, the character of the basins is completely determined by the Narrows. As a consequence, sediment transport in the northern part of Outer Harbour is dominated by the ebb flows. Transport in Central Harbour and the southern part of Indian Arm are dominated by the flood flows. The behaviour in Inner Harbour, being enclosed by the Narrows on both sides, is regulated by a combination of ebb and flood flow.

Interestingly, sediment pathways in Outer Harbour show only export of sediment and no import into the inlet. This raises the question how sediment enters the system and whether river supply is the only source of sediment into the inlet. There is, however, potential for transport from the Strait of Georgia into Burrard Inlet. Very high waves (σ 3 m) open up pathways along the shores of Outer Harbour, directed into the inlet (Figure G.20). Moreover, hydrodynamic analysis showed water motion from Outer Harbour towards First Narrows (Figure 5.5), suggesting that very fine suspended particles are able to enter the inlet.

Transport patterns in Central Harbour

The net transports in Central Harbour are the largest of all of Burrard Inlet and are governed by the transport patterns during flood. Sediment enters Central Harbour via Second Narrows, where it is transported by high velocities. The main 'pathway' for this sediment meanders through the basin and connects to the shore at the eastern end of the TWN reserve. Here, a sediment 'divergence point' can be found, where part of the sediment moves westward along the shore into the eddy in front of Maplewood Mudflats (eddy I in Figure 7.1). The main pathway moves eastward and detaches from the shore at the southern tip of Cates Park, taking material from the shorelines and Cates Park with it to deeper waters and finally north into Indian Arm. Another eddy forms on the eastern side of Cates Park (eddy II).

Conceptually, Central Harbour can be presented as a channel running through the basin, surrounded by several flats (Figure 7.1). This deeper channel, where the largest flow velocities can be found, coincides exactly with the main sediment pathway described in the previous paragraph. It is possible that this channel was scoured out by the high currents from the Narrows. As the channel deepens, currents concentrate in the channel, deepening it further. There is however not enough evidence to support this statement. Depth measurements from 1893 show the depths in Central Harbour have not significantly changed since then, which means that this channel and flat structure has developed prior to 1893 (Stewart and Boulton, 1893).

This channel is flanked by shallower flats, on which velocities are lower and eddies form (eddy I, II and III in Figure 7.1). It is considered plausible that these eddies act as a sink, as the center of each eddy is relatively shallow, which could indicate deposition. The locations of the eddies correspond

to areas with finer sediment composition, another indication for deposition (Harper, 2020, McLaren, 1994). Moreover, the SedTRAILS results show that sediment trajectories are rarely able to 'escape' once they enter the eddy. All pathways interacting with an eddy continue to spiral inward and end in the center of the eddy. However, again no evidence of the depth changing over time due to deposition could be found (Stewart and Boulton, 1893).

Indian Arm likely acts as a sink as well. Due to the flood dominance in Central Harbour and the southern part of Indian Arm, caused by the accelerated flood flow in Second Narrows, there are sediment pathways leading into Indian Arm. No sediment pathways are observed coming out of Indian Arm. This observation is consistent with the physical setting of Indian Arm. Due to the deep waters and low flow velocities in this fjord, resuspension of sediment is unlikely.

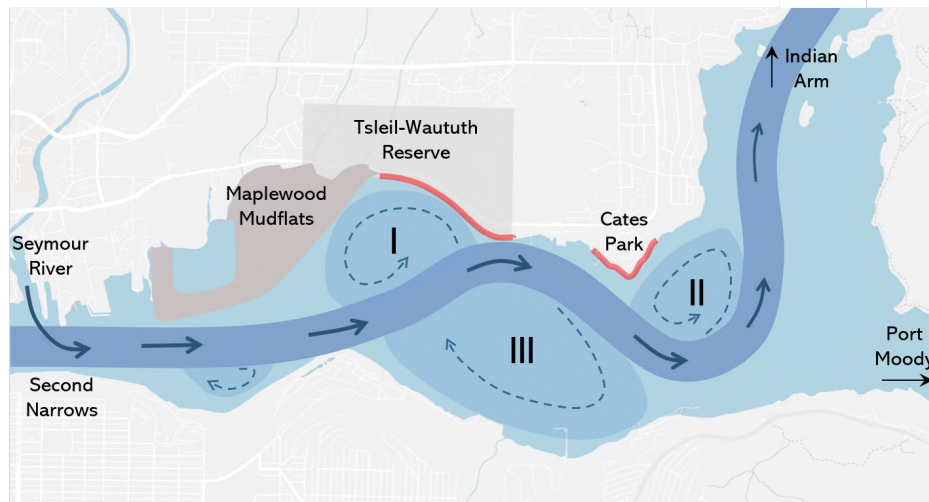


Figure 7.1: Conceptual map showing the sediment transport system of Central Harbour. The shorelines experiencing erosion are indicated in red. Sediment enters Central Harbour via the Second Narrows and generally follows the trajectory indicated in dark blue. This is the main channel, where the largest depths and highest flow velocities can be found. This channel is flanked by shallower flats on which velocities are lower and eddies form.

Effect of wind and waves

The effect of wind and waves on the sediment transports is rather limited. The transport patterns and the magnitude of the transport vectors remain largely the same compared to the tide-only reference scenario. Only in the 'sensitivity scenario' with an extreme storm, wind and waves are able to significantly alter the circulation patterns during ebb and low tide. However, during flood, when tidal currents in Central Harbour are strongest, even this scenario is not able to cause a serious deviation in the transport. This tidal domination on the flow and transport patterns is consistent with the physical characteristics of Burrard Inlet, where the tidal flows are relatively strong. Moreover, wave heights in Central Harbour are low due to its sheltered location (Beatty, 2021, Thomson, 1981).

Comparing the scenarios for strong wind and high waves, their effect on the circulation is similar. Between average winds and average waves, there is a notable difference: the effects of average winds on the circulation are minimal, with velocity deviations in the order of 0.01 m/s. The impact of average waves on the velocities is notably larger, in the order of 0.3 m/s. This difference can however not be attributed purely to the presence of waves. The wind speed for average waves was increased from 1.9 m/s to 4.0 m/s in order to obtain representative wave heights in the area of interest. Hence, the observed difference could be caused by the difference in wind speed between both 'average' scenarios. In order to isolate the effect of waves on the transport patterns, it is better to compare the scenarios for strong wind and high waves as they are truly identical except for the presence of waves.

It should be noted that this model does not resolve enhanced erosion due to the presence of waves (see Section 3.4 - Nearshore erosional processes). Waves have the potential to mobilize sediment and enhance erosion. Wave breaking exerts a force on the shoreline and can thus increase erosion rates. Moreover, the orbital motion in the water column caused by waves enhances shear stresses on

the bed and stirs up sediment. As soon as sediment is mobilized, it can be transported by currents (Bosboom and Stive, 2015). The measured wave heights by Beatty (2021) might not significantly affect the transport vectors, however, they might increase shoreline erosion, which is not captured in the model. Consequently, if the height and wave energy of waves attacking the shores increases due to increased shipping activities in Central Harbour, this can lead to increased erosion.

Moreover, under storm conditions, a larger area of Maplewood Mudflats could be submerged due to a water level set-up. This could enhance sediment transport on the intertidal areas under certain wind or wave directions, which is not included in the model (Section 3.4 - Set-up Effects).

Implications of the transport patterns for TWN

The shoreline retreat in front of the TWN reserve and Cates Park can be assessed by investigating the changes in sediment supply to and withdrawal from the area.

Combining the transport patterns observed in Central Harbour with findings of enhanced erosion can explain much of the erosion observed by the Tsleil-Waututh community. The sediment transport pathways show that as soon as shoreline sediment is mobilized, it tends to move away from the shoreline with an end destination either in one of the eddies (eddy I and II) or in Indian Arm, which can both be considered sediment sinks (Figure 7.2). This means that increased erosion leads to increased transport of sediment away from the TWN shorelines and Cates Park. This sediment is lost into sediment sinks and cannot supply the shoreline anymore.

It is plausible that in the last decades, erosion processes and sediment mobilization along these shorelines have increased. Possible causes for this are an increased wave attack on the shorelines due to shipping activities, and the loss of shoreline vegetation as described in Section 7.3.2

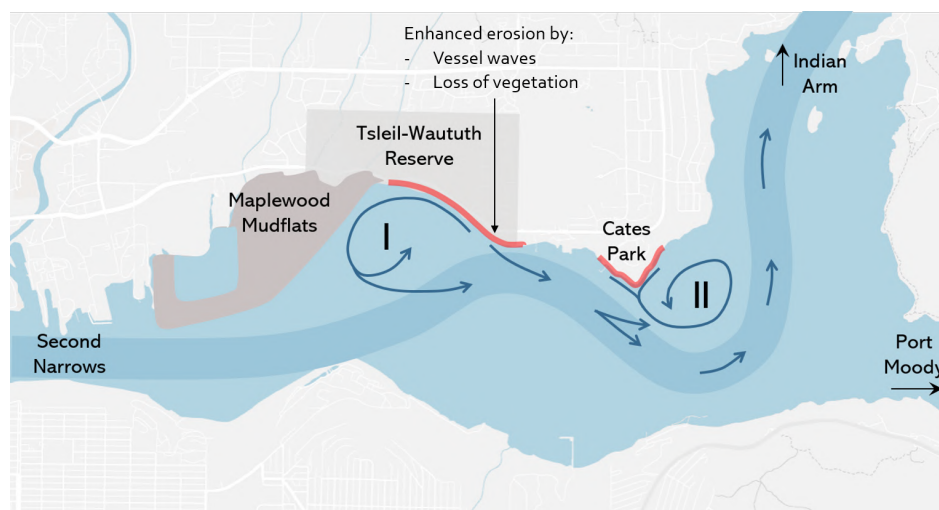


Figure 7.2: Conceptual map showing the withdrawal of sediment from eroding shorelines. The shorelines experiencing erosion are indicated in red. Sediment mobilization has increased by enhanced wave action and loss of shoreline vegetation. Sediment originating from the TWN shoreline tends to move directly into eddy I or to follow the main pathway into eddy II or up to Indian Arm. Sediment from Cates Park is transported directly into eddy II.

Adding to this enhanced erosion, sediment supply to the area has probably reduced. Visualizing the sediment pathways that are able to reach the eroding shorelines along the TWN reserve and Cates Park in a reversed SedTRAILS run showed that most sediment reaching this area enters the basin via Second Narrows, where the Seymour River delta is located (Figure 7.3). Since Seymour River has been dammed, only a fraction of the initial sediment load is likely to reach Burrard Inlet (section 7.3.2). However, further research is needed on the sediment retention rate of Seymour Falls dam to validate this statement. Moreover, as quantitative information on the sediment fluxes in Seymour River and Burrard Inlet is not available, it is difficult to estimate the significance of sediment input by Seymour River to the system.

The affected shores are areas of importance to the Tsleil-Waututh Nation. At Cates Park, an archaeological site is exposed to erosion. This location is of high cultural importance to TWN, and the archaeological deposits have both cultural and scientific significance to the Nation (TWN Communica-

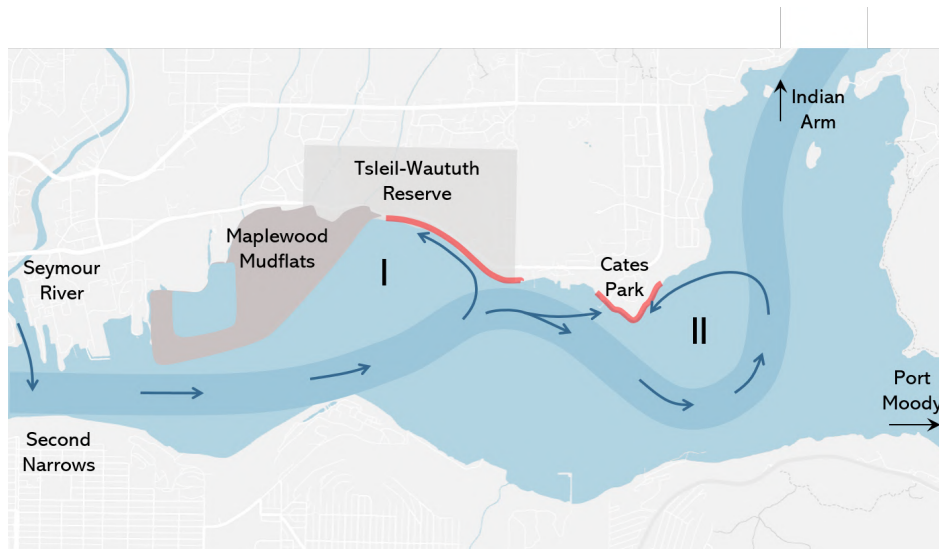


Figure 7.3: Conceptual map showing the sediment supply towards the eroding shorelines. The shorelines experiencing erosion are indicated in red. Sediment that is able to reach these areas enters Central Harbour via Second Narrows. In this way, Seymour River is able to feed these shorelines. The sediment load supplied by Seymour River has likely decreased since the river has been dammed.

tion, 2018). Shorelines of the reserve are eroding, leading to loss of land for TWN members' properties and damage to infrastructure.

7.2. Sensitivity

The modelled flow in Burrard Inlet is very stable with regard to flows in the Strait of Georgia. In the process of setting up the model, there were some initial problems with the boundary conditions, leading to unrealistically high velocities (in the order of 200 m/s) in the Strait of Georgia. The velocities in Burrard Inlet, however, were barely affected by this. The flow the inlet is driven by the water level modulation rather than the flows in the Strait of Georgia.

While water level data was available for multiple locations spread equally over the inlet, limited velocity data was available for calibration. The only two measurement stations providing velocity data are located in First and Second Narrows. Despite the advantageous locations (velocities are highest in First and Second Narrows, hence these locations are most critical for calibration), validating the modeled velocity at more measurement locations would have been valuable. Due to limited amount of calibration data, sensitivity of the flows to the used model settings is particularly important. The model has been calibrated using a range of Manning coefficients ($0.02 - 0.05 \text{ s/m}^{\frac{1}{3}}$) and a range of initial salinities (0 - 33 PSU). The largest root mean squared error for velocities in the Narrows for any combination of calibration parameters is 0.30 m/s, which amounts to roughly 15% of the peak velocity (using a peak velocity of 1.5 to 2.5 m/s in respectively First and Second Narrows). Based on these values, the sensitivity of the modeled velocities to the model parameters is considered to be within an acceptable range.

7.3. Effect of human interventions

The effects of shoreline changes on the sediment transport have been modeled. In Section 7.3.1, these results are interpreted. Apart from the shoreline changes, there have been other human interventions that have the potential to affect sediment transport (Figure 7.4), which will be evaluated in Section 7.3.2.

7.3.1. Modeled shoreline changes

Hydrodynamic changes

Due to shoreline changes, the tidal prism of Burrard Inlet has decreased over the past 2 centuries. Moreover, the tidal range has increased. This effect is stronger as the tidal wave propagates deeper into the inlet. The model shows an increase of 30 cm (7 - 8 %) in Second Narrows. A possible explanation for this is that the tidal wave was dampened by the wide and shallow intertidal area in 1792. With the loss of intertidal area, flow became less friction dominated and resonance of the tidal wave increased. Other changes to the shoreline that reduce friction in the inlet, such as the replacement of vegetated shorelines by hard, vertical structures, have not been implemented in the model. Hence, it is possible that the decrease in tidal range has been even stronger in reality than predicted by the model.

As a consequence of this increased tidal range, water levels at high tide are higher than they used to be for the same mean sea level. This could possibly explain some of the effects mentioned by Harper (2020), indicating that TWN elders observed a rise in high water levels that could not be explained by sea level rise only.

The shoreline changes have a significant effect on flows and transport patterns in Burrard Inlet. Velocity changes are in the order of 1.5 m/s in First Narrows and 0.5 m/s in the basins. These velocity alterations are significantly stronger than the effects observed for wind and waves.

The high velocities observed in First Narrows correspond with historical records. In the late 1800s and early 1900s there have been several ships grounding and sinking in First Narrows due to the strong tidal currents. In 1911, First Narrows was dredged to deepen and widen the channel, in order to permit safer passage (Armitage, 2001). Pre-dredging velocities in the First Narrows would range up to 6 knots (3 m/s) in both ebb and flood flows (Baines, 1957), corresponding very well with the peak velocities found by the model (Figure 6.2a).

Changes in sediment transport

Due to the velocity changes, the net sediment transport out of First Narrows in both directions has reduced significantly since 1792. According to the net transport maps, sediment transport out of Second Narrows decreased likewise (6.5). This decrease is however not visible in the sediment flux through the cross-section in Second Narrows (Figure 6.4b). A possible explanation for this discrepancy is the fact that the graph in Figure 6.4b only shows the flux through one cross-section, which may not be an accurate representation as the flow accelerates strongly in the Narrows and is thus highly spatially variable.

The SedTRAILS pathways indicate the consequences of the changed transport vector fields. As Figures 6.8a, 6.8b, 6.9a, and 6.9b show, the changing pathways have striking consequences for the eroding areas. It is remarkable how large the effect of subtle changes in the transport vectors is on the sediment pathways. While the transport vectors generally show the same patterns, the change in curvature that is found in eddy I (Figure 6.5) results in completely different pathways. Compared to 1792, pathways in 2019 move much further away from the shores. For the TWN shorelines, the SedTRAILS results suggest that grains eroding under the 1792 shoreline conditions would usually end up along the same shorelines or on Maplewood Mudflats. Moreover, less trajectories moving east end up in Indian Arm. For Cates Park, the same picture arises. Using the same conditions, the same source locations and the same runtime, more pathways move away from the shores now compared to 1792. These results suggest that the changing shorelines have altered the sediment transport patterns in a way that sediment that is mobilized along the vulnerable shores now has a larger tendency to move away. If the same amount of sediment would get mobilized in the 1792 and 2019 scenario, more sediment would be retained to the shorelines in the 1792 case.

It is emphasized that these results should be treated with caution, as there are many uncertainties to this model run. Since only the shorelines and depth in intertidal areas have been changed, this is not an accurate representation of Burrard Inlet in 1792. This model isolates the effect of the shifted shorelines and increased intertidal area to give an indication how they could have affected transport

patterns. Other factors such as bathymetric changes, river discharges, tidal boundary forcing, and sea level rise are not included.

7.3.2. Other human interventions

Many of the changes that have been made to Burrard Inlet cannot be captured in a model at this moment, due to a lack of available data on the historic situations. An overview of the changes that have the potential to affect sediment transport is given in Figure 7.4. These will be evaluated qualitatively in this section.

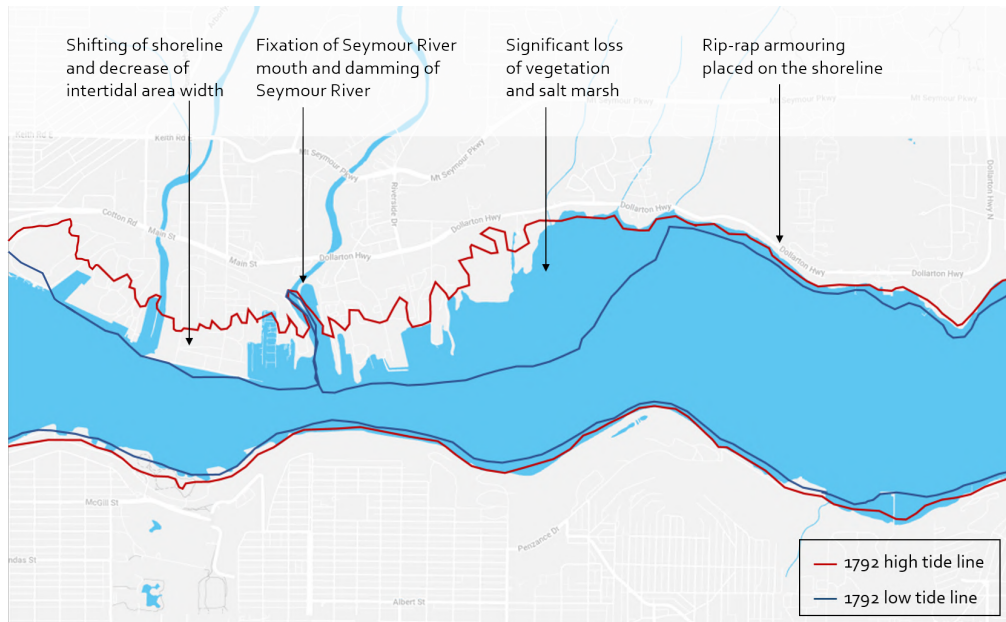


Figure 7.4: Map of Second Narrows and Central Harbour giving an overview of the most important human interventions that have a potential to affect sediment transport.

Shifting of the shoreline and decrease of intertidal area width

The results of the landward shift of the shoreline are captured in the model results as described above. Important consequences are the increase in tidal range and the changes in transport pathways.

Since 1792, the intertidal area has narrowed significantly, especially in the Narrows. These intertidal areas likely acted as wide, shallow foreshores with gentle slopes, which dampen wave heights and improve resilience of the shoreline by reducing wave attack (Battjes and Groenendijk, 2000, Penning et al., 2015). In this way, the tidal flats may have protected the shorelines from erosion. Now that the intertidal area has reduced, shorelines are more exposed to high waves and faster currents, making them more prone to erosion.

Confinement of Seymour River mouth and damming of Seymour River

Both Seymour River and Capilano River have been dammed in the 1950s and 1960s (Armstrong, 1990, Metro Vancouver, n.d.), which has likely substantially reduced their sediment load. A study by USGS surveying sediment loads and river morphology for 21 dams in the western United States found that sediment concentrations and suspended loads were decreased markedly for hundreds of kilometers downstream of the dams (Williams and Wolman, 1984). Other studies confirm these reduced sediment loads: comparing sediment in the Yangtze river upstream and downstream of the Three Gorges Dam showed a 77% sediment retention rate by the dam (Li et al., 2021). In the Muga river in the southern Pyrenees, sediment trapping in the reservoir even reached up to 95% (Piqué et al., 2017).

For numerous dammed rivers, coarsening and armouring of the river bed downstream of the dam and coarsening of the river delta was observed (Piqué et al., 2017, Yang et al., 2018). Moreover, river deltas were observed to undergo a change from accretion to an erosional trend (Yang et al., 2018).

The examples mentioned above are used to give a first indication to the possible effects of river damming. It should be noted that these rivers are very different from Seymour river in terms of their environmental settings, climatic conditions and discharges, and are therefore not necessarily representative of the effects of damming for Seymour river. However, these examples do show that the sediment trapping and downstream erosion and coarsening can be very substantial.

An example in a more similar environment is Elwha River in Washington, discharging into the Salish Sea. Here, a dam removal project was undertaken, removing two major dams from the river. This increased sediment fluxes by approximately two orders of magnitude. Moreover, significant shoreline accretion was observed at the river mouth (Warrick et al., 2019).

Therefore, it is likely that damming of Seymour river has contributed to the erosion and coarsening sediment composition in the river mouth and surrounding area (including Maplewood Mudflats and the shoreline in front of the TWN reserve). Before Cleveland dam (damming Capilano river) was built in the 1950s, the river deposited significant amounts of sediment into First Narrows and dredging activities were needed to keep the channel open for ship traffic (Baines, 1957). Some sources even state that "Burrard inlet would have turned into Burrard Lake" without human interventions, suggesting that the sediment discharge of Capilano river was very significant (Armstrong, 1990, Armitage, 2001). Lynn Creek and Seymour River, which both empty into Second Narrows, did not carry such large sediment loads under ordinary conditions. However, before damming, they would rise rapidly after a heavy rainfall and move everything from clay to small boulders, which would then be deposited in Second Narrows, from where it can be transported into Central Harbour (Baines, 1957).

Moreover, the river mouth has been fixed, which means that Seymour River now discharges directly into the high-current regime of Second Narrows. Maplewood Mudflats is the former delta of Seymour River. It is possible that due to confinement of the river mouth, sediment delivered by Seymour River no longer has an opportunity to slowly settle on the low-energy tidal flats but is directly washed away by the fast currents in Second Narrows.

Significant loss of vegetation and salt marsh

There has been a significant loss of shoreline and underwater vegetation along the shoreline in front of the TWN Reserve. Extensive kelp beds and eelgrass started disappearing in the late 1960s (Burrard Inlet Science Symposium, 2017). This loss of vegetation can potentially have enhanced shoreline erosion.

Kelp beds are known to dampen wave energy in shallow water and are able to substantially reduce nearshore wave heights (Løvås and Tørum, 2001, Mork, 1996). Moreover, eelgrass promotes a depositional environment and sediment retention. Eelgrasses influence local hydrodynamics as they induce drag on the flow and dampen near-bed velocities, thereby reducing shear stresses near the bed (Hansen and Reidenbach, 2012, Fonseca et al., 1982). One study observed how an estuarine environment changed from a highly depositional environment to an erosional environment after an estuary-wide loss of eelgrass. 90% of the monitored locations that had lost eelgrass experienced erosion, while locations under similar flow conditions where eelgrass was detained underwent a mean accretion (Walter et al., 2020).

The area has also experienced a reduction in salt marsh environment. Salt marshes were continuous from Seymour river to the eastern corner of Maplewood Mudflats and have been reduced to less than 1/10th of their original extent, from 43 ha to 2.4 ha (Harper, 2020). The salt marsh has been removed by industrial developments east of Seymour River and the landfill in Maplewood Conservation area (Harper, 2020). However, salt marsh vegetation is known to be useful for erosion control and effective in stabilizing eroding shorelines in many sheltered coastal areas (Knutson and Inskeep, 1982, Broome et al., 1992). Furthermore, salt marshes enhance the trapping of fine sediments by the sheltered environment they create (Christiansen et al., 2000). In this way, the loss of salt marsh might be related to the coarsening observed at Maplewood Mudflats. This is, however, a complex process where many factors can play a role, and needs further research.

To conclude, it is very plausible that the decrease in shoreline and underwater vegetation has led to increased vulnerability of these shorelines to erosion.

7.4. Comparison to existing knowledge

The current available knowledge on the sediment transport and changes that have been observed in the inlet comes from various sources. Several studies have been done on the hydraulic (Genwest Systems Inc., 2019) and sedimentary (McLaren, 1994, Harper, 2020) behaviour of Burrard Inlet. Moreover, there is ample knowledge within the Tseil-Waututh community on the changes that have been observed in the area (Harper, 2020, Burrard Inlet Science Symposium, 2017, Tseil-Waututh Nation Climate Summit, 2018). The results and interpretations from this study are reflected on by making a comparison to this information.

7.4.1. Full inlet/larger scale patterns

Sediment transport study by Mc Laren

The transport patterns found in this study are compared to those found in the study by McLaren (1994) that is described in Section 2.4.1.

Both studies predict transport out of First Narrows into Outer Harbour, along the northern shore (Figure 7.5, number 1). In Inner Harbour (number 2), the results between the studies differ. This study predicts two eddies in Inner Harbour, one counterclockwise that is associated with the ebb currents from Second Narrows and one clockwise, forced by the flood currents from First Narrows. The study by Mc Laren, however, predicts one counterclockwise eddy in the central/south side of the basin and westward directed transport on the northern side. Remarkably, this pattern described by Mc Laren matches more the patterns observed in Inner Harbour that are found in the sensitivity runs for different tidal cycles (Figure B.5 and B.6). As the morphological tide in this study was chosen to obtain representative transport for Central Harbour and did not focus on Inner Harbour (see Section 3.4 - Input reduction techniques), it is well possible that the results found by Mc Laren are more representative for Inner Harbour.

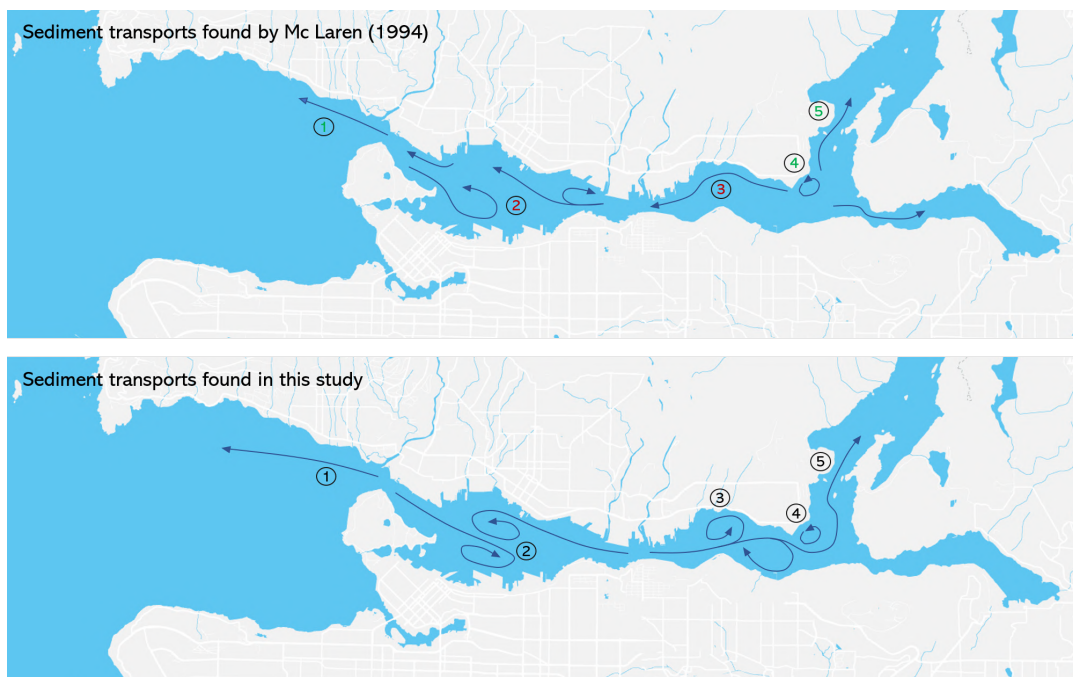


Figure 7.5: Upper map: general sediment transport trends as found by McLaren 1994. The different sections of Burrard Inlet are labeled using the numbers 1 to 5. Green numbers are used in areas where the transport patterns match reasonably well, while red numbers are used in areas where both transport studies give contradicting results. Bottom map: the sediment transport trends as found in this study using SedTRAILS, based on Figure 5.11.

In the area of interest, Central Harbour, the transport patterns differ significantly (Figure 7.5, number 3). Mc Laren predicts a continuous westward transport from Central Harbour towards Second Narrows. Moreover, the Mc Laren findings indicate deposition everywhere in Central Harbour (McLaren, 1994). Statements by the TWN about ongoing erosion contradict these findings. It should be noted here that Mc Laren was the least confident about the results found in Central Harbour. Correlations in the grain

size trends along these transport lines were weak and the net accretion trend was uncertain. The Mc Laren results indicating depositional transport towards Second Narrows are highly unlikely, given the strong net transport vectors moving out of Second Narrows towards Central Harbour.

Both studies indicate the presence of a counterclockwise eddy east of Cates Park (4). Moreover, there is agreement in the northwards transport predicted up to Indian Arm (5). Mc Laren indicates that the transport towards Indian Arm is depositional, which is in agreement with our findings of Indian Arm acting as a sink (McLaren, 1994). In Indian Arm and Port Moody, high contaminant concentrations were found in the sediment samples, confirming that primarily deposition and little resuspension takes place in these areas.

The method used by Mc Laren has been evaluated by LeRoux and Rojas (2007). They have pointed out that the method has an implicit subjectiveness because the lines of transport have been chosen by the researcher. When comparing the method used by Mc Laren to other methods on a test site, the method showed the same general macro-scale patterns as other, more refined methods. However, because the Mc Laren method did not pick up local transports and seasonal variations, they found the method to be less refined than other methods (LeRoux and Rojas, 2007).

There are several other drawbacks to determining transport patterns based on the grain size of bottom sediment samples. Transport trends can vary in time and the depth with which samples penetrate into the bottom determines which time period the sample represents. To be able to get relevant results for current trends, samples should be taken as shallow as possible, preferably from the top 1 cm. If the sample is taken too deep, the obtained trends are more of an indication of past circumstances than of the present. Moreover, the presence of bedforms can influence the results. Sediment samples taken from the crest of a ripple are generally finer than those taken from a trough, which can lead to trends that are more related to the bed structure than to the actual transport direction (LeRoux and Rojas, 2007).

Oil spill models

The study executed by Genwest Systems Inc. (2019) to simulate an oil spill in Burrard Inlet is the only other study using Lagrangian particle tracking to visualize transport of matter (be it sediment or oil) through the inlet.

The general transport directions and patterns correspond. The strong export from the Narrows into the basins is captured in both studies, as well as the circulation patterns in the basins. Both studies predict that Indian Arm acts as a sink. The shape of the main transport pathway found in this study (Figure 7.1) corresponds with the pathways for oil particles.

The spilled oil tracks show much more motion and larger connectedness compared to the sediment transport pathways and resemble more the hydrodynamic pathways that were computed in Section 5.1.1 (Figure 5.5). The circulation in Inner Harbour is different as well. Moreover, the study predicts oil particles moving into Port Moody, whereas Port Moody was found to be relatively detached in this study. Genwest Systems Inc. (2019) found that wind had a significant role in the pathways and final locations of the oil particles.

These different trends can partly be explained by the different focus of the studies. This study describes the motion of sediment particles, which are distributed over the depth. As a 2D model was used, the depth-averaged velocity is used to model the transport of sediment. By contrast, oil particles float on the water surface and are thus transported by surface currents, which can differ from the depth-averaged currents and are often stronger influenced by the wind, which can be the reason why the influence of wind was found to be stronger than in this study. Additionally, oil particles themselves are assumed to interact with wind (Genwest Systems Inc., 2019). As oil particles do not have a settling velocity, their transport is not dependent on how energetic the flow regime is, which explains the longer pathways and larger connectedness.

7.4.2. Central Harbour

The study done by Harper (2020) focuses specifically on the sediment transport patterns in Central Harbour, as described in Section 2.4.2. The findings by Harper (2020) support the model results and interpretations about sediment transport. The high-energy zone found by Harper (2020) correspond almost perfectly with the area in which the Delft3D FM model predicts the highest velocities and where the main line of sediment transport is found (Figure 7.6). At moderate- and low-energy zones described by Harper (2020), the model predicts eddies and lower flow velocities. Additionally, the fact that the

eddies have been classified as low-energy zones with finer sediment compositions supports the theory that deposition takes place in the eddies.

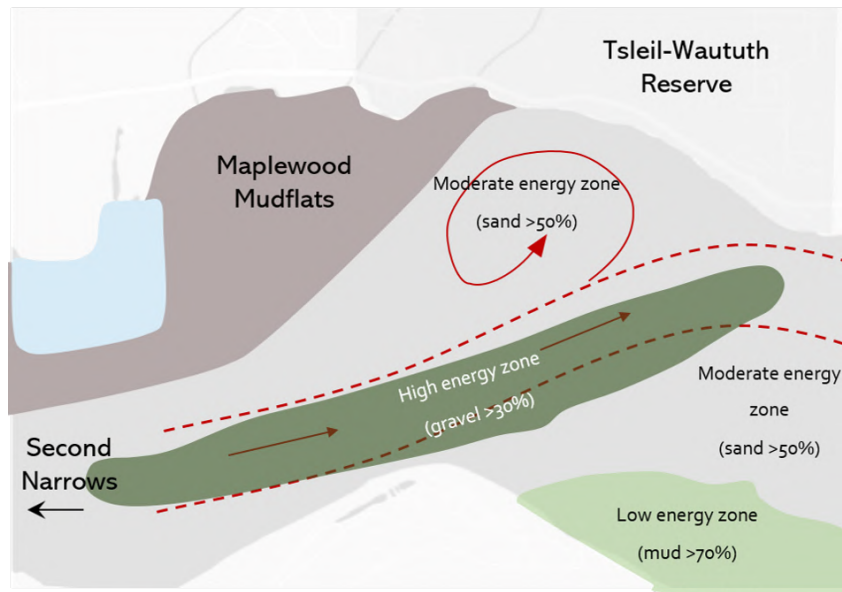


Figure 7.6: Map indicating the high-energy and moderate/low-energy zones constructed by Harper (2020). The main sediment pathways in Central Harbour as established in this study are indicated in red.

The sediment transport directions found by Harper (2020) correspond to the net transport vectors and SedTRAILS results (Figure 7.7). The flow circulation in front of TWN is captured in Harper's results, as well as eastwards flow at the 'divergence point'.

The study conducted by Harper (2020) is detailed and thorough, relating shoreline and seabed characteristics with the goal of resolving sediment transport patterns focused specifically on Central Harbour and the TWN shoreline. The good match between the results of these studies gives confidence in our model performance in the area of interest.

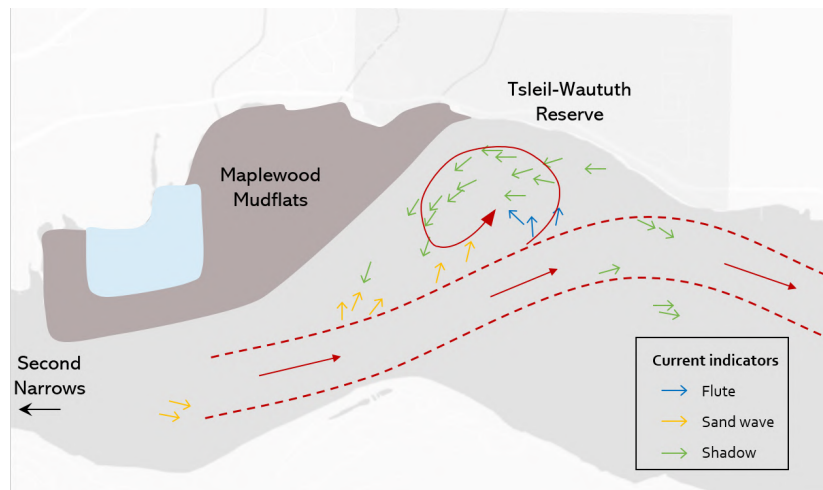
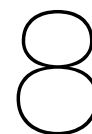


Figure 7.7: Map indicating the sediment transport directions along the bed as constructed by Harper (2020). The main sediment pathways in Central Harbour as established in this study are indicated in red.



Conclusion and recommendations

The aim of this research was to estimate the sediment transport pathways through Burrard Inlet and get more insight in the processes responsible for sediment transport in the inlet. In order to do this, the system behaviour was assessed in terms of flows and sediment transport. Transport pathways have been visualized using SedTRAILS. The importance of various hydrodynamic processes such as tide, wind, and waves was compared and the effect of shoreline alterations was investigated. Special attention was given to Central Harbour, where the TWN community is located and shoreline erosion has been observed.

8.1. Conclusion

The main research question was as follows:

What are the sediment transport pathways into, within and out of Burrard Inlet and what is the role of the different hydrodynamic processes and of human interventions on these patterns?

In order to answer this research question, a numerical model of the area has been developed, simulating hydrodynamics and sediment transport in the inlet. This depth-integrated, morphostatic Delft3D FM model with a curvilinear grid was developed for the Strait of Georgia. This model was nested inside a larger model covering the Puget Sound area and the Salish Sea, to obtain the boundary conditions. At the seaward boundaries, a water level time series was prescribed and river forcing was included in the model. A spatially uniform wind field was imposed on the model domain using five wind scenarios, covering representative and extreme wind situations. Seven wave scenarios were implemented by coupling the Delft3D FM model to the spectral wave model SWAN.

The model was calibrated and validated using all available water level and velocity data and has shown to perform well, with velocity deviations in the order of 5% in the Narrows. Water levels show a root mean squared error of less than 10 cm for all measurement locations, demonstrating that the propagation of mean water level and variance throughout the inlet has been simulated correctly.

Using this model, the sub-questions have been answered:

1. What are the sediment transport pathways under present-day average conditions?

Flows in Burrard Inlet are governed by the topography and bathymetry. The presence of First and Second Narrows dominates the flow, and correspondingly the sediment transport patterns, due to the strong accelerations in these constricted areas.

As a result of the presence of Second Narrows, sediment transport patterns in Central Harbour are determined by the flood flows. Very little transport occurs in Central Harbour during ebb. During flood, the strongest transports in Central Harbour are concentrated in the flow channel depicted in Figure 7.1. Adjacent to this channel, eddies form in shallower areas with lower velocities.

As soon as sediment from the TWN shorelines and Cates Park is mobilized, it tends to move away from the shoreline with an end destination either in one of the eddies or in Indian Arm, which can both be considered as sediment sinks (Figure 7.2). Thus, the eroding sediment generally does not deposit along these shorelines but is lost into sediment sinks.

2. What are the sources of sediment entering Burrard Inlet and how do they redistribute within the inlet?

The rivers discharging into Burrard Inlet (Capilano River, Seymour River and Lynn Creek) have the potential to feed the basins with sediment. From the transport pathways, it follows that Capilano River will mostly feed Outer Harbour (Figure 5.15). Material from Lynn Creek circulates along the northern shores of Second Narrows and eventually moves into Inner Harbour. Finally, Central Harbour is supplied with sediment by Seymour River.

Performing a reverse SedTRAILS analysis showed that material reaching the eroding shorelines along the TWN reserve and Cates Park originates from Second Narrows, where the mouth of Seymour River is located (Figure 7.3). Therefore, Seymour River is an important source to these shorelines. Damming of Seymour River in the 1950s has likely reduced the sediment supply to Central Harbour and the eroding shorelines specifically.

Transport pathways for sediments originating from the Fraser River delta have been investigated. However, the results are not conclusive about whether this transport is possible. Further research on the behaviour of sediment in the Fraser river delta and the connection between Fraser delta and Burrard Inlet is needed. The results do show that waves play an important role in enabling this sediment transport (Figure 5.16b).

3. What is the role of tidal currents, wind, and wind waves on the transport pathways?

The flow in Burrard Inlet is strongly tide-dominated. The effect of wind and waves on the transport patterns (direction, strength and overall pathways) is very limited. However, waves have the potential to increase the transport capacity along the vulnerable shorelines.

Moreover, waves may increase erosional processes on the shoreline. These nearshore processes were not well resolved by the model. However, this increased erosion may have severe consequences when combined with the transport pathways in Central Harbour. Sediment that is mobilized along the vulnerable shores tends to quickly move away from the shoreline (see research question 1). Therefore, increased erosion due to waves leads to increased transport away from the shoreline.

4. What is the effect and sensitivity of the shoreline alterations that have taken place in the last two centuries on the transport patterns?

Since first European contact in 1792, the shoreline of Burrard Inlet has changed at various locations, due to industrial and urban developments, and dredging activities. At several locations, the inlet has been narrowed and intertidal area was lost.

A model run was performed implementing the shorelines from 1792 to assess the effect of these shoreline changes on the transport pathways. The results of this scenario should however be treated with caution, as there are many uncertainties to the 1792 scenario. It is emphasized that this model isolates the effect of the shifted shorelines and increased intertidal area, and that other factors such as bathymetric changes, the effect of river damming, changes in tidal boundary forcing, and sea level rise are not included.

As a result of the shoreline changes, the tidal prism in Burrard Inlet (measured by the amount of water entering and leaving through First Narrows at each tide) has decreased and the tidal range has increased. Dredging operations in the early 1900s have widened the channel at First Narrows, decreasing the peak flow velocities from 3 m/s to 1.5 m/s. The net sediment transport field directed out of the Narrows was stronger for both Narrows in 1792 (Figure 6.5).

Investigating the transport pathways of sediment originating from the eroding shorelines along the TWN reserve and Cates Park shows that in 1792, material mobilized along these banks was more likely to be re-deposited there when compared to present-day shorelines (Figures 6.8a and 6.9a). Running the model with the 1792 shorelines showed more sediment trajectories ending along the TWN reserve shorelines and at Maplewood Mudflats with fewer pathways terminating in deeper waters, thus feeding the shoreline, rather than losing sediment to sink locations.

Other changes to Burrard Inlet that possibly affected sediment transport are the damming of Seymour River, increased shipping activities, loss of intertidal area, and the removal of vegetation. Due to these changes, sediment supply to the vulnerable shorelines has likely decreased after Seymour river was dammed. Moreover, erosion and sediment mobilization has potentially increased because of the disappearing vegetation, intertidal area loss, and increased wave energy due to shipping activities.

8.2. Recommendations

This study has estimated the sediment transport pathways through the inlet and obtained more insight in the processes responsible for transport in Burrard Inlet. This can be seen as a first step towards the design and evaluation of effective measures to prevent further erosion. The recommendations for further research are organized into four categories: 1) A description of which data would be valuable to collect. 2) Possible improvements to the model. 3) An overview of how the existing model can be applied to gain more information. 4) Suggestions of which measures to counteract erosion could be investigated.

8.2.1. Data collection

Gathering additional data in Burrard Inlet would help to further calibrate and verify the model, and to be able to use the model to obtain more information, such as to quantify sediment transports. The most urgent data needs are described in this section.

Shoreline monitoring

One of the difficulties in this study was the lack of knowledge on the exact intensity and locations of the erosion problems.

In Cates Park, locations of erosion are relatively well documented, including photographs of eroding sites (TWN Communication, 2018). For the shoreline in front of the Tsleil-Waututh reserve, there are mostly spoken accounts of erosion (Tsleil-Waututh Nation Climate Summit, 2018, Harper, 2020). It is unclear which locations are most vulnerable and erosion rates are largely unknown. At Maplewood Mudflats, contradictory accounts are even heard on whether erosion or accretion occurs (Burrard Inlet Science Symposium, 2017). This makes it difficult to verify the behaviour observed in the model.

As the Tsleil-Waututh Nation is looking to understand the processes leading to erosion and to design solutions to combat this erosion, having a clear overview of the locations and rates of erosion is an essential first step. A suggestion would be to perform regular GPS measurements of the cross-sectional profile at strategic locations along the shoreline, or aerial LiDAR surveys to cover the entire shoreline in detail. In this way, erosion rates can be determined and vulnerable locations can be identified. Adding to regular measurements, performing extra measurements before and after storm events would give valuable information on whether the erosion observed can be attributed mostly to storm events or whether it is more of a gradual process.

Moreover, the TWN should bundle all existing knowledge on the erosion problems and sediment transport patterns in Burrard Inlet. For further research, it is valuable to have a comprehensive overview to be able to better target future work and avoid doing double work.

Sediment load of rivers

This study showed that there are sediment pathways from the mouths of Capilano River, Seymour River and Lynn Creek into Burrard Inlet. However, no data was available on the amount and grain size of the sediment provided by these rivers. Hence, the importance of these rivers as sediment sources to the system could not be determined. An indication of their contribution could be given by comparing the sediment load of these rivers to the total amounts of sediment in the system.

Studies on other dammed rivers showed that damming can significantly reduce the sediment load of a river (Li et al., 2021, Piqué et al., 2017). Moreover, river damming can lead to severe erosion and coarsening of the river delta (Piqué et al., 2017, Yang et al., 2018). In order to further assess the influence of human interventions, it would be useful to obtain an estimate of the river sediment load before and after damming for Capilano River (Cleveland Dam, built in the 1950s (Armstrong, 1990)) and Seymour River (Seymour Falls Dam, built 1959-1961 (Metro Vancouver, n.d.)). This would provide an estimate to what extent the sediment supply has reduced due to damming.

Sediment flux through Burrard Inlet

In general, no data is available on amounts of sediment moving through Burrard Inlet at each tidal cycle. The only information on sediment in the inlet are the sediment samples taken by Mc Laren (1994), which report the distribution of grain sizes through the inlet.

Due to the lack of data on sediment fluxes, this study could give only qualitative results on the pathways of sediment. The quantitative results on the sediment transport should be interpreted as the

maximum potential transport capacity in a case of unlimited supply. As the transport capacity in First and Second Narrows is very large, sediment transport in Burrard Inlet is likely supply-limited.

Velocity measurements

For the calibration of this model, velocity data was only available at First and Second Narrows (SalishSeaCast, 2021). Obtaining velocity data at different locations in Burrard Inlet would be valuable in further calibrating and validating the model. Ideally, this velocity data would be collected at strategic points within the basins and not only along the shorelines, as velocities directly along the shorelines are usually very low.

Moreover, in case a 3D model will be developed, velocity measurements over a range of depths would be needed in order to accurately calibrate this model.

Wind and wave data

At this moment, only wind data at Point Atkinson and the TWN reserve is available in Burrard Inlet (Government of Canada, 2021b, Beatty, 2021). A uniform wind field based on the wind conditions as measured in front of the TWN reserve (Beatty, 2021) is applied in the model simulations. As Central Harbour is much more sheltered than the outer parts of Burrard Inlet and the Strait of Georgia, this wind field is known to be incorrect for the largest part of the model domain. In order to obtain a better approximation of the spatial wind field, wind data at various locations inside Burrard Inlet would be needed.

Supposing the wave-driven erosion will be studied in more detail (eg. using a detailed model to resolve nearshore processes), it would be valuable to gather wave data at a range of water depths in front of the shore, to gather data on the wave evolution as waves approach the shore.

8.2.2. Model improvements

Several assumptions and simplifications are made in the model used in this study. This section describes possible improvements to the model, and why these improvements would be valuable.

Wave-driven erosion

The Tsleil-Waututh Nation is particularly interested in the contribution of vessel waves in the observed shoreline erosion. This study investigated the effect of waves on the transport pathways. However, the model did not resolve erosional processes due to waves. Moreover, vessel waves were not specifically included in the model formulations and no distinction was made between vessel waves and wind waves for the transport pathways. Further research should be done on the role of the vessel waves on the shoreline erosion, e.g. using a more detailed model focussing specifically on Central Harbour. This can for example be done using XBeach: a recent study was able to successfully simulate ship waves using Xbeach, showing good agreement for primary waves (which is often the main concern regarding shoreline erosion) and simulating the overall secondary wave field pattern (Almström et al., 2021).

3D model

Due to the interaction of freshwater supplied by rivers and salty water penetrating the inlet in Outer Harbour, a weak estuarine circulation is set up in Burrard Inlet. Furthermore, the deep water exchange between Burrard Inlet and Indian Arm is driven by fluctuations in the vertical density structure (deYoung and Pond, 1988, Stacey et al., 2002). As a depth-integrated model is used for this study, these effects are not included. Even though it is assumed that tidal currents dominate the flow patterns, the exact role and importance of these density-driven effects on the vertical flow structure is yet unknown (Wu et al., 2019, Stacey, 2005). Further research into the importance of these effects would be valuable. Provided the vertical density structure has a significant effect on flow and transport rates, a 3D model could be set up to model the influence on the sediment transport pathways. This comes with the challenge that very little information is available to verify a 3D model. In order to validate such a model, in-situ velocity, salinity, and temperature measurements over a range of depths should be carried out.

Using a 3D model enables to assess the effect of changing river discharges more accurately, as the river discharge influences salinity and density gradients in the inlet. Possible use of this would be to compare the current situation to a higher or more variable discharge that may have been present before damming, or to assess the sensitivity the flow to changes in the river discharge.

Investigate transports in the Fraser Delta

The development of a 3D model could aid in further understanding possible sediment transports from the Fraser delta into Burrard Inlet. The results of this research are not conclusive about whether sediment supplied by Fraser river is able to enter Burrard Inlet. Some evidence suggest that this might be possible: an aerial picture taken of the Fraser river delta after severe flooding in the upstream catchment area, causing massive sediment discharge, shows that the sediment plume is able to penetrate at least into Outer Harbour (Figure F.2, ADAM platform, 2021). Moreover, the SedTRAILS pathways for hydrodynamics in the Fraser delta show possible transport of the finest cohesive fractions into Burrard Inlet as well (Figure F.1). More research could increase the understanding of Fraser delta and the potential pathways from Fraser delta into Burrard Inlet. Moreover, research should be done to the conditions that open up these pathways, such as certain wind or wave directions and the Fraser discharge.

Fraser river has a high freshwater discharge and buoyancy effects will likely play a role in the dynamics of the sediment plume in the Strait of Georgia. Thus, a 3D model might be needed to accurately resolve these processes.

In case further research demonstrates that Fraser river sediments are able to reach Burrard Inlet, it should be investigated how the sediment discharge of Fraser river has changed over the years, e.g. due to damming in the upstream catchment area. In case Fraser river contributes to a significant amount to Burrard Inlet's sediment budget, changes in the Fraser river sediment supply could also have affected Burrard Inlet.

8.2.3. Application of the existing model

In this study, a depth-averaged Delft3D-FM model has been developed and calibrated. Apart from the results generated in this research, the model can be applied in the future to answer a range of other questions concerning flow and sediment transport in Burrard Inlet.

Effect of sea level rise

The Delft3D FM model that has been built for this study can be used to gather more information on how the system will respond to future changes. By increasing the water levels in the model's boundary forcing, the effect of sea level rise to the sediment transport patterns can be observed.

Influence of grain size

A variety of grain sizes is present in Burrard Inlet, ranging from very fine mud to coarse gravel and cobblestones (McLaren, 1994, McLaren, 1995). Each of those grain sizes has a different critical velocity at which it is picked up and transported. The coarsening observed at for instance Maplewood Mudflats could potentially be explained by erosion of the finer particles. Investigating the transport pathways for a range of grain sizes could enlighten whether different grain sizes follow different pathways and are more likely to end up at a certain location.

Investigating the influence of grain size would be valuable in combination with the sediment supply and grain size distributions, as transport in Burrard Inlet is likely to be supply-limited. Sediment samples taken by McLaren (1994) show that bottom sediments are coarser in the Narrows and the main channels, while they are finer in low-energy areas such as Port Moody. These spatial distributions in grain size availability could affect the transport patterns.

Assess the impact of planned interventions

Using the model, the impact of future land-use and infrastructure projects can be investigated. Examples of these interventions are large-scale shoreline changes or large dams. Additionally, the model can be used to assess possible solutions to the current erosion problems. However, when applying the model to assess potential interventions, the model limitations should be kept in mind. For small-scale interventions (such as the placement of groynes along the shoreline), the model resolution of the current model is insufficient. Furthermore, the current depth-averaged model may not give accurate results when investigating changes in the freshwater flow, such as a changing river discharge, because density-driven effects are not taken into account. Moreover, a long spin-up time (at least 2 months) should be taken into account when altering the freshwater influx, unless a non-uniform initial salinity is applied.

8.2.4. Possible measures to counteract erosion

This research demonstrated that the current erosion problems are related to an interaction of increased erosion and decreased sediment supply with the dominant transport patterns moving sediment away from the shore. Altering the transport patterns within Burrard Inlet and Central Harbour specifically is difficult and would require large scale operations with possibly unforeseeable consequences.

The most realistic short-term mitigation approach can be found in measures to stabilize the shoreline and decrease the mobilization of sediment: if sediment is not mobilized, it can consequently not be transported away from the shore. Regarding the nature of the erosion and the sediment transports at the location, potential solutions should meet the following criteria: they should stabilize the shoreline, dampen waves, and reduce flow velocities directly along the shores and on the mudflats. In this way, a more low-energy, depositional environment can be created along the shores.

Some examples of solutions meeting these criteria are described below. It is stressed that each of these solutions should be investigated in more detail before being applied.

- **Vegetation:** The shoreline in front of the TWN reserve used to be covered with a thick and dense layer of kelp and seagrass, which has now disappeared (Burrard Inlet Science Symposium, 2017). This vegetation layer likely contributed to stabilizing the shoreline, as kelp beds and seagrasses are known to dampen waves, reduce near-bed velocities, and promote a depositional environment where sediment is retained (Mork, 1996, Hansen and Reidenbach, 2012). Moreover, the salt marsh vegetation on Maplewood Mudflats has been drastically reduced to less than 1/10th of its original extent (Harper, 2020). Salt marsh vegetation is known to be effective in stabilizing eroding shorelines in many sheltered coastal areas and trapping fine sediments (Knutson and Inskeep, 1982, Broome et al., 1992, Christiansen et al., 2000). Therefore, restoring the vegetation along the TWN shoreline and on Maplewood Mudflats has the potential to decrease the mobilization of sediment by dampening waves and flow velocities. Moreover, incoming sediments can be retained in the depositional environment created by the vegetation, which may counteract the coarsening of the beaches that has been going on. Additionally, restoring vegetations has positive effects for biodiversity and promotes a habitat for fish, which aligns with the Tsleil-Waututh Nation's goals on restoring the inlet's ecological health (Lilley et al., 2017, Tsleil-Waututh Nation, 2019)
- **(Vegetated) foreshore:** The construction of a shallow foreshore has the potential to protect the existing shoreline from erosion as the gentle slopes dampen waves reaching the shoreline (van Eekelen and Bouw, 2020, Battjes and Groenendijk, 2000). Moreover, wave energy on the beach is reduced, which leads to less sand losses (Penning et al., 2015). Additionally, planting vegetation on this shallow foreshore enhances the capacity for sediment trapping and the dampening of waves and currents. However, the effect of a shallow foreshore on the local circulation should be investigated.
- **Clam gardens:** A specific type of shallow foreshore can be found in clam gardens, which is an ancient Indigenous technique (Jackley et al., 2016). Clam gardens consist of a flat terrace at the low-tide level, with a rock wall built at its seaward end (Smith et al., 2019). The terrace is submerged at high water and dry at low water, which provides an optimal clam habitat and enables harvesting at low tide. Simultaneously, this acts as a shallow foreshore, protecting the actual shoreline and trapping sediment on the terrace (Jackley et al., 2016). Clams and other types of shellfish are able to stabilize the bed and break waves, making them suitable for erosion protection (van Eekelen and Bouw, 2020). Additional benefits include sustainable food production using ancient First Nations techniques and ecosystem improvements.

Bibliography

- ADAM platform. (2021). *Tweet by ADAM platform, showing an aerial picture of the sediment plume in the Fraser delta: "Extreme rainfall in British Columbia, Canada caused severe flooding and massive sediment discharge, as shown by #Copernicus #Sentinel2 on Nov. 16. #BCStorm #ClimateAction #ClimateEmergency #flooding*. <https://twitter.com/PlatformAdam/status/1460983971685322757>
- Alden, A. (2020). *All about sediment grain size*. <https://www.thoughtco.com/all-about-sediment-grain-size-1441194>
- Almström, B., Roelvink, D., & Larson, M. (2021). Predicting ship waves in sheltered waterways – an application of xbeach to the stockholm archipelago, sweden. *Coastal Engineering*, 170, 104026. <https://doi.org/https://doi.org/10.1016/j.coastaleng.2021.104026>
- Armitage, D. (2001). *Burrard inlet, a history*. Harbour Publishing.
- Armstrong, J. (2010). *Windstorm hammers Vancouver Island*. Retrieved July 8, 2021, from <https://www.theglobeandmail.com/news/british-columbia/windstorm-hammers-vancouver-island/article1366510/>
- Armstrong, J. (1990). *Vancouver Geology* [Edited by Charlie Roots and Chris Staargaard]. Cordilleran Section, Geological Association of Canada.
- Attard, M., Venditti, J., & Church, M. (2014). Suspended sediment transport in fraser river at mission, british columbia: New observations and comparison to historical records. *Canadian Water Resources Journal*. <https://doi.org/http://dx.doi.org/10.1080/07011784.2014.942105>
- Baines, W. D. (1957). Tidal currents in constricted inlets. *Coastal Engineering Proceedings*, 1(6), 31. <https://doi.org/10.9753/icce.v6.31>
- Battjes, J. A., & Groenendijk, H. W. (2000). Wave height distributions on shallow foreshores. *Coastal Engineering*, 40(3), 161–182. [https://doi.org/https://doi.org/10.1016/S0378-3839\(00\)00007-7](https://doi.org/https://doi.org/10.1016/S0378-3839(00)00007-7)
- BC Hydro. (2019). *Storm report: the most damaging storm in BC Hydro's history*. BC Hydro.
- Beatty, S. (2021). *Tsleil-Waututh Wave Monitoring*. MarineLabs Data Systems Inc.
- Booij, N., Ris, R., & Holthuijsen, L. (1999). A third-generation wave model for coastal regions, part 1: model description and validation. *Journal of Geophysical Research*, 104 (C4), 7649–7666.
- Bosboom, J., & Stive, M. (2015). *Coastal Dynamics 1*. Delft Academic Press.
- British Columbia Ministry of Environment. (2016). *Indicators of Climate Change for British Columbia: 2016 Update*. Ministry of Environment, British Columbia, Canada.
- Broome, S., S.M., R., & Seneca, E. (1992). In C. Burgess (Ed.), *Shoreline erosion control using marsh vegetation and low-cost structures*. Sea Grant.
- Burrard Inlet Science Symposium. (2017). *Talk: Physical Oceanography: Indigenous and Western Science Perspectives*. <https://twinsacredtrust.ca/biss-yas-videos-slides/>
- Christiansen, T., Wiberg, P., & Milligan, T. (2000). Flow and sediment transport on a tidal salt marsh surface. *Estuarine, Coastal and Shelf Science*, 50(3), 315–331. <https://doi.org/https://doi.org/10.1006/ecss.2000.0548>
- City of Vancouver. (2006). *After the Stanley Park windstorm*. Retrieved August 27, 2021, from <https://vancouver.ca/parks-recreation-culture/stanley-park-restoration.aspx>
- Coastal and Ocean Resources. (2018). *ShoreZone Habitat Mapping Summary Report for the Burrard Inlet survey area*. Coastal and Ocean Resources, prepared for Tsleil-Waututh Nation.
- Deltares. (2021). *D-Flow Flexible Mesh User Manual*. Deltares.
- deYoung, B., & Pond, S. (1988). The Deepwater Exchange Cycle in Indian Arm, British Columbia. *Estuarine Coastal and Shelf Science*, 26, 285–308.
- deYoung, B., & Pond, S. (1989). Partition of Energy Loss from the Barotropic Tide in Fjords. *Journal of Physical Oceanography*, 19, 246–252.
- Elias, E., & Pearson, S. (2020). *SedTRAILS - Sediment TRANsport visualization & Lagrangian Simulator*. Deltares.
- Fisheries and Oceans Canada. (2020). *Non-Navigational (NONNA) Bathymetric Data*. Retrieved June 15, 2021, from <https://data.chs-shc.ca/login>

- Fisheries and Oceans Canada. (2021). *Oceanic Forecast - water level observation data*. Retrieved June 15, 2021, from <https://www.tides.gc.ca/Eng/data#s2>
- Fonseca, M., Fisher, J., Ziemann, J., & Thayer, G. (1982). Influence of the seagrass, *Zostera marina* L., on current flow. *Estuarine, Coastal and Shelf Science*, 15(4), 351–364. [https://doi.org/https://doi.org/10.1016/0272-7714\(82\)90046-4](https://doi.org/https://doi.org/10.1016/0272-7714(82)90046-4)
- Genwest Systems Inc. (2019). *Oil Spill Trajectory Modeling Report in Burrard Inlet for the Trans Mountain Expansion Project*. Genwest Systems Inc.
- Government of Canada. (2021a). *Historical wave data; Halibut Bank [C46146]*. Retrieved August 27, 2021, from <https://www.meds-sdmm.dfo-mpo.gc.ca/isdm-gdsi/waves-vagues/data-donnees/data-donnees-eng.asp?medsid=C46146>
- Government of Canada. (2021b). *Historical weather and climate data; Point Atkinson*. Retrieved August 27, 2021, from https://climate.weather.gc.ca/climate_data/hourly_data_e.html
- Hansen, J., & Reidenbach, M. (2012). Wave and tidally driven flows in eelgrass beds and their effect on sediment suspension. *Marine Ecology Progress Series*, 448, 271–287. <https://doi.org/https://doi.org/10.3354/meps09225>
- Harper, J. (2020). *Coastal and Marine Processes Inner Burrard Inlet*. Coastal and Ocean Resources, prepared for Tsleil-Waututh Nation.
- Honderich, H. (2021). *Why Canada is mourning the deaths of hundreds of children*. Retrieved July 8, 2021, from <https://www.bbc.com/news/world-us-canada-57325653>
- Hume, T. M. (2005). Tidal prism. In M. L. Schwartz (Ed.), *Encyclopedia of coastal science* (pp. 981–982). Springer Netherlands. https://doi.org/10.1007/1-4020-3880-1_320
- Jackley, J., Gardner, L., Djunaedi, A., & Salomon, A. (2016). Ancient clam gardens, traditional management portfolios, and the resilience of coupled human-ocean systems. *Ecology and Society*, 21(4). <https://doi.org/https://doi.org/10.5751/ES-08747-210420>
- Knutson, P., & Inskeep, M. (1982). *Shoreline erosion control with salt marsh vegetation*. USACE Coastal Engineering Research Center.
- LeRoux, J., & Rojas, E. (2007). Sediment transport patterns determined from grain size parameters: Overview and state of the art. *Sedimentary Geology*, 202, 473–488.
- Li, S., Xu, Y. J., & Ni, M. (2021). Changes in sediment, nutrients and major ions in the world largest reservoir: Effects of damming and reservoir operation. *Journal of Cleaner Production*, 318, 128601. <https://doi.org/https://doi.org/10.1016/j.jclepro.2021.128601>
- Lilley, P., deKoning, P., Konovsky, J., & Doyle, B. (2017). *Burrard Inlet Action Plan*. Tsleil-Waututh Nation and Kerr Wood Leidal.
- Løvås, S. M., & Tørum, A. (2001). Effect of the kelp *Laminaria hyperborea* upon sand dune erosion and water particle velocities. *Coastal Engineering*, 44(1), 37–63. [https://doi.org/https://doi.org/10.1016/S0378-3839\(01\)00021-7](https://doi.org/https://doi.org/10.1016/S0378-3839(01)00021-7)
- Mazzotti, S., Jones, C., & Thomson, R. E. (2008). Relative and absolute sea level rise in western Canada and northwestern United States from a combined tide gauge-gps analysis. *Journal of Geophysical Research: Oceans*, 113(C11). <https://doi.org/https://doi.org/10.1029/2008JC004835>
- McLaren, P. (1994). *Sediment Transport in Vancouver Harbour: Implications to the Fate of Contaminated Sediments and/or Dredged Material Disposal*. GeoSea Consulting, for Burrard Inlet Environmental Action Program (BIEAP).
- McLaren, P. (1995). *The Sediment Transport Regime of Outer Burrard Inlet: Environmental Implications*. GeoSea Consulting, for Burrard Inlet Environmental Action Program (BIEAP).
- Metro Vancouver. (n.d.). *Seymour Falls Dam Factsheet*. http://www.metrovancouver.org/services/water/WaterPublications/SeymourFallsDam_Factsheet.pdf
- Morin, J. (2015). *Tsleil-Waututh Nation's History, Culture and Aboriginal Interests in Eastern Burrard Inlet*. Tsleil-Waututh Nation.
- Mork, M. (1996). Wave attenuation due to bottom vegetation. In J. Grue, B. Gjevik, & J. E. Weber (Eds.), *Waves and nonlinear processes in hydrodynamics* (pp. 371–382). Springer Netherlands. https://doi.org/10.1007/978-94-009-0253-4_30
- Nijman, R., & Swain, L. (1990). *Ambient Water Quality Objectives for Burrard Inlet Coquitlam-Pitt River Area*. Ministry of Environment, Water Management Branch, Resource Quality Section.
- Pawlowicz, R., Beardsley, B., & Lentz, S. (2002). Classical tidal harmonic analysis including error estimates in Matlab using T-Tide. *Computers Geosciences*, 28, 929–937.

- Penning, W., Steetzel, H., van Zanten, R., Fiselier, J., de Lange, H., Vuik, V., Ouwekerk, S., & van Thiel de Vries, J. (2015). Natural Foreshores as an alternative to traditional dike re-enforcements: a field pilot in the large shallow lake Markermeer, the Netherlands. *36th IAHR World Congress*.
- Piqué, G., Batalla, R., López, R., & Sabater, S. (2017). The fluvial sediment budget of a dammed river (upper muga, southern pyrenees). *Geomorphology*, 293, 211–226. <https://doi.org/https://doi.org/10.1016/j.geomorph.2017.05.018>
- SalishSeaCast. (2021). *FVCOM model data download*. Retrieved June 15, 2021, from <https://salishsea.eos.ubc.ca/erddap/info/ubcSSFVCOM-VHFR-BaroclinicR12/index.html>
- Smith, N., Lepofsky, D., Toniello, G., Holmes, K., Wilson, L., Neudorf, C., & Roberts, C. (2019). 3500 years of shellfish mariculture on the northwest coast of north america. *Plos One*. <https://doi.org/https://doi.org/10.1371/journal.pone.0211194>
- Stacey, M. (2005). Review of the Partition of Tidal Energy in Five Canadian Fjords. *Journal of Coastal Research*, 214, 731–746.
- Stacey, M., Pieters, R., & Pond, S. (2002). The simulation of Deep Water Exchange in a Fjord: Indian Arm, British Columbia, Canada. *Journal of Physical Oceanography*, 32, 2753–2765.
- Stevens, A., Elias, E., Pearson, S., Kaminsky, G., Ruggiero, P., Weiner, H., & Gelfenbaum, G. (2020). *Observations of Coastal Change and Numerical Modeling of Sediment-Transport Pathways at the Mouth of the Columbia River and its Adjacent Littoral Cell*. USGS.
- Stewart, W. J., & Boulton, J. G. (1893). *Map of Burrard Inlet*, 1–1. <https://searcharchives.vancouver.ca/burrard-inlet-6>
- Thomson, R. (1981). *Oceanography of the British Columbia Coast*. Department of Fisheries of Oceans, Institute of Ocean Sciences.
- Truth and Reconciliation Commission Canada. (2015). *Canada's Residential Schools: The Final Report of the Truth and Reconciliation Commission of Canada, volume 1*. McGill-Queen's Press MQUP.
- Tsleil-Waututh Nation. (n.d.-a). *Assessment of the Trans Mountain Pipeline and Tanker Expansion Proposal*. Treaty, Lands and Resources Department, Tsleil-Waututh Nation.
- Tsleil-Waututh Nation. (n.d.-b). *Tsleil-Waututh Nation - Our Story*. Retrieved February 11, 2021, from twnation.ca/our-story
- Tsleil-Waututh Nation. (2019). *Understanding Our Community's Climate Change Vulnerabilities*. Tsleil-Waututh Nation and Kerr Wood Leidal.
- Tsleil-Waututh Nation. (2020). *Project Terms of Reference: Understanding Sediment Dynamics and Shoreline Erosion in Burrard Inlet*. Tsleil-Waututh Nation.
- Tsleil-Waututh Nation. (2021). *Reconstructed historic shorelines from 1792*. Data provided by the Tsleil-Waututh Nation.
- Tsleil-Waututh Nation Climate Summit. (2018). *Talk: TWN Perspective*. https://www.youtube.com/watch?v=f3k_1IJV00U&list=PLoc7WcV5-h2UT8rpk-O6mynv7CSGdp2_I&index=13
- TWN Communication. (2018). *Whey-Ah-Wichen/Cates Park Archaeological Site (DhRr-8) Erosion Report*. Treaty, lands and resources department of the Tsleil-Waututh Nation, Toniello, G.
- USDA Forest Service. (2004). *Reference tables for Manning values*. Retrieved October 15, 2021, from http://www.fsl.orst.edu/geowater/FX3/help/8_Hydraulic_Reference/Mannings_n_Tables.htm
- van Eekelen, E., & Bouw, M. (2020). *Building with Nature*. nai010 publishers.
- vanRijn, L. (2007). Unified view of sediment transport by currents and waves. I: Initiation of motion, bed roughness, and bed-load transport. *American Society of Civil Engineers*, 133, 649–667.
- Walter, R. K., O'Leary, J. K., Vitousek, S., Taherkhani, M., Geraghty, C., & Kitajima, A. (2020). Large-scale erosion driven by intertidal eelgrass loss in an estuarine environment. *Estuarine, Coastal and Shelf Science*, 243, 106910. <https://doi.org/https://doi.org/10.1016/j.ecss.2020.106910>
- Warrick, J., Stevens, A., Miller, I., Harrison, S., Ritchie, A., & Gelfenbaum, G. (2019). World's largest dam removal reverses coastal erosion. *Scientific Reports*, 9. <https://doi.org/https://doi.org/10.1038/s41598-019-50387-7>
- Water Office Canada. (2021). *Historical Hydrometric Data Map Search*. Retrieved June 15, 2021, from https://wateroffice.ec.gc.ca/google_map/google_map_e.html?map_type=historical&search_type=province&province=BC
- Williams, G. P., & Wolman, M. G. (1984). *Downstream effects of dams on alluvial rivers*. USGS Professional Paper.

- Wilson, K. (2018). *Pulling Together: A guide for Indigenization of post-secondary institutions. A professional learning series*. BC Campus.
- Wilson, K., & Henderson, J. (2014). *First Peoples: A guide for Newcomers*. Province of British Columbia, Greater Vancouver.
- Wu, Y., Hannah, C., O'Flaherty-Sproul, M., MacAulay, P., & Shan, S. (2019). A modeling study on tides in the Port of Vancouver. *Anthropocene Coasts*, 2, 101–125.
- Yang, H., Yang, S., Meng, Y., Xu, K., Luo, X., Wu, C., & Shi, B. (2018). Recent coarsening of sediments on the southern yangtze subaqueous delta front: A response to river damming. *Continental Shelf Research*, 155, 45–51. <https://doi.org/https://doi.org/10.1016/j.csr.2018.01.012>



Calibration

This appendix displays the match of water levels and velocities at various measuring stations after calibration, indicating the model performance. An initial salinity of 10 PSU is used, applying a salinity of 30 PSU on the seaward boundaries and a salinity of 0 PSU on all river fluxes. Moreover, a manning coefficient of $0.040 \text{ s/m}^{1/3}$ is used. Figures A.1a, A.1b, A.2a and A.2b show the calibration results for water levels, validated at six measuring stations distributed equally over the inlet (for the locations of the measuring stations, see Figure 4.1). Figures A.3a, A.3b, A.4a and A.4b show the calibration results for the velocities, validated for measuring stations in First and Second Narrows.

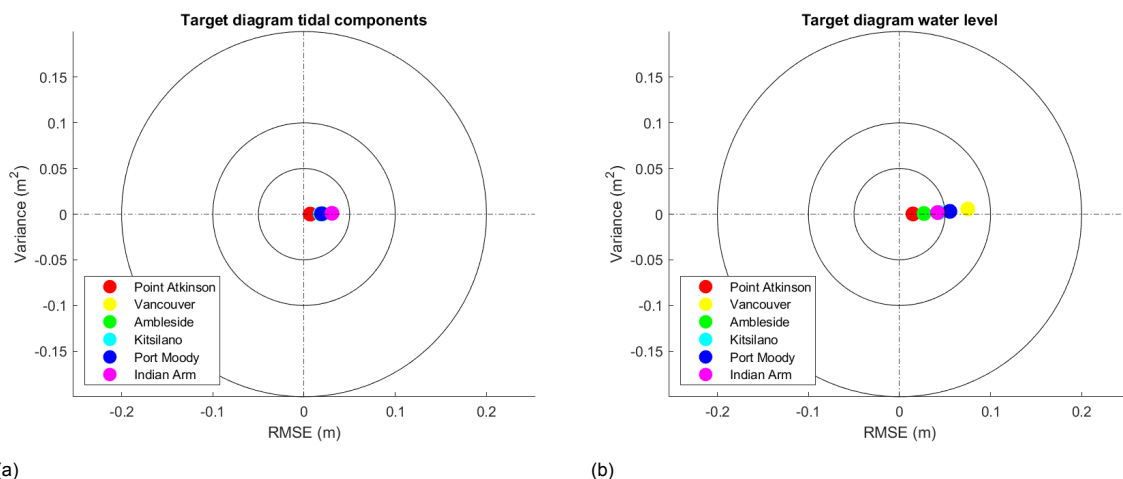
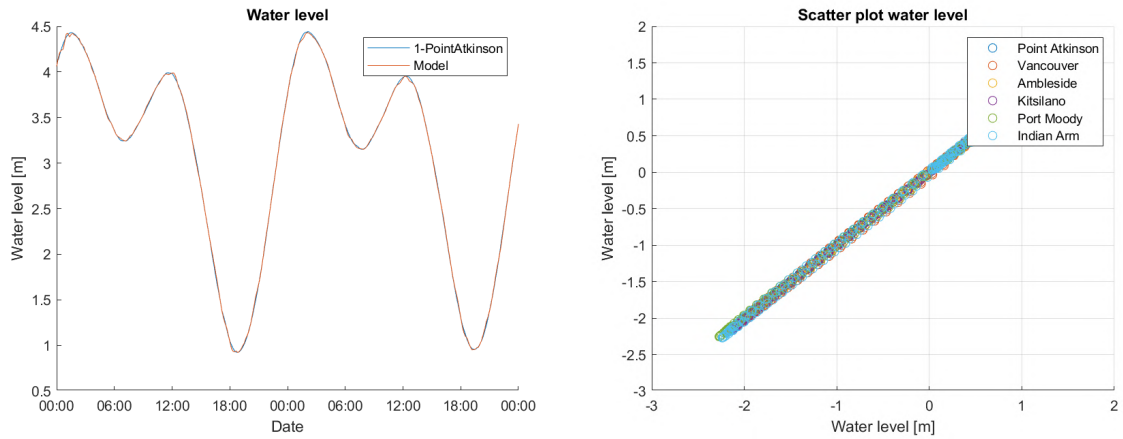
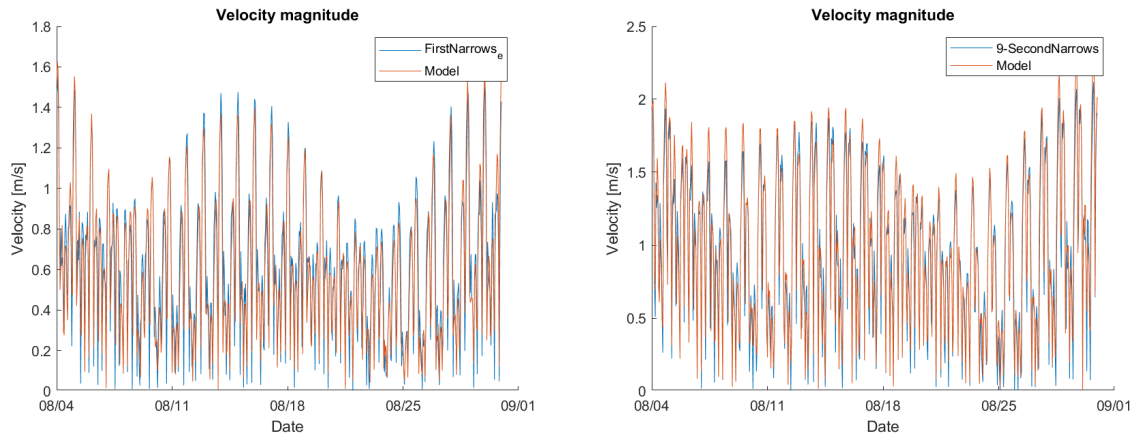


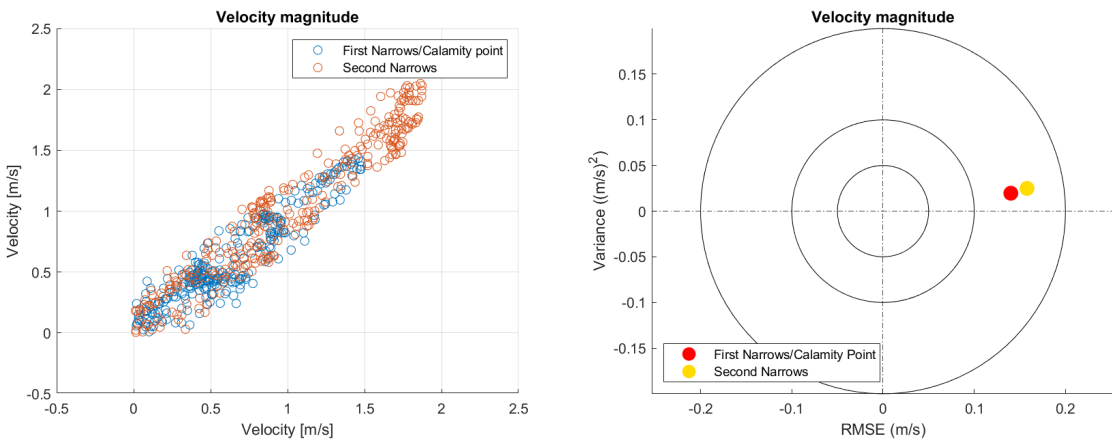
Figure A.1: a) Target diagram showing the root mean squared error (RMSE) and variance for the tidal components on several measuring stations. Points located closer to the center indicate a lower error, i.e. a better model performance. b) Target diagram showing the root mean squared error (RMSE) and variance for the modeled water level on several measuring stations.



(a) (b)
 Figure A.2: a) Measured and modeled water levels at Point Atkinson. b) Scatter plot of the observed and modeled water levels at various measuring station. The measured water level is given on the x axis and the modeled water level on the y-axis.



(a) (b)
 Figure A.3: a) Plot comparing the observed and modeled velocity in First Narrows. b) Plot comparing the observed and modeled velocity in Second Narrows.



(a) (b)
 Figure A.4: a) Scatter plot of the observed and modeled velocities. The measured velocity is given on the x axis and the modeled velocity on the y-axis. b) Target diagram showing the root mean squared error (RMSE) and variance for the velocity in First and Second Narrows. Points located closer to the center indicate a lower error, i.e. a better model performance.

B

Morphological tide

B.1. Selection of the morphological tide

The net sediment transport is plotted using arrows in order to compare the sediment transport trends and identify the representative tidal cycle. In this appendix, the net sediment transport for the full year (April 2019 to April 2020, Figure B.1), for August 2019 (Figure B.2), which was chosen to be representative for the long term trends. Finally, the double tidal cycle from 14-08 12:10 to 15-08 12:50 was selected to be the most representative tidal cycle (Figure 5.1).

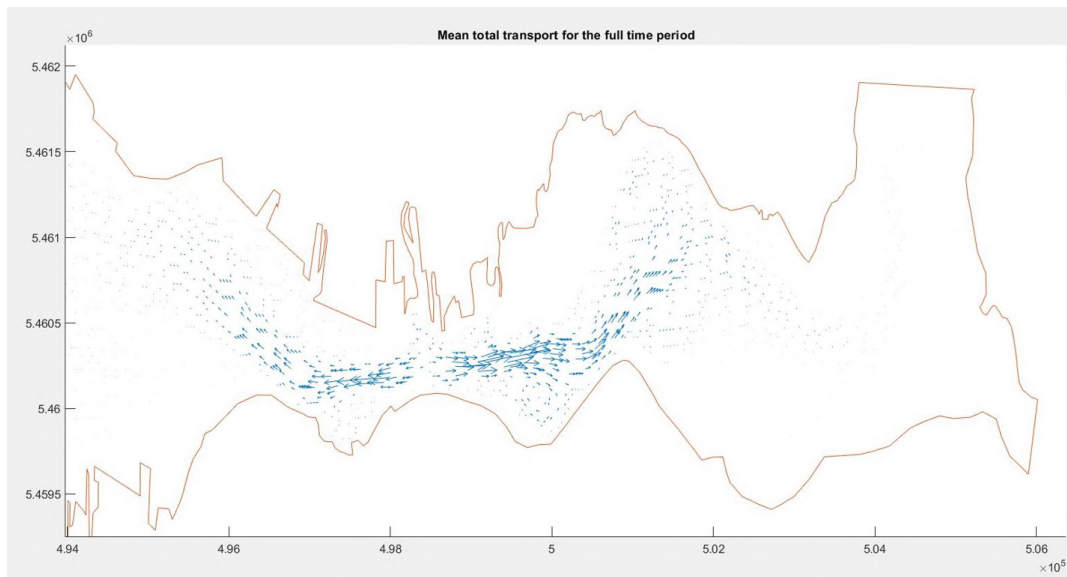


Figure B.1: Visualization of the net sediment transport vectors for the full year (April 2019 to April 2020).

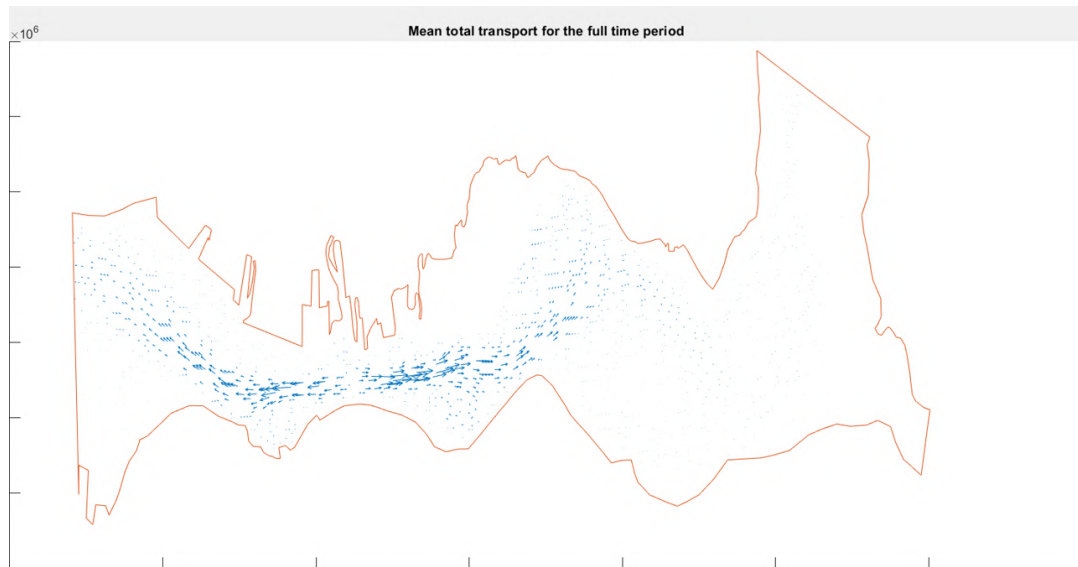


Figure B.2: Visualization of the net sediment transport vectors for August 2019.

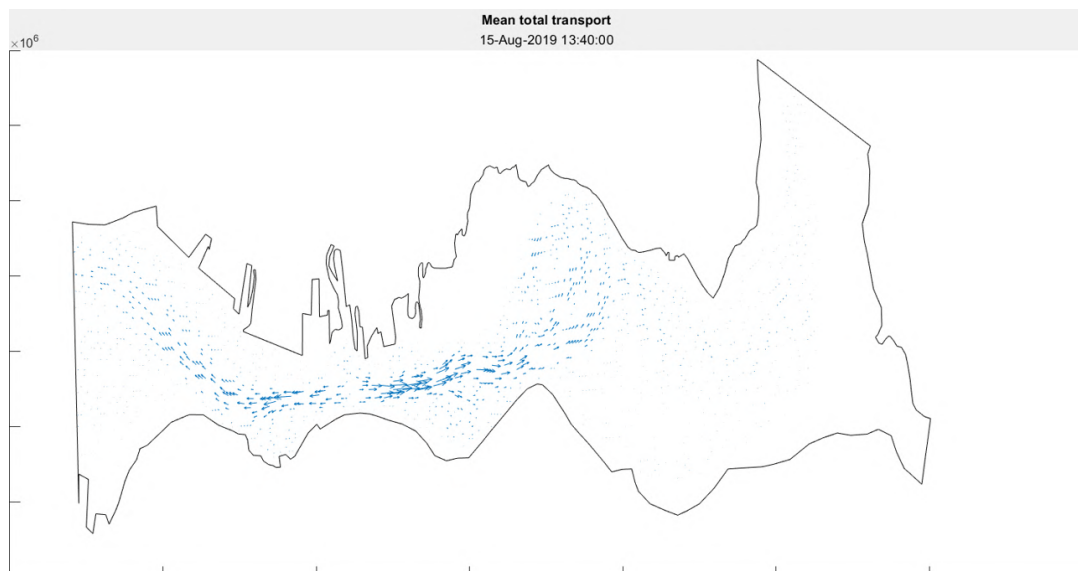


Figure B.3: Visualization of the net sediment transport vectors for the selected double tidal cycle (14-08 12:10 to 15-08 12:50).

B.2. Sensitivity runs for tidal cycles

After the representative tidal cycle has been chosen, some sensitivity runs are performed to check the effects of using a time period in a different stage of the spring-neap tidal cycle and see how sensitive the resulting transport patterns are to the choice of tidal cycle.

For this, the periods of 18-08 15:00 to 19-08 15:50 (spring going to neap) and 21-08 17:30 to 22-08 18:40 (neap tide) are used. Their stages in the spring-neap tidal cycle are presented in Figure B.4.

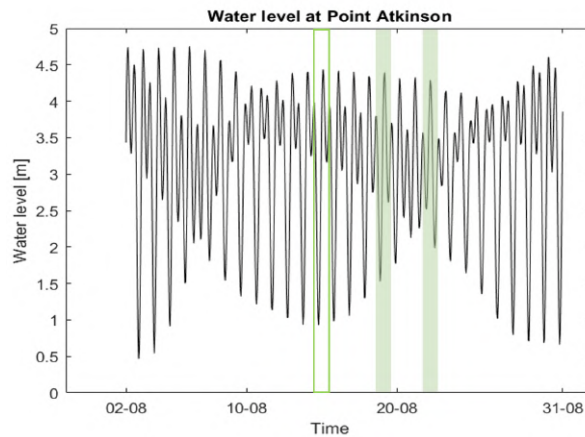


Figure B.4: The spring-neap tidal cycle of August 2019. The tidal cycles that are used for the sensitivity runs are highlighted in green. The tidal cycle that is selected to be representative (14-08 12.10 to 15-08 12.50) is indicated using a green contour line.

In Central Harbour, the transport patterns are found to be very similar for all three tidal cycles (Figure B.5 and B.6). In the run at neap tide (21-08 17:30 to 22-08 18:40), the transport is less strong but still shows the same patterns (Figure B.6). The transport vectors can be found in Figure B.7, B.8, B.9 and B.10.

In Inner Harbour, the differences are larger (Figure B.5 and B.6). Both 'reference' tidal cycles show one large counterclockwise eddy in the center of Inner Harbour, instead of a counterclockwise eddy in the north and a clockwise one in the south as was found for the selected representative tidal cycle.

Based on the persistence of the key transport patterns for the different tidal cycles, the sensitivity to the selected tidal cycle on the scale of the inlet is limited.

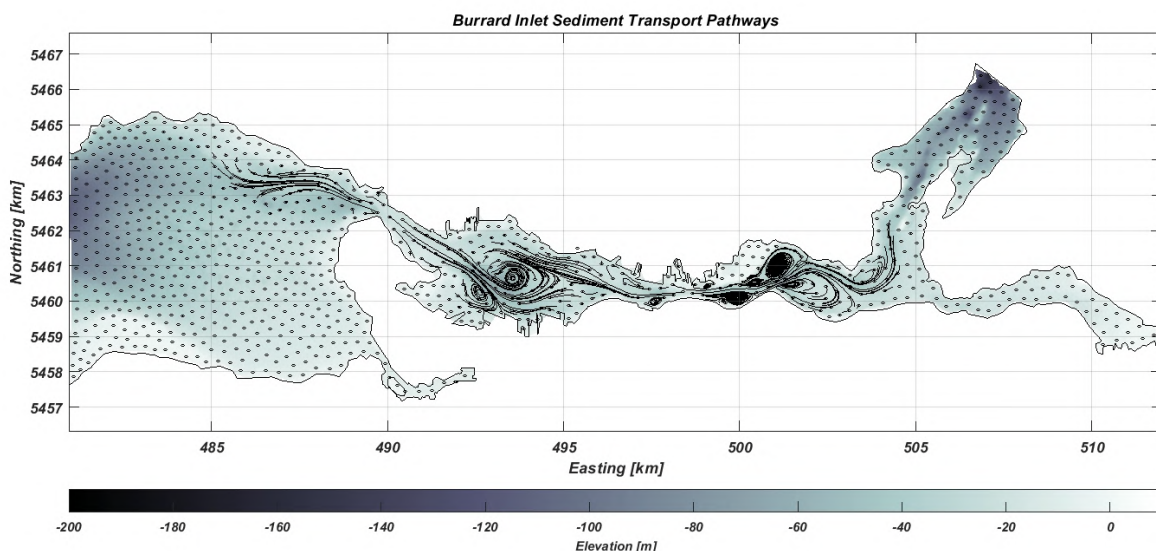


Figure B.5: Sediment transport pathways for the tidal cycle from 18-08 15:00 to 19-08 15:50 (spring going to neap).

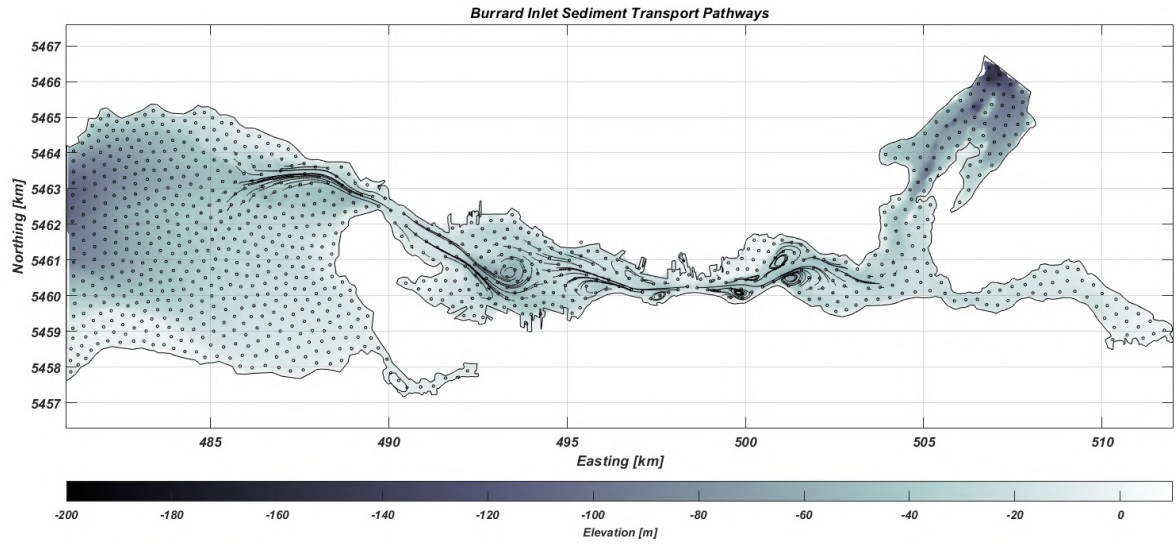


Figure B.6: Sediment transport pathways for the tidal cycle from 21-08 17:30 to 22-08 18:40 (neap tide)

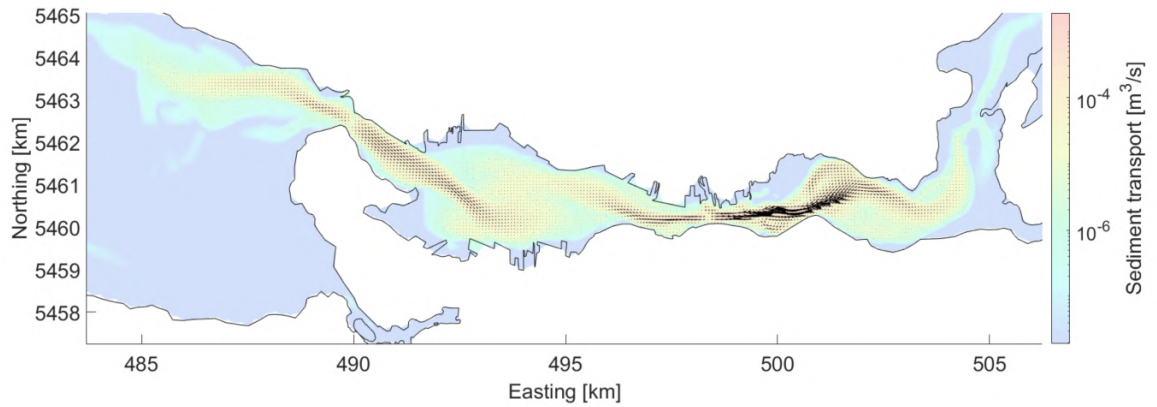


Figure B.7: Net transport vectors for the tidal cycle from 18-08 15:00 to 19-08 15:50 (spring going to neap) for Burrard Inlet.

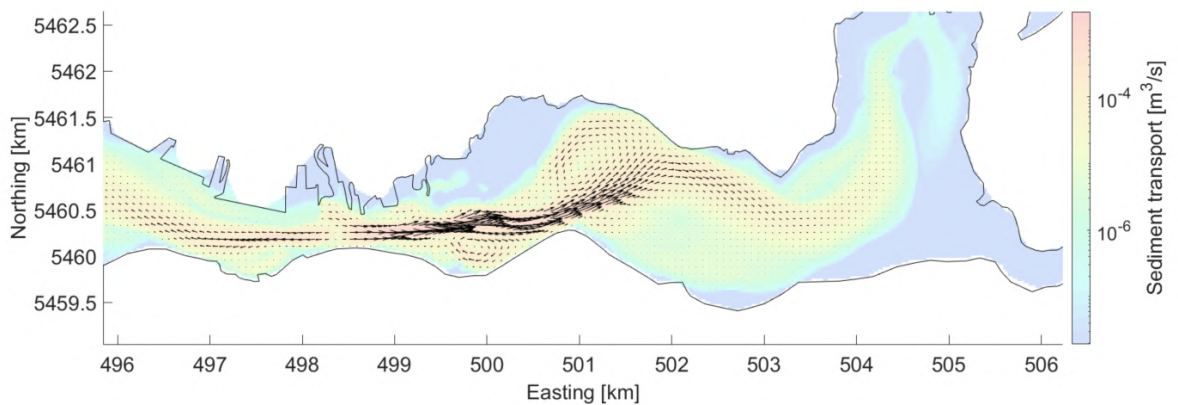


Figure B.8: Net transport vectors for the tidal cycle from 18-08 15:00 to 19-08 15:50 (spring going to neap) zoomed in on Central Harbour.

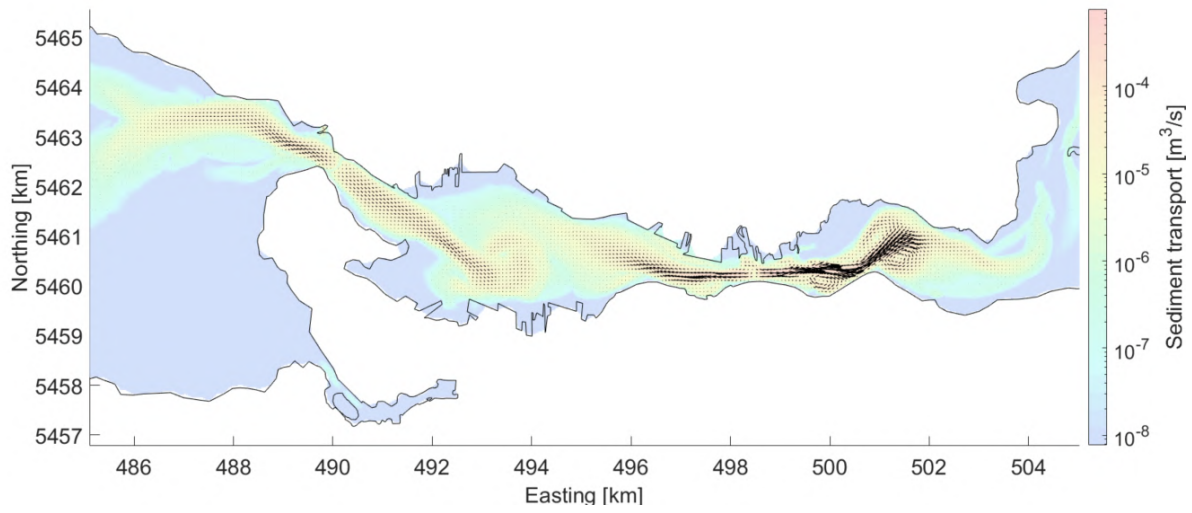


Figure B.9: Net transport vectors for the tidal cycle from 21-08 17:30 to 22-08 18:40 (neap tide) for Burrard Inlet.

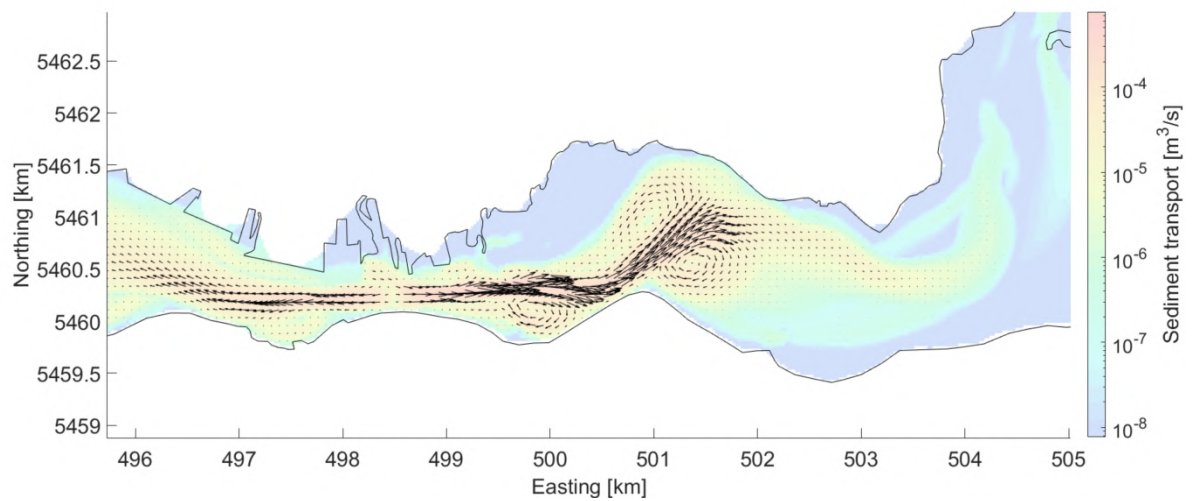


Figure B.10: Net transport vectors for the tidal cycle from 21-08 17:30 to 22-08 18:40 (neap tide) zoomed in on Central Harbour.

Velocity analysis

This appendix contains the maps showing the velocities in Burrard Inlet, averaged over the ebb and flood periods of the tidal cycle. The dominant ebb and flood periods (ebb 1 and flood 1) are analyzed in Section 5.1. The trends found during the weaker ebb and flood events (ebb 2 and flood 2) are displayed here in Figures C.1 and C.2.

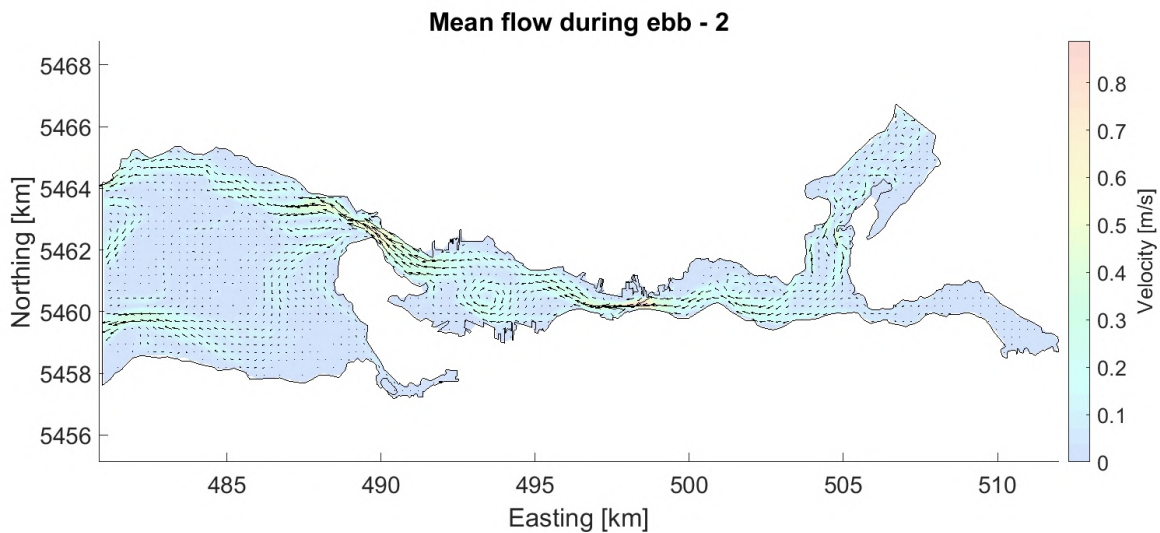


Figure C.1: Maps showing the velocities in Burrard Inlet averaged over the second ebb period.

Section 5.2 explains the sediment transport patterns that can be found in Burrard Inlet. Transport patterns are dominated by the presence of First and Second Narrows. Plotting the net transport vectors shows transport away from the Narrows in both directions. This can be explained by the strong accelerations taking place in the Narrows, which is elaborated on in Section 5.2 using maps of the velocity, sediment concentration and sediment transport flux for Second Narrows as an example. Figure C.3 shows how the same principle applies for First Narrows as well, where the strong velocity increase in the Narrows results in transport moving away from First Narrows during both flood and ebb tide.

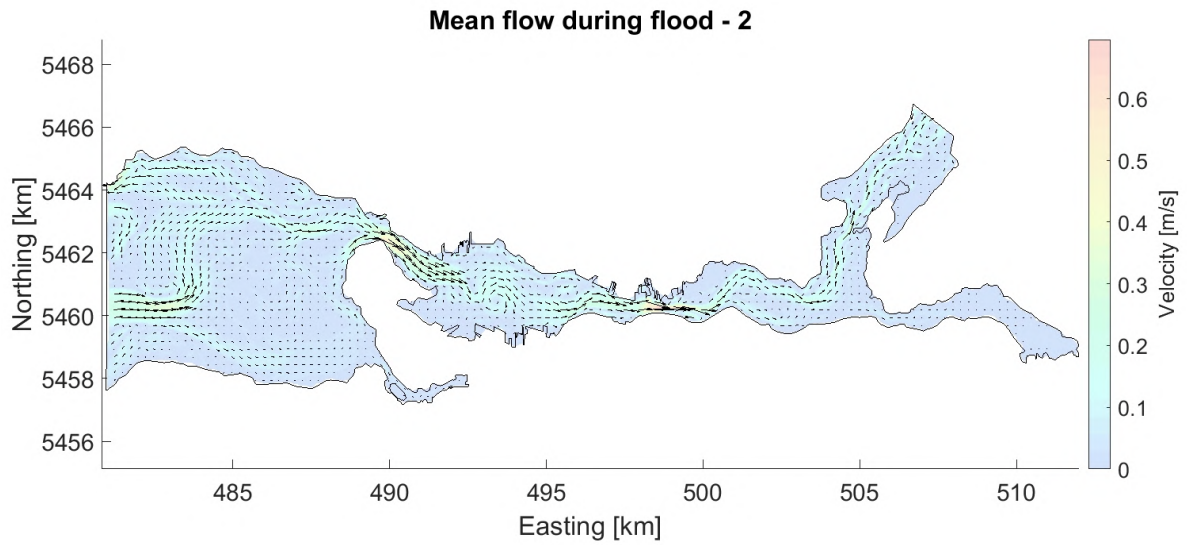


Figure C.2: Maps showing the velocities in Burrard Inlet averaged over the second flood period.

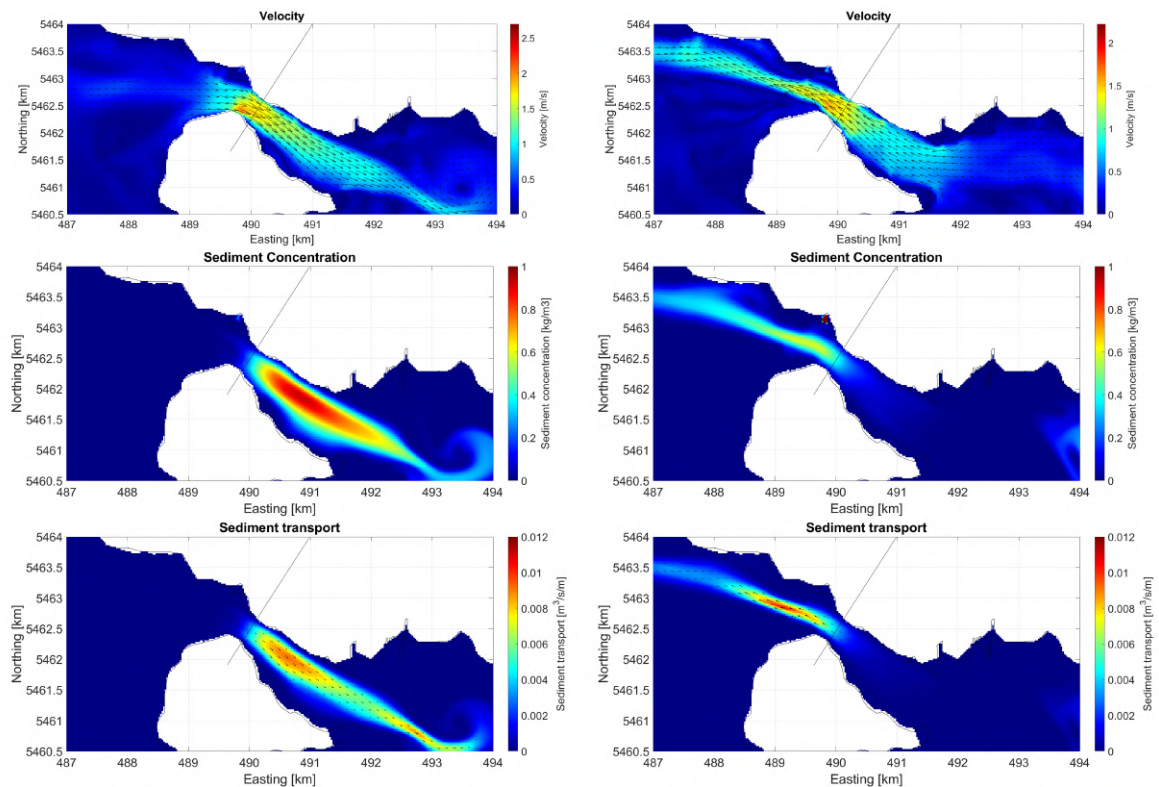


Figure C.3: Left panels: Velocity, sediment concentration and sediment transport in First Narrows during peak flood. Right panels: velocity, sediment concentration and sediment transport in First Narrows during peak ebb. Net transport moves away from the Narrows in both directions. At the location of the black line, the center of the constriction, sediment transport is limited.

D

SedTRAILS for hydrodynamics

SedTRAILS runs for hydrodynamics have been performed in order to visualize the patterns of water motion and the connections between the different basins. Figure D.1 shows what a SedTRAILS run for hydrodynamics would look like if source points would be placed all over the inlet. Due to the long and dispersive pathways, this results in a chaotic picture, in which no trends can be distinguished.

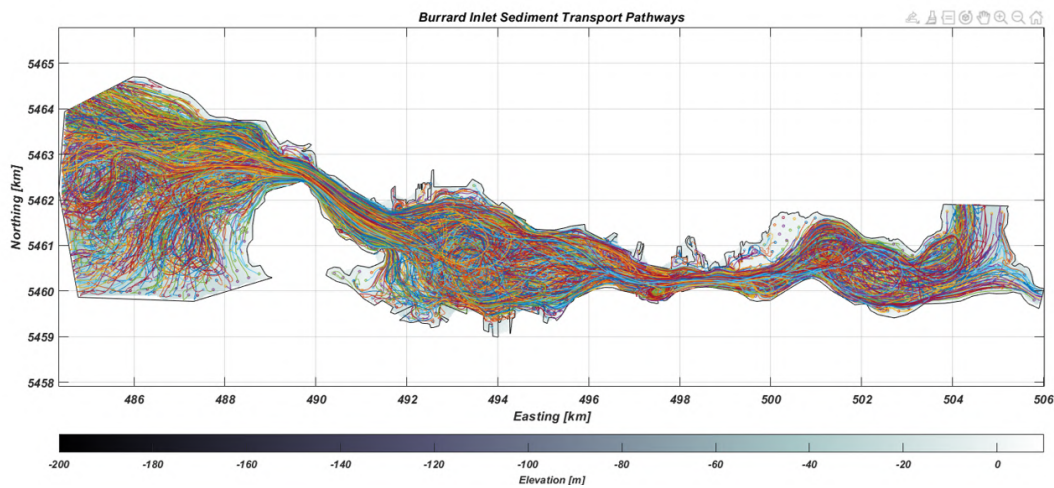


Figure D.1: SedTRAILS run for hydrodynamics with source points everywhere in the inlet: this results in a chaotic figure where individual pathways are impossible to distinguish.

In order to be able to distinguish separate trajectories and get an overview of how water moves through Burrard Inlet, a SedTRAILS simulation has been done for each section of the inlet, containing source points only in this section. This shows the possible pathways for water originating in this section during one tidal cycle, and gives an indication of the connectivity within the inlet. The sections that are implemented are: First Narrows (Figures D.2 and D.3), Second Narrows (Figures D.4 and D.5), Central Harbour (Figures D.6 and D.7), the TWN shorelines (Figures D.8 and D.9), Inner Harbour (Figures D.10 and D.11), and Outer Harbour (Figures D.12 and D.13).

Moreover, each simulation has been performed for two 'release moments': at high water slack (just before ebb) and low water slack (just before flood). An overview of the results of each simulation can be found in this appendix.

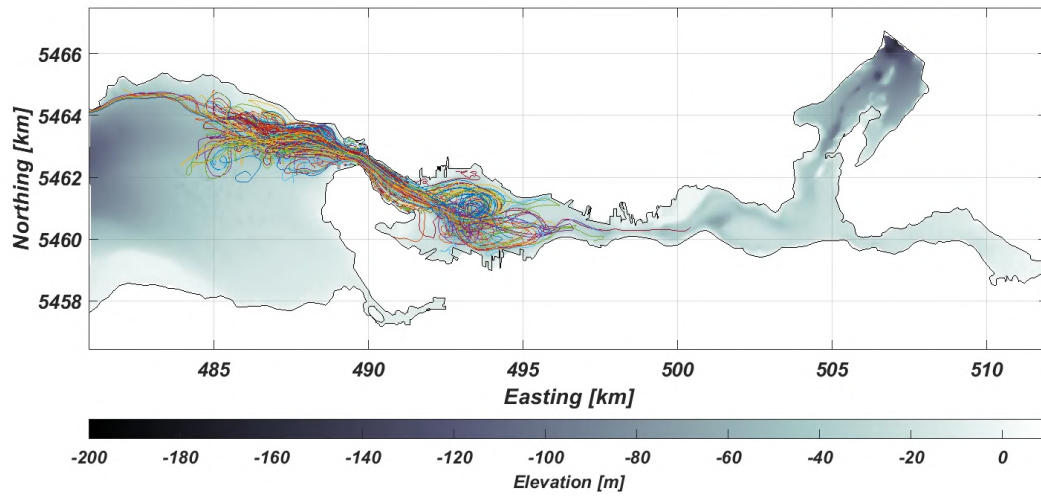


Figure D.2: SedTRAILS run for hydrodynamics with source points in First Narrows. Release moment: high water slack.

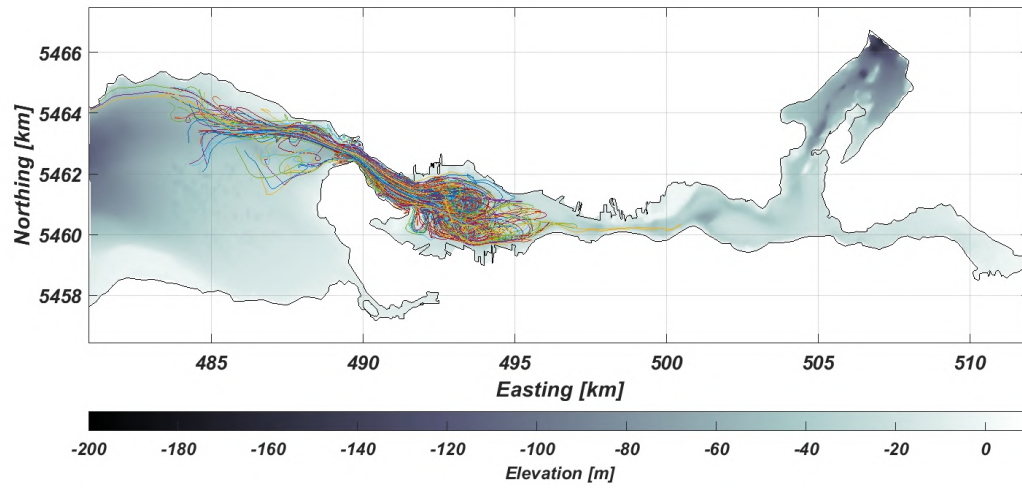


Figure D.3: SedTRAILS run for hydrodynamics with source points in First Narrows. Release moment: low water slack.

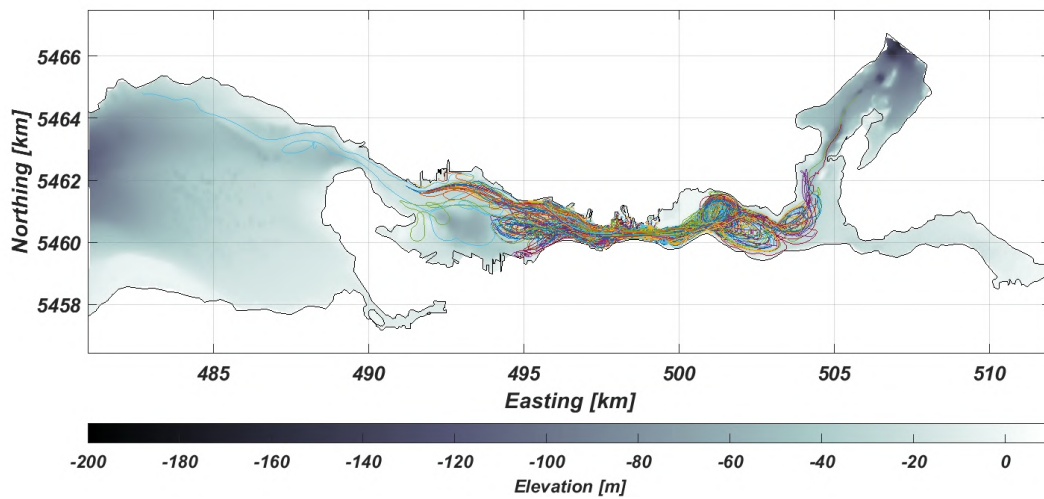


Figure D.4: SedTRAILS run for hydrodynamics with source points in Second Narrows. Release moment: high water slack.

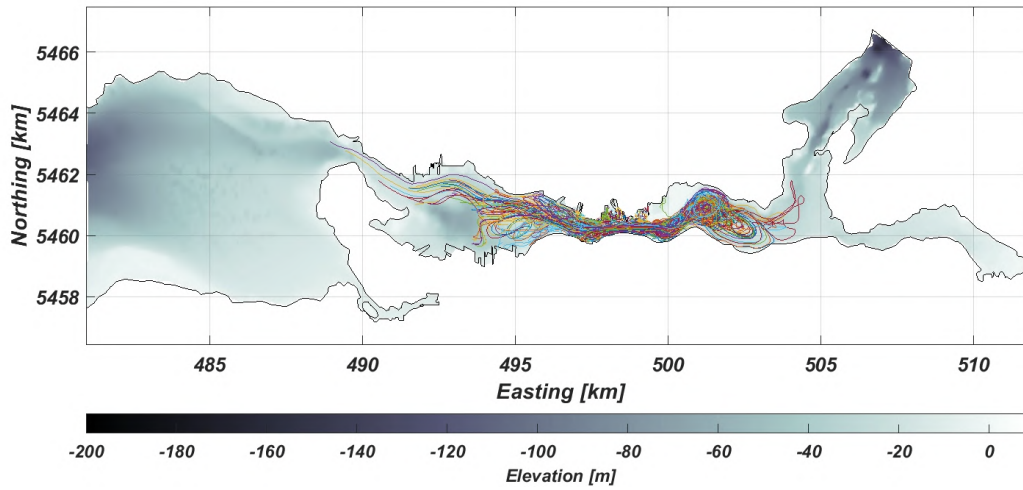


Figure D.5: SedTRAILS run for hydrodynamics with source points in Second Narrows. Release moment: low water slack.

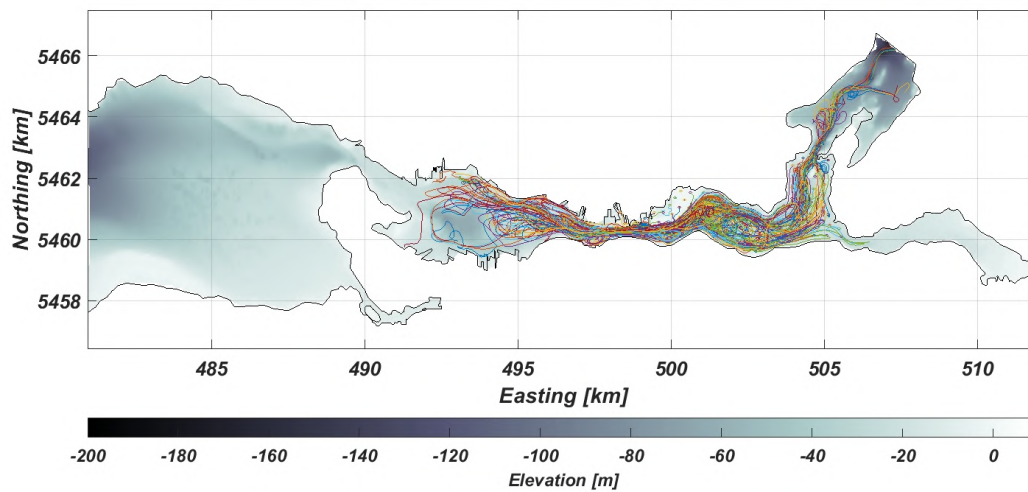


Figure D.6: SedTRAILS run for hydrodynamics with source points in Central Harbour. Release moment: high water slack.

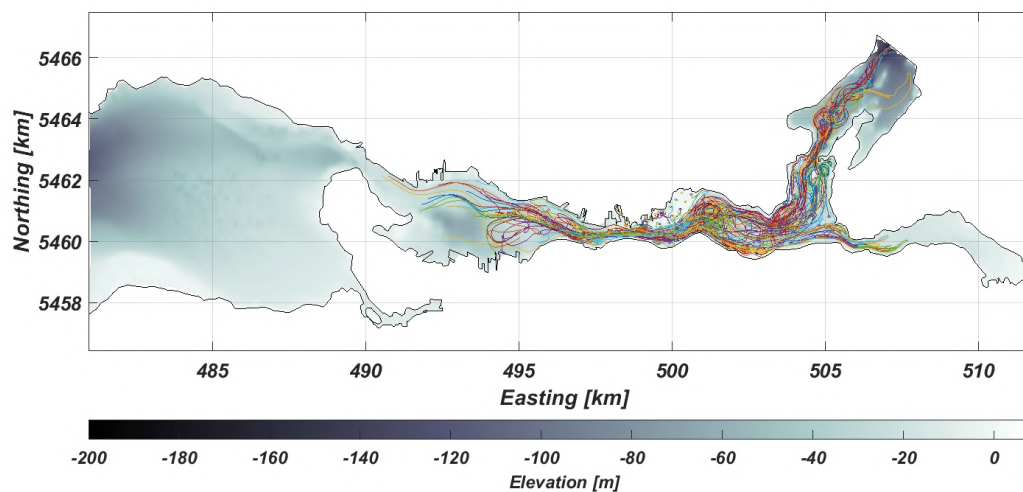


Figure D.7: SedTRAILS run for hydrodynamics with source points in Central Harbour. Release moment: low water slack

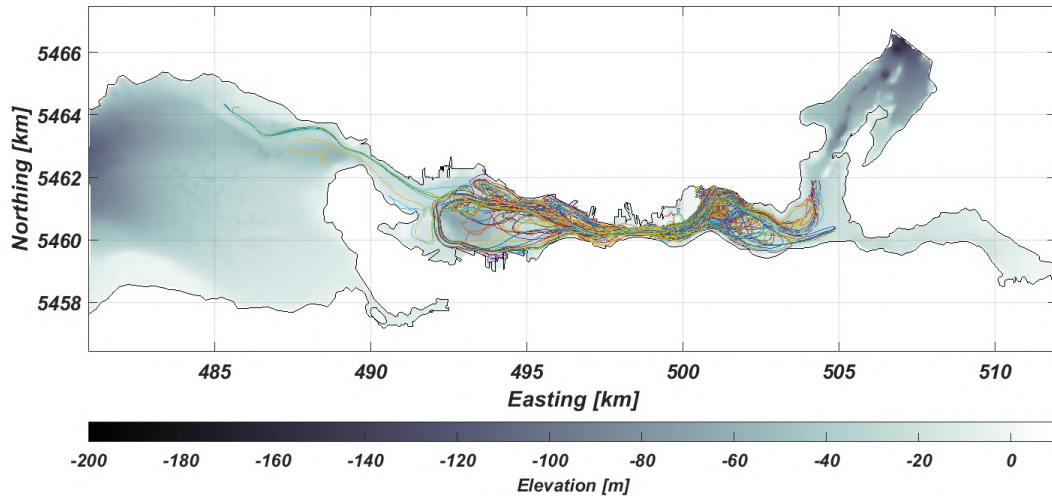


Figure D.8: SedTRAILS run for hydrodynamics with source points along the TWN shoreline. Release moment: high water slack.

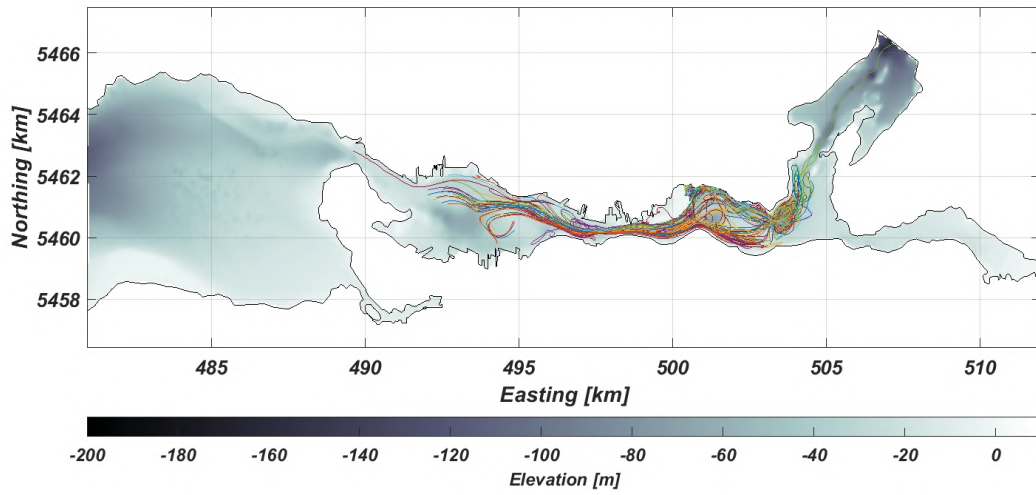


Figure D.9: SedTRAILS run for hydrodynamics with source points along the TWN shoreline. Release moment: low water slack.

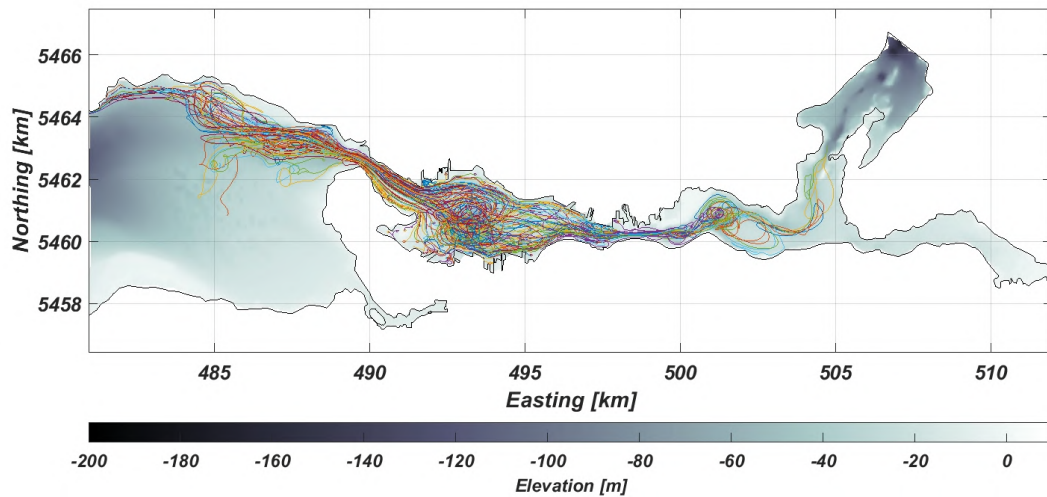


Figure D.10: SedTRAILS run for hydrodynamics with source points in Inner Harbour. Release moment: high water slack

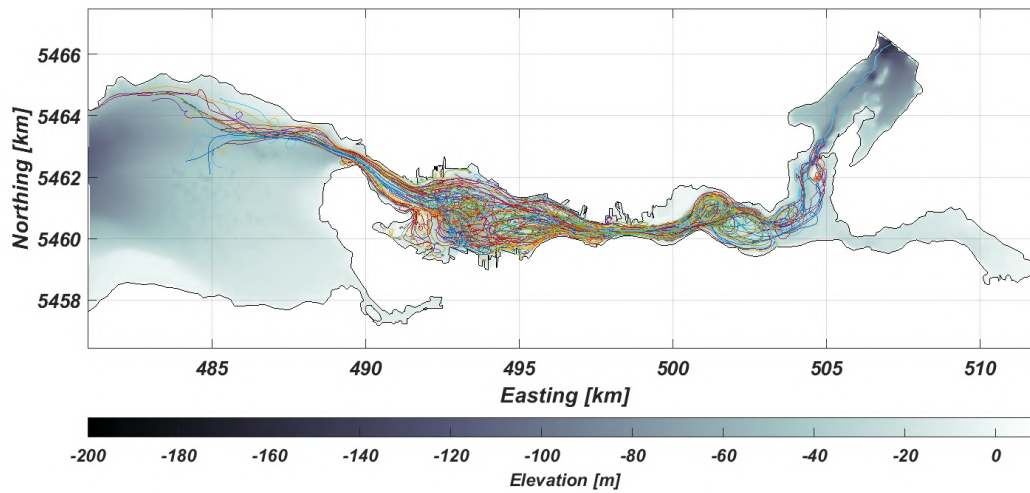


Figure D.11: SedTRAILS run for hydrodynamics with source points in Inner Harbour. Release moment: low water slack

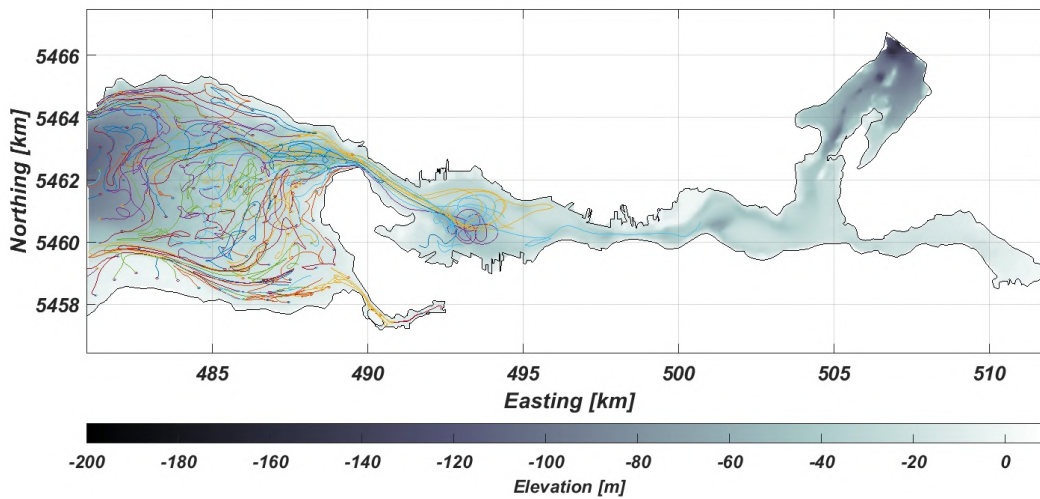


Figure D.12: SedTRAILS run for hydrodynamics with source points in Outer Harbour. Release moment: high water slack

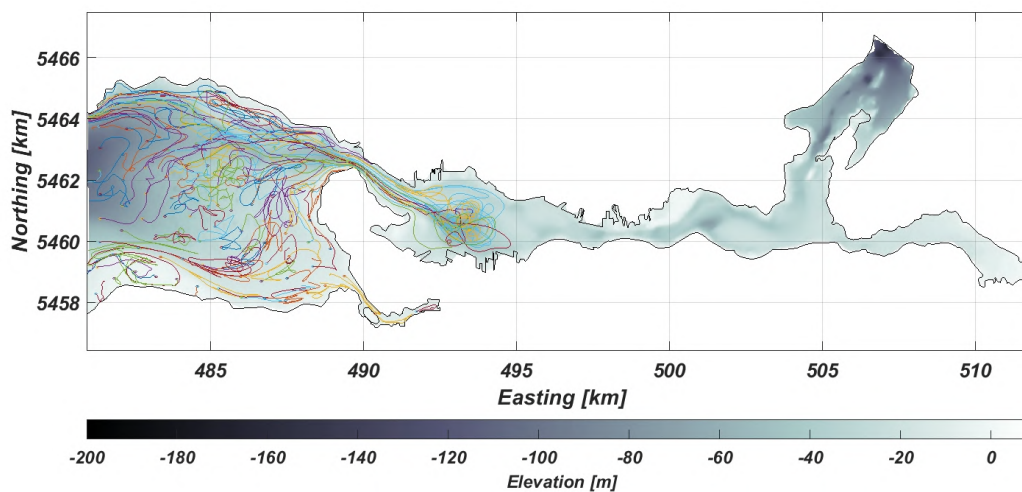


Figure D.13: SedTRAILS run for hydrodynamics with source points in Outer Harbour. Release moment: low water slack

Sediment Transport Pathways

The sediment transport pathways have been analyzed by running SedTRAILS for each basin separately: Outer Harbour (Figure E.1), First Narrows (Figure E.2), Inner Harbour (Figure E.3), Second Narrows (Figure E.4) and Central Harbour (Figure E.5). Moreover, Figures E.6 and E.7 zoom in on the pathways in Central Harbour.

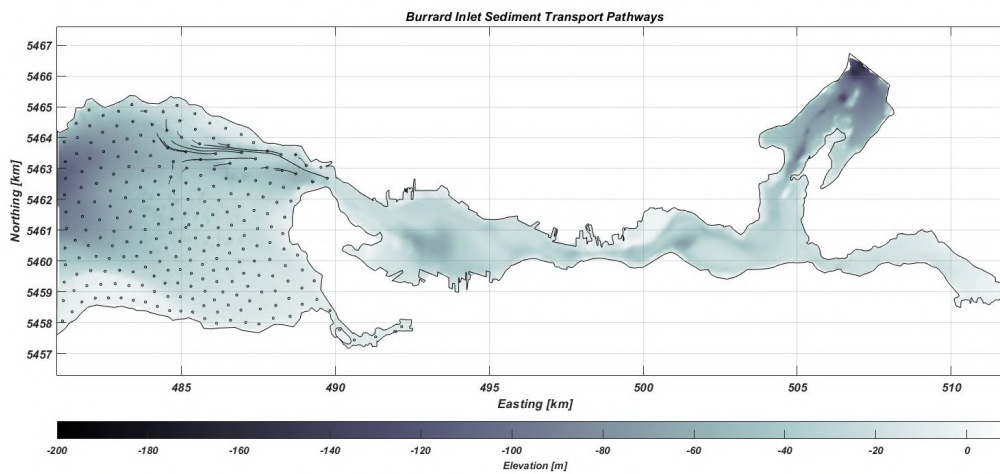


Figure E.1: SedTRAILS run for Outer Harbour, with a sediment size of 70 micron, a runtime of 20 days and an acceleration factor of 20.

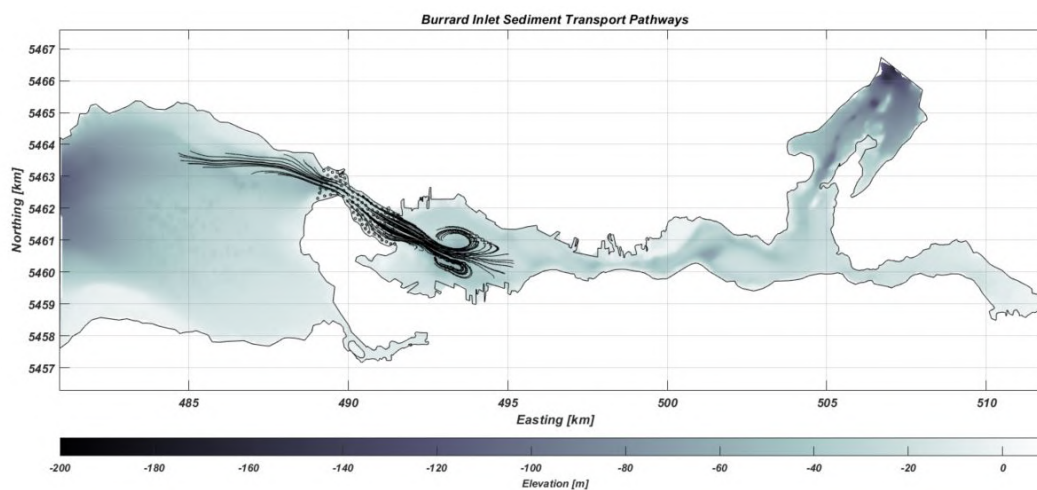


Figure E.2: SedTRAILS run for First Narrows, with a sediment size of 70 micron, a runtime of 20 days and an acceleration factor of 20.

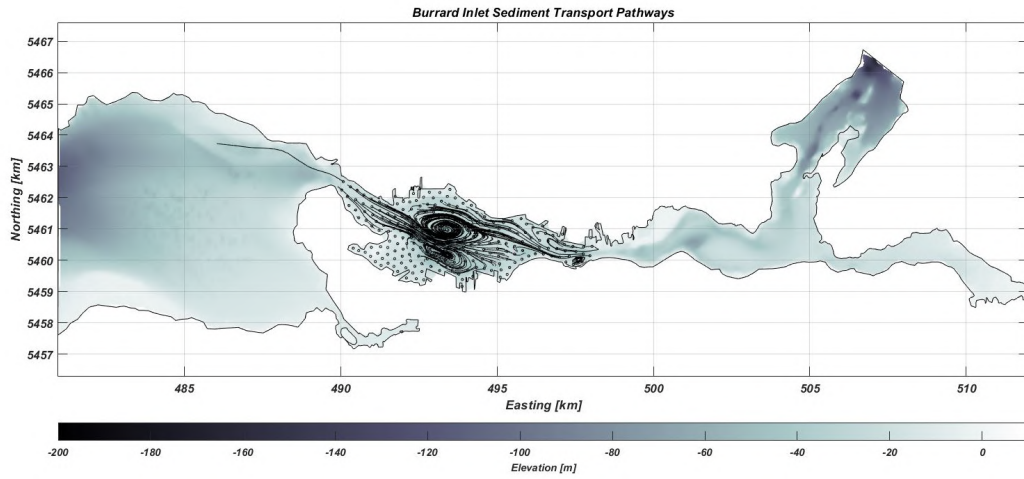


Figure E.3: SedTRAILS run for Inner Harbour, with a sediment size of 70 micron, a runtime of 20 days and an acceleration factor of 20.

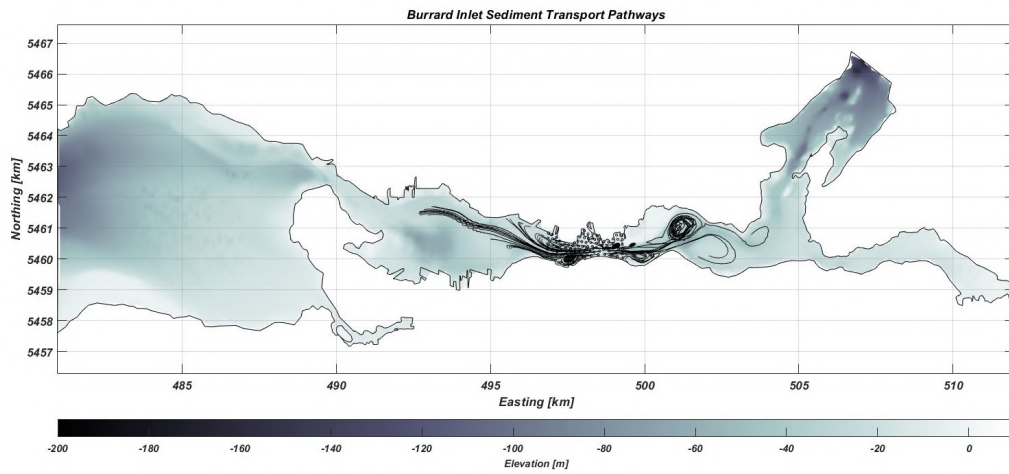


Figure E.4: SedTRAILS run for Second Narrows, with a sediment size of 70 micron, a runtime of 20 days and an acceleration factor of 20.

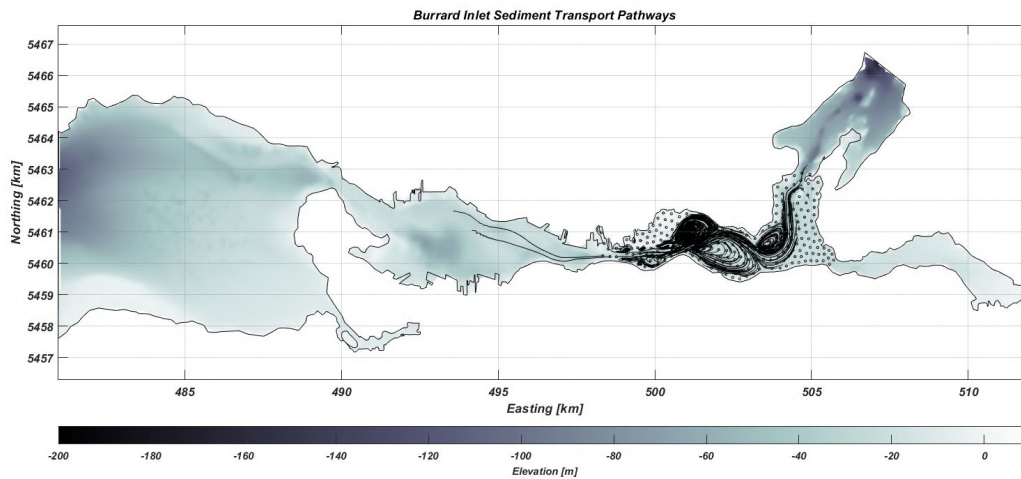


Figure E.5: SedTRAILS run for Central Harbour, with a sediment size of 70 micron, a runtime of 20 days and an acceleration factor of 20.

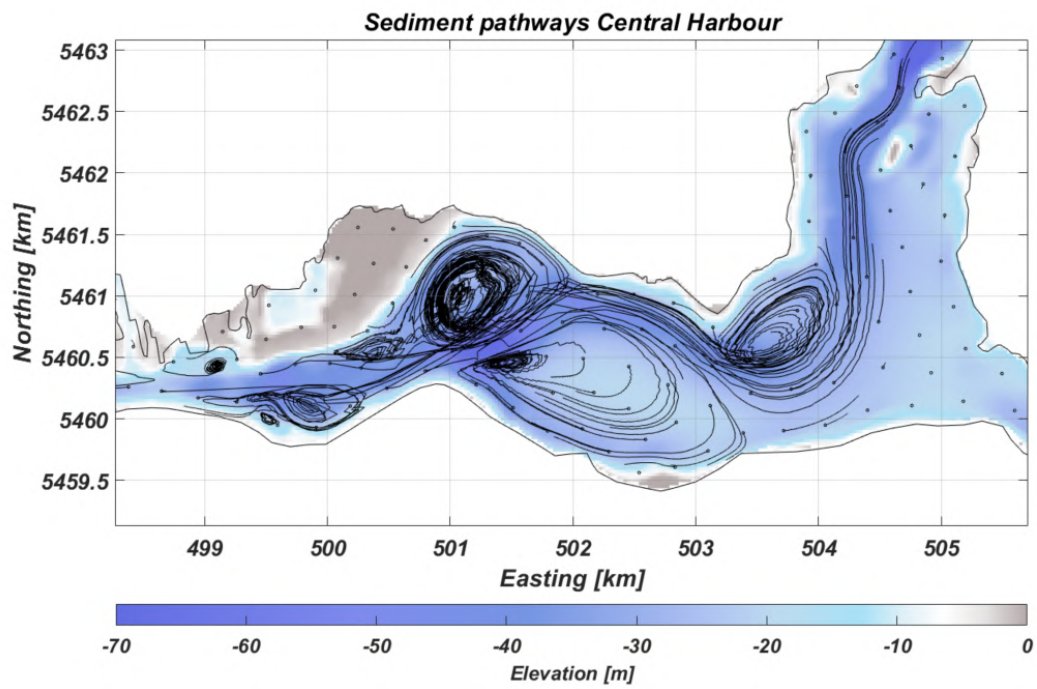


Figure E.6: SedTRAILS run for Central Harbour, with a sediment size of 70 micron, a runtime of 20 days and an acceleration factor of 20.

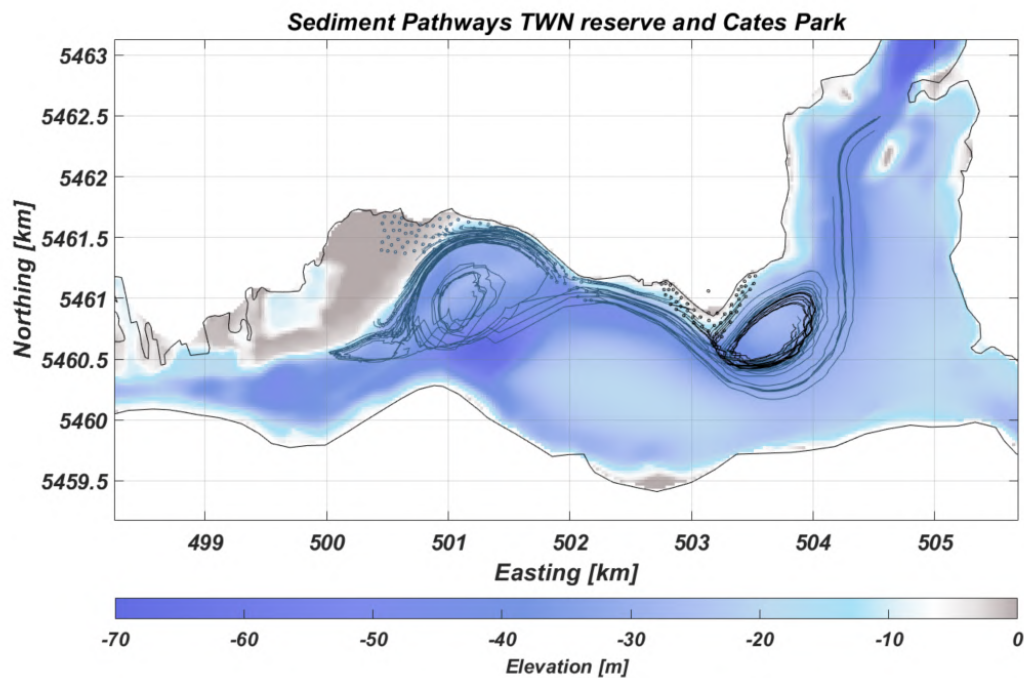


Figure E.7: SedTRAILS run for the TWN reserve shoreline and Cates Park, with a sediment size of 70 micron, a runtime of 20 days and an acceleration factor of 20.

F

Fraser river

Results of the SedTRAILS runs visualizing the sediment pathways in the Fraser Delta for various wave conditions are given in this appendix. Adding to the sediment pathways, a SedTRAILS run for hydrodynamics is done to get an indication of the upper limit of the possible pathways for fine suspended sediment (Figure F.1). Moreover, an aerial picture of Fraser river is included, which shows how far the sediment plume can reach out into the Strait of Georgia and Burrard Inlet (Figure F.2).

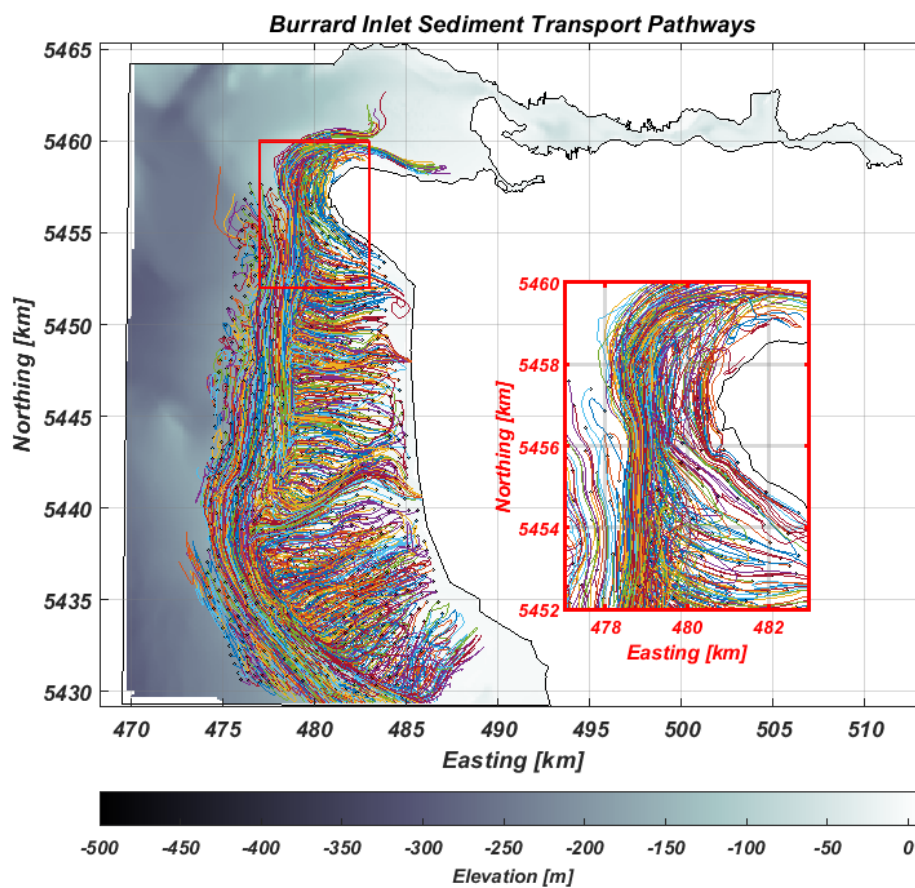


Figure F.1: SedTRAILS run for hydrodynamics on the Fraser delta. The zoomed inset box shows Point Grey, which separates the Fraser delta from Burrard Inlet.



Figure F.2: Aerial picture of the Sediment Plume of Fraser river, suggesting that some sediments from Fraser river might be able to reach Burrard Inlet (ADAM platform, 2021)

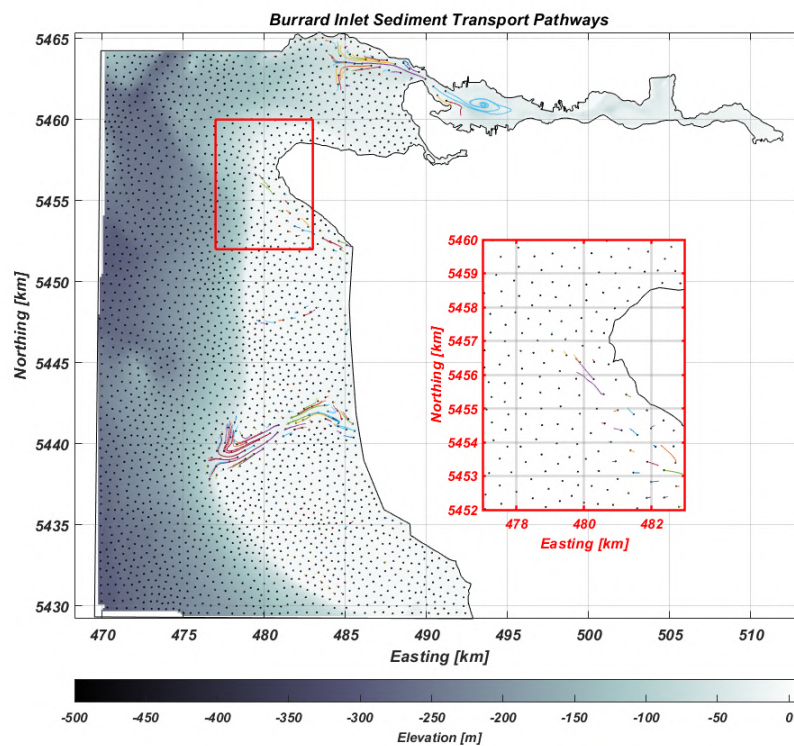


Figure F.3: SedTRAILS run including the Fraser river delta with high waves ($H_s = 1.64$ m) from the east. Runtime is 50 days and an acceleration factor of 30 is used. The zoomed inset box shows Point Grey, which separates the Fraser delta from Burrard Inlet.

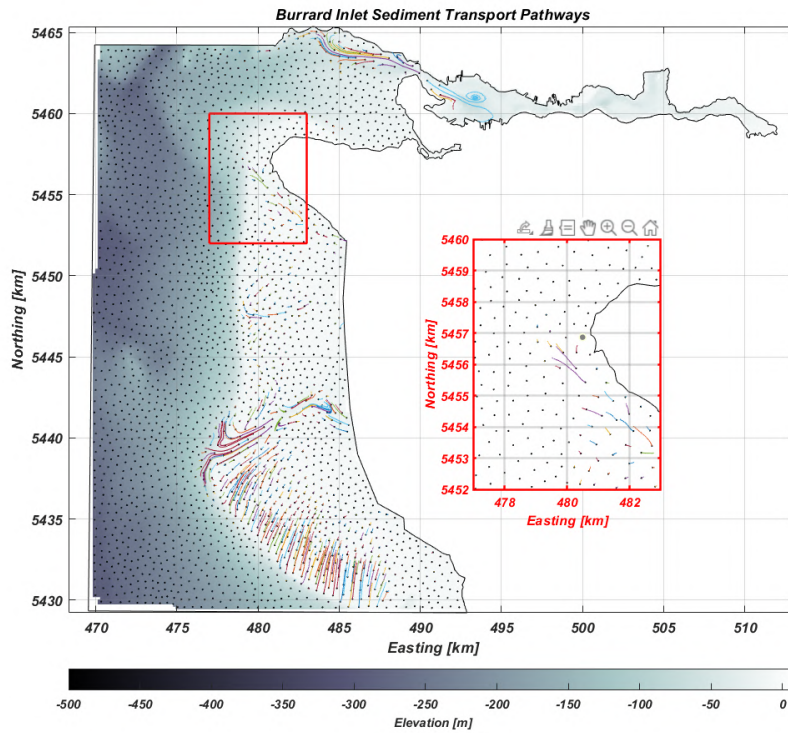


Figure F.4: SedTRAILS run including the Fraser river delta with high waves ($H_s = 1.64$ m) from the south. Runtime is 50 days and an acceleration factor of 30 is used. The zoomed inset box shows Point Grey, which separates the Fraser delta from Burrard Inlet.

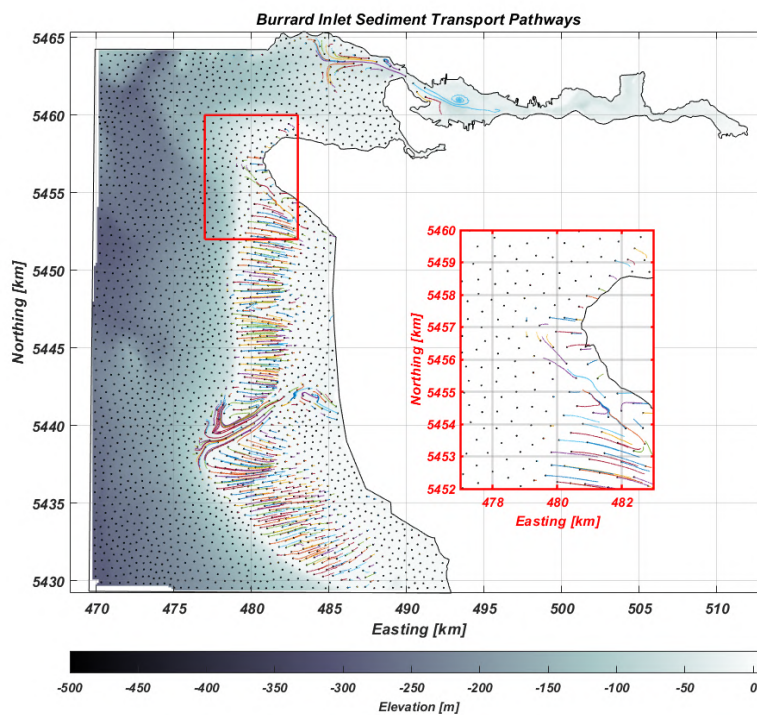


Figure F.5: SedTRAILS run including the Fraser river delta with high waves ($H_s = 1.64$ m) from the west. Runtime is 50 days and an acceleration factor of 30 is used. The zoomed inset box shows Point Grey, which separates the Fraser delta from Burrard Inlet.

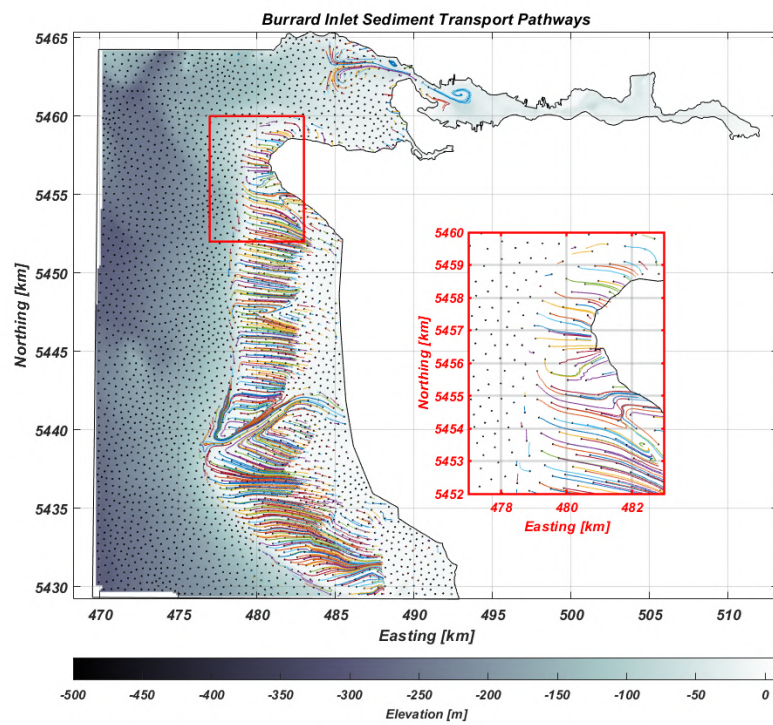


Figure F.6: SedTRAILS run including the Fraser river delta with extreme waves ($H_s = 3.5$ m) from the west. Runtime is 50 days and an acceleration factor of 30 is used. The zoomed inset box shows Point Grey, which separates the Fraser delta from Burrard Inlet.

G

Waves

G.1. Wave heights

This appendix gives an overview the wave heights in Burrard Inlet as simulated by SWAN for the seven wave scenarios (Figures G.1 until G.7). An overview of the wave scenarios that are used is given in Table 3.3.

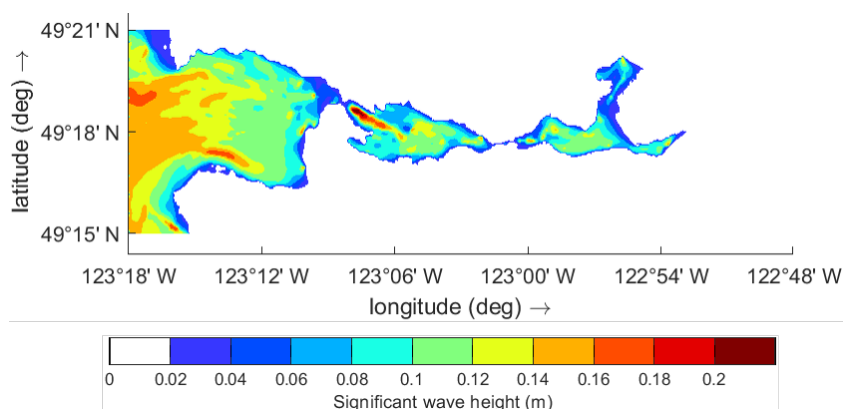


Figure G.1: Average East: Significant wave height in Burrard Inlet as simulated by SWAN for average wave heights (H_{sig} at boundary = 0.38 m) and an average wind speed (4.0 m/s) from the east.

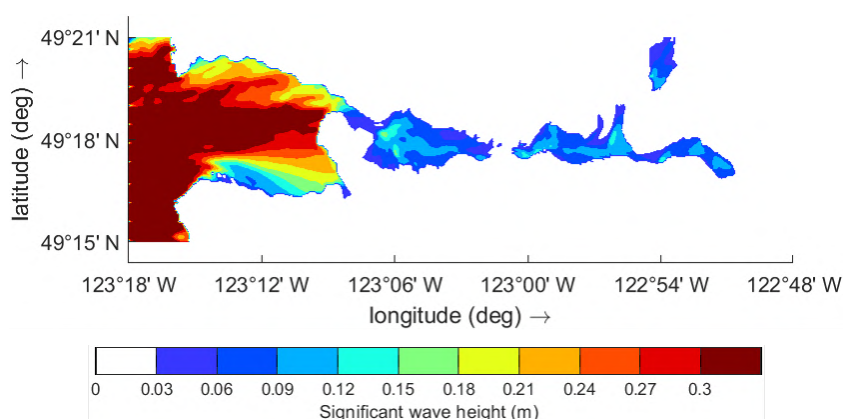


Figure G.2: Average West: Significant wave height in Burrard Inlet as simulated by SWAN for average wave heights (H_{sig} at boundary = 0.38 m) and an average wind speed (4.0 m/s) from the west.

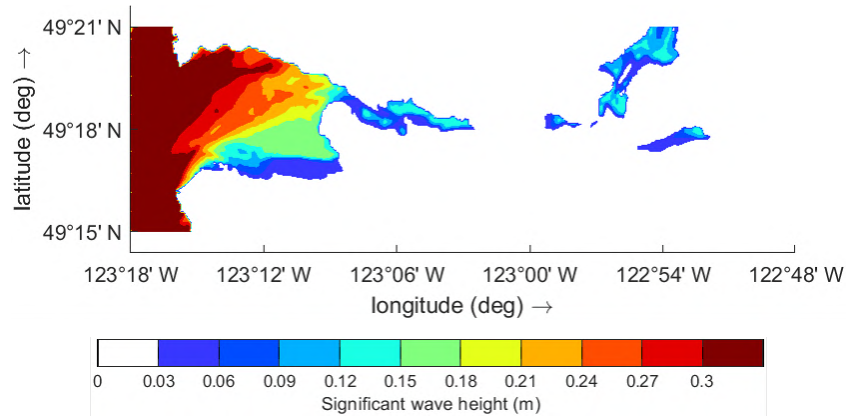


Figure G.3: Average South: Significant wave height in Burrard Inlet as simulated by SWAN for average wave heights (H_{sig} at boundary = 0.38 m) and an average wind speed (4.0 m/s) from the south.

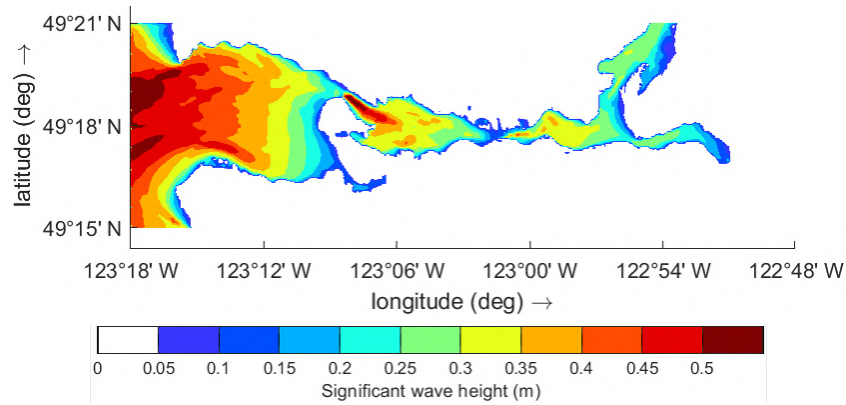


Figure G.4: High East: Significant wave height in Burrard Inlet as simulated by SWAN for high wave heights (H_{sig} at boundary = 1.64 m) and a strong wind speed (8.69 m/s) from the east.

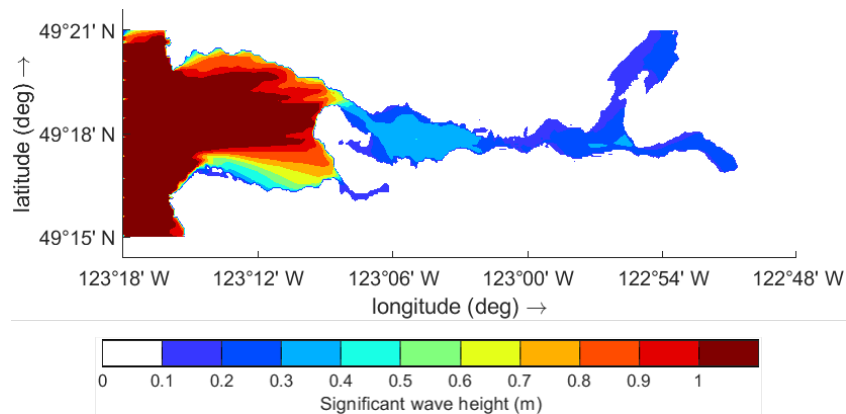


Figure G.5: High West: Significant wave height in Burrard Inlet as simulated by SWAN for high wave heights (H_{sig} at boundary = 1.64 m) and a strong wind speed (8.69 m/s) from the west.

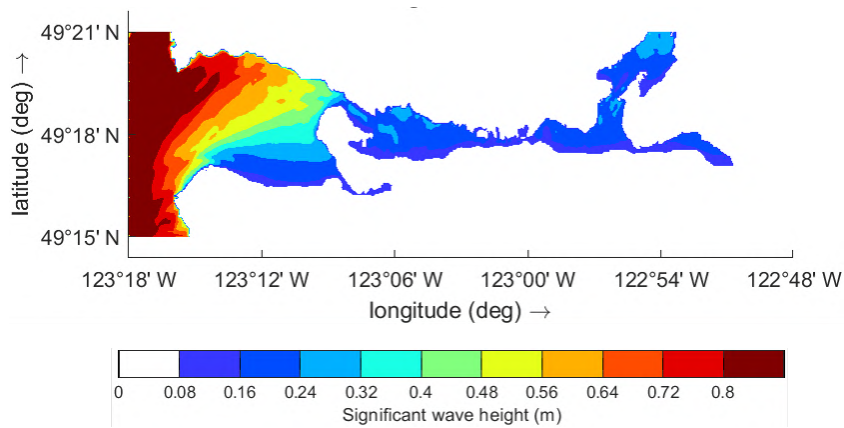


Figure G.6: High South: Significant wave height in Burrard Inlet as simulated by SWAN for high wave heights (H_{sig} at boundary = 1.64 m) and a strong wind speed (8.69 m/s) from the south.

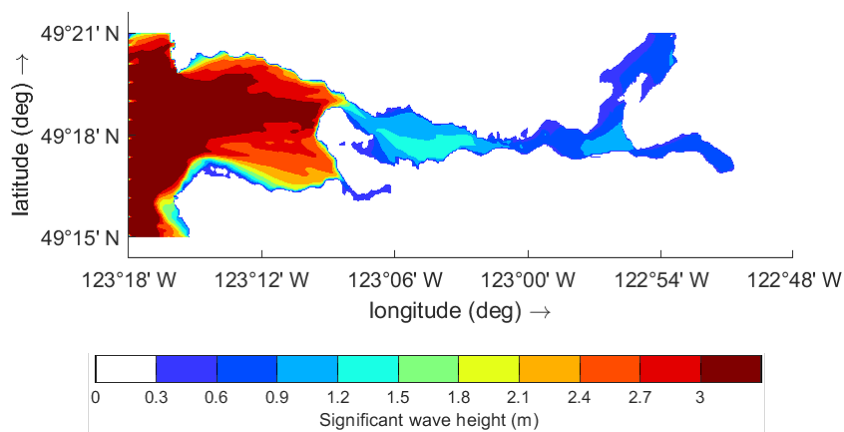


Figure G.7: Extreme West: Significant wave height in Burrard Inlet as simulated by SWAN for extreme wave heights (H_{sig} at boundary = 3.5 m) and a strong wind speed (24.2 m/s) from the west.

G.2. Wave-driven changes to net transport

Figures G.8 to G.14 show the wave-driven changes to the net sediment transport in Central Harbour. The arrows show the directions of the transport vectors. In areas highlighted in red, transport without waves is stronger. In areas highlighted in blue, transport with waves is stronger. In most images, the 'shift' in main transport line can be observed, as well as an increase in strength along the vulnerable shorelines.

Figure G.15 shows the local offshore-directed currents described in Section 3.2

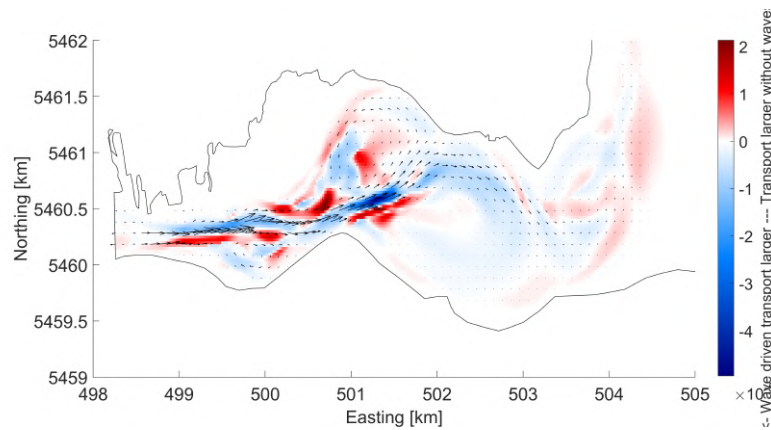


Figure G.8: Average East: Net transports over the full period for average waves (H_{sig} at boundary = 0.38 m) and an average wind speed (4.0 m/s) from the east.

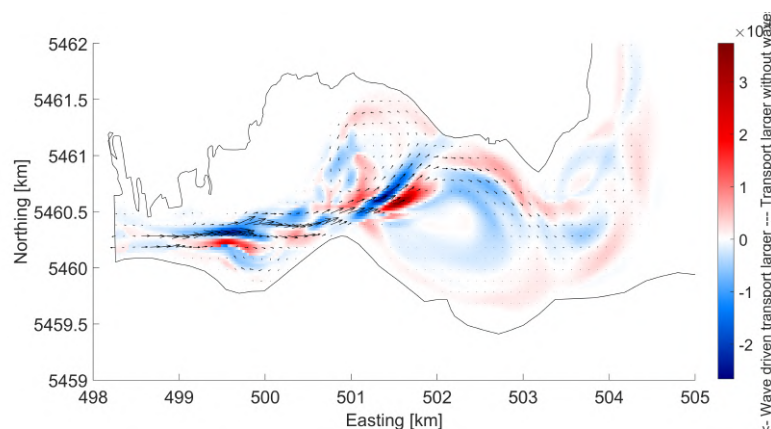


Figure G.9: Average West: Net transports over the full period for average waves (H_{sig} at boundary = 0.38 m) and an average wind speed (4.0 m/s) from the west.

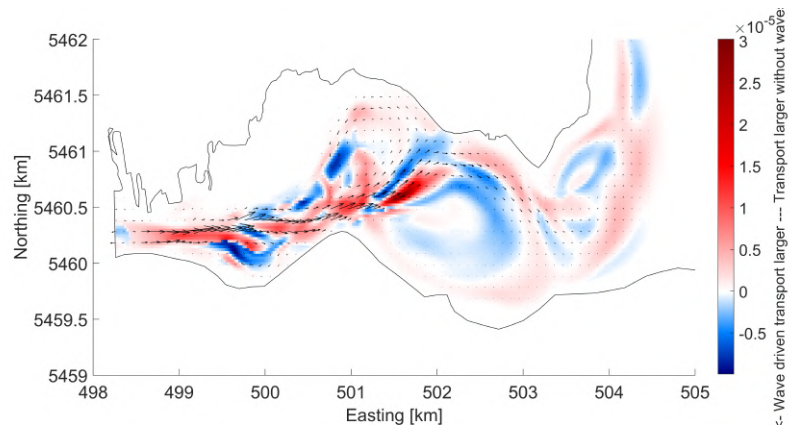


Figure G.10: Average South: Net transports over the full period for average waves (H_{sig} at boundary = 0.38 m) and an average wind speed (4.0 m/s) from the south.

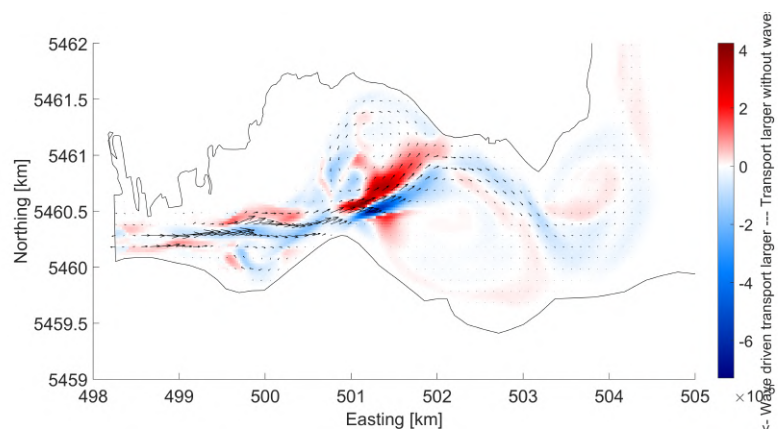


Figure G.11: High East: Net transports over the full period for high waves (H_{sig} at boundary = 1.64 m) and a strong wind speed (8.69 m/s) from the east.

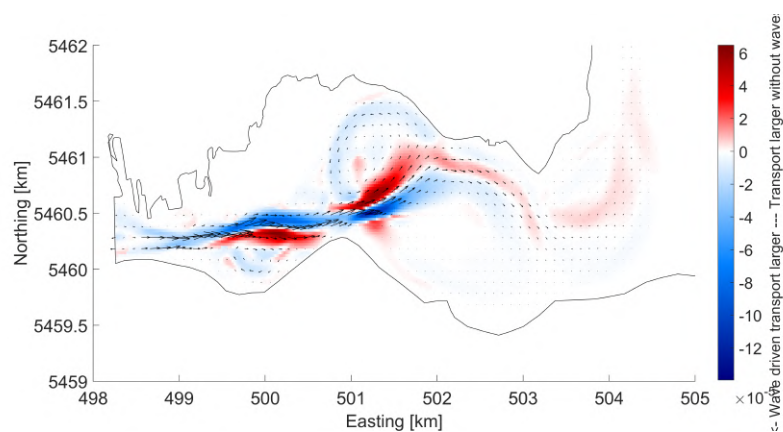


Figure G.12: High West: Net transports over the full period for high waves (H_{sig} at boundary = 1.64 m) and a strong wind speed (8.69 m/s) from the west.

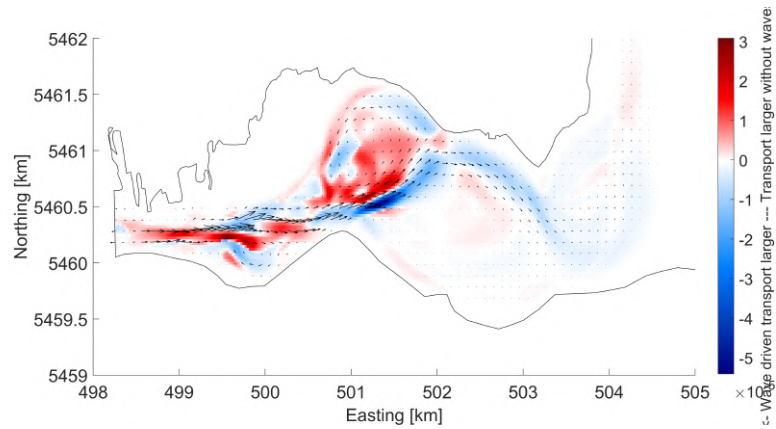


Figure G.13: High South: Net transports over the full period for high waves (H_{sig} at boundary = 1.64 m) and an strong wind speed (8.69 m/s) from the south.

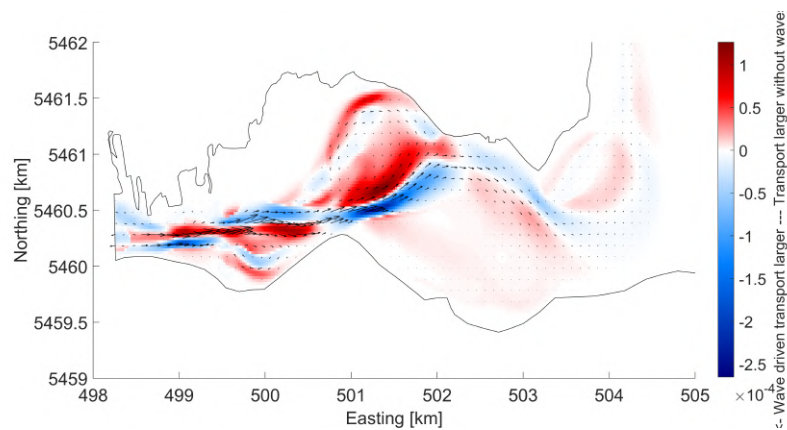


Figure G.14: Extreme West: Net transports over the full period for extremely high waves (H_{sig} at boundary = 3.5 m) and an extreme wind speed (24.2 m/s) from the west.

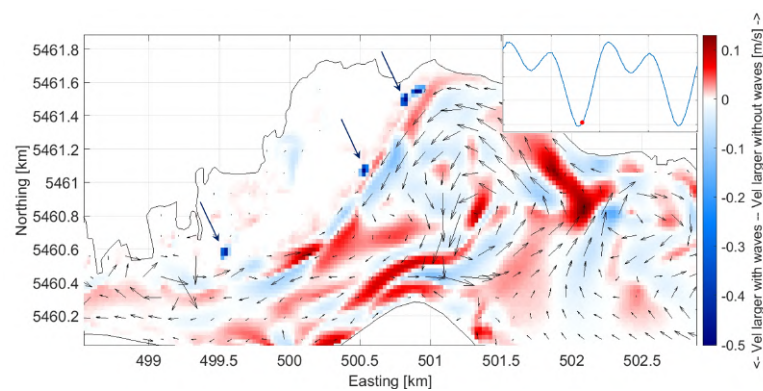


Figure G.15: Velocities for high waves from the south during low water. The wave-driven local offshore currents are indicated with arrows.

G.3. SedTRAILS pathways for waves

For each wave scenario, the SedTRAILS visualization of the transport pathways is shown (Figures G.16 until G.20).

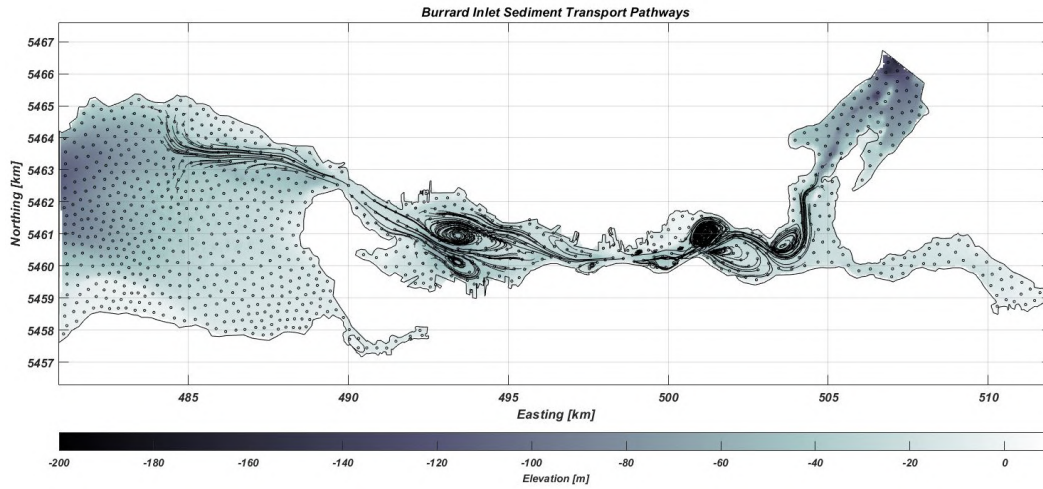


Figure G.16: Average East: SedTRAILS run with average wave heights (0.38 m) and an average wind speed (4.0 m/s) from the east.

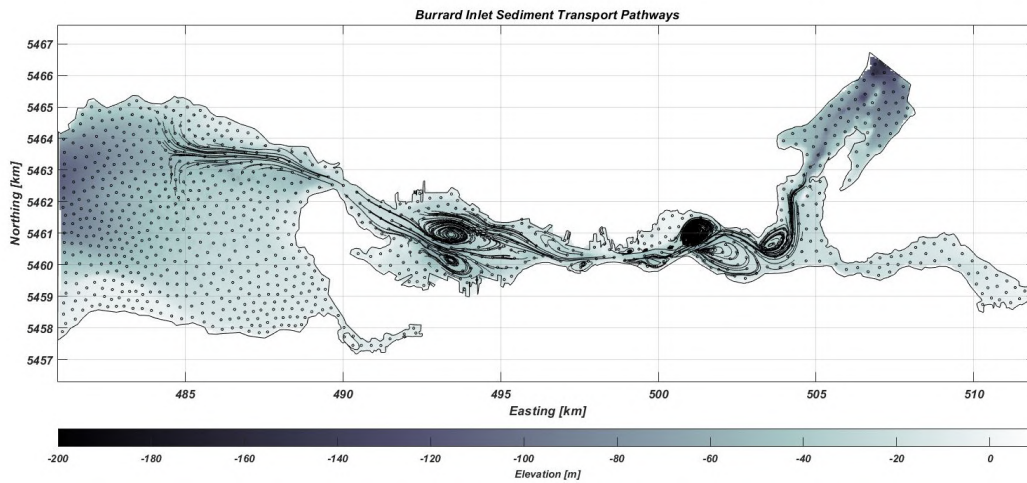


Figure G.17: Average West: SedTRAILS run with average wave heights ($H_s = 0.38$ m) and an average wind speed (4.0 m/s) from the west.

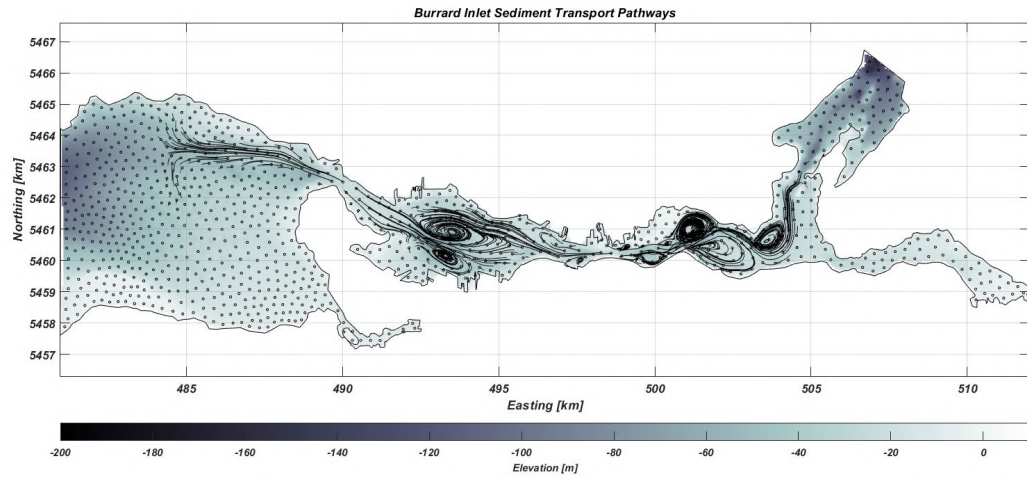


Figure G.18: High East: SedTRAILS run with high waves ($H_s = 1.64$ m) and strong wind (8.69 m/s) from the east.

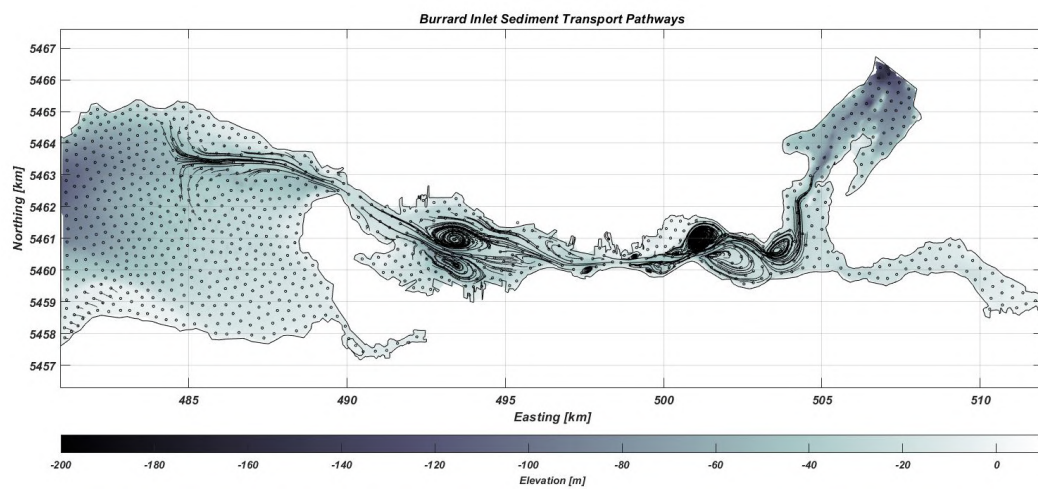


Figure G.19: High West: SedTRAILS run with high waves ($H_s = 1.64$ m) and strong wind (8.69 m/s) from the west.

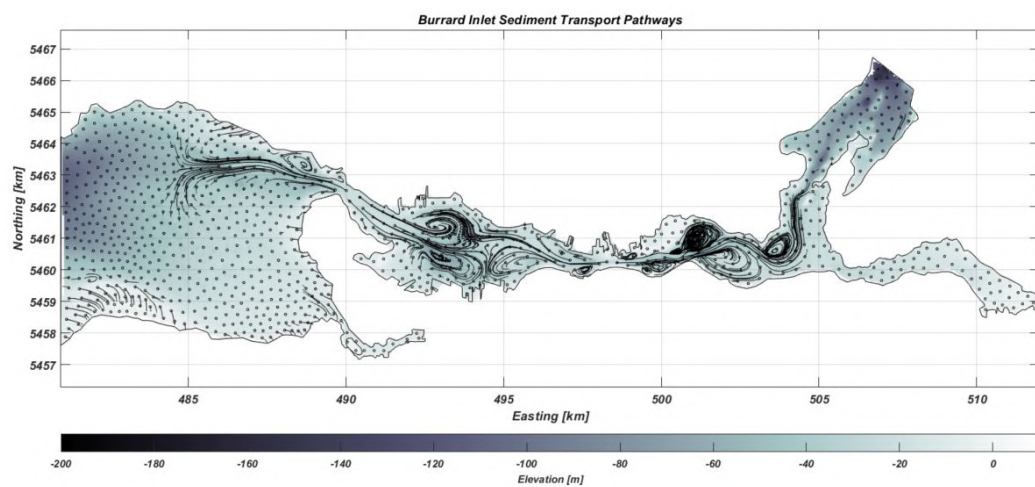
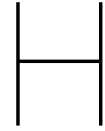


Figure G.20: Extreme West: SedTRAILS run with extreme waves ($H_s = 3.5$ m) and extreme wind (24.2 m/s) from the west.



Human Interventions

Two model runs are performed using the reconstructed shorelines from 1792 (Tsleil-Waututh Nation, 2021), assigning intertidal areas a height of respectively 1m and 2m. This appendix presents the results for both scenarios.

Figure H.1 shows which areas of False Creek are not covered by the grid.

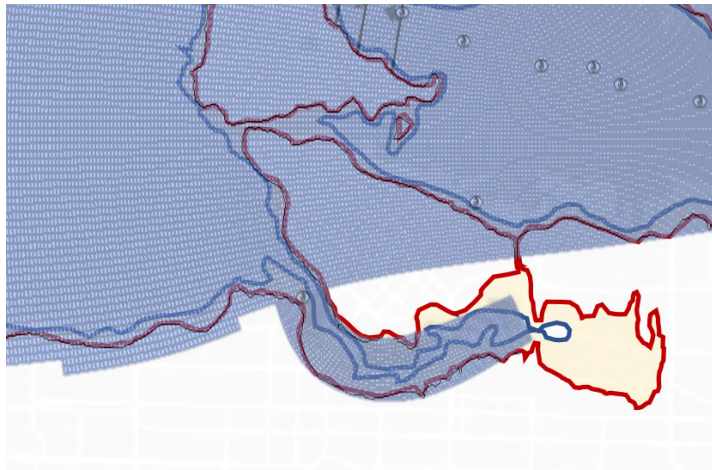


Figure H.1: A map of the historic shorelines (high water line in red, low water line in blue, with the intertidal areas indicated in yellow). The used grid is plotted over the historic shorelines, showing the areas of False Creek that are not covered by the grid.

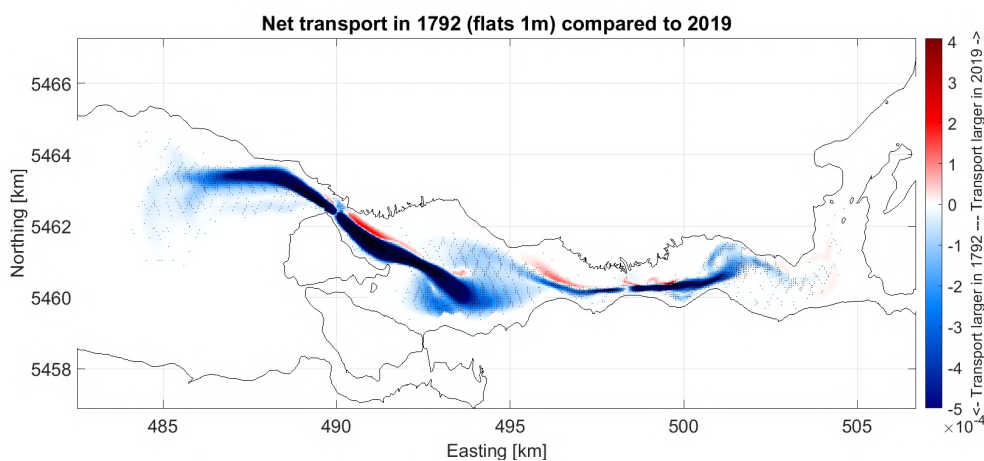


Figure H.2: Comparison of the net transports over the full simulation period for the 1792 (flats 1m high) and 2019 shorelines. In blue areas, transport vectors were stronger in 1792. In red areas, transport vectors are stronger in 2019.

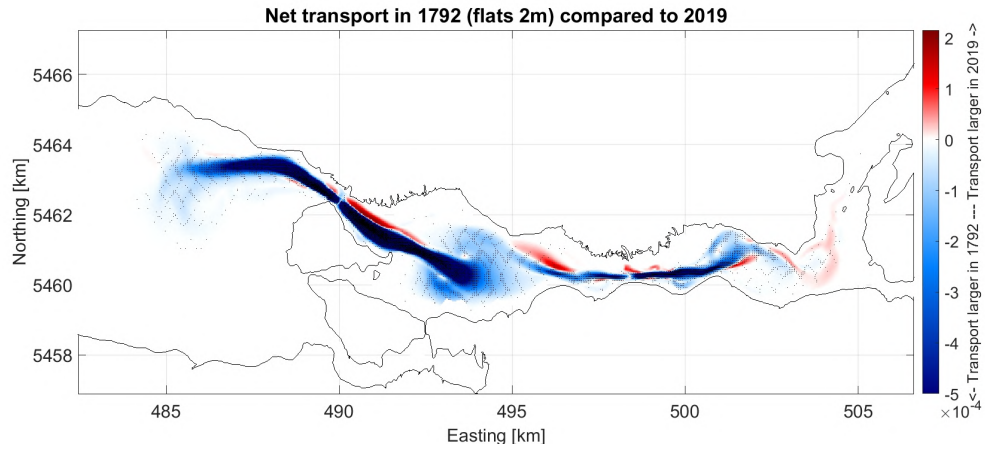


Figure H.3: Comparison of the net transports over the full simulation period for the 1792 (flats 2m high) and 2019 shorelines. In blue areas, transport vectors were stronger in 1792. In red areas, transport vectors are stronger in 2019.

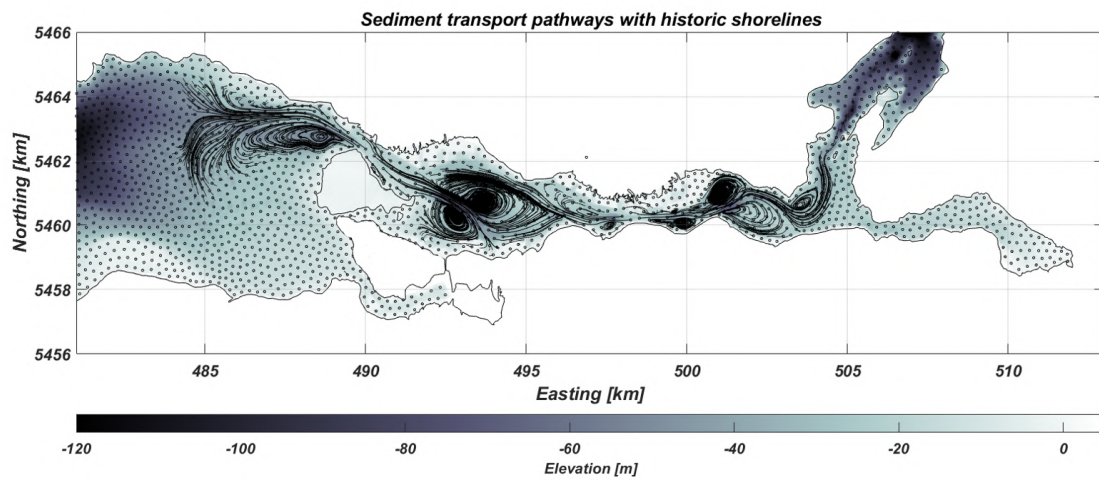


Figure H.4: SedTRAILS performed of Burrard Inlet for tidal flats of 1m high.

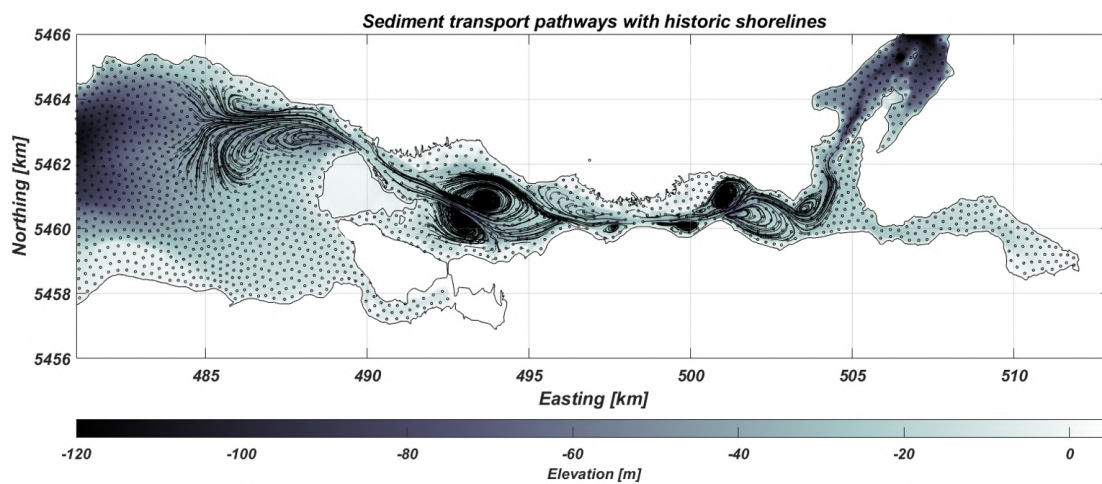
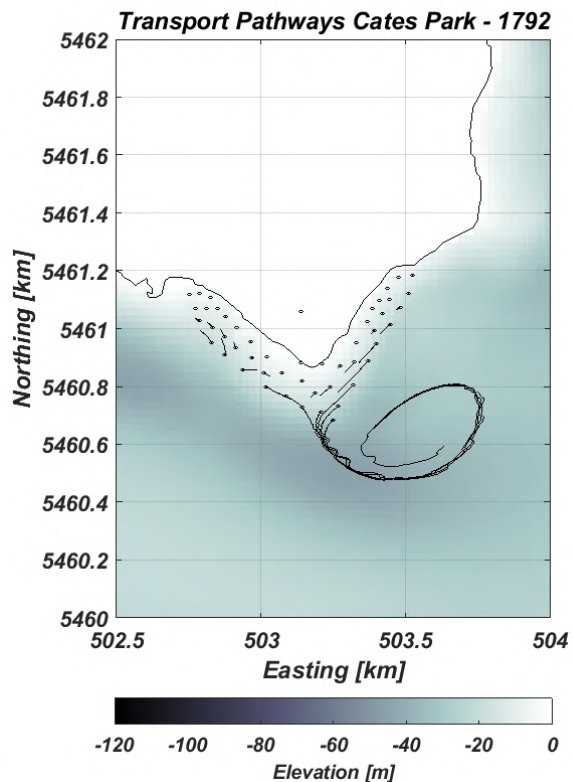
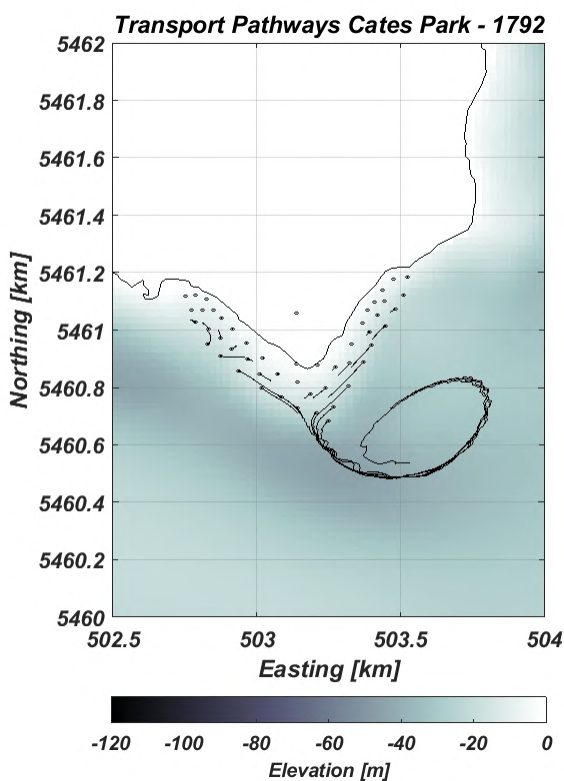


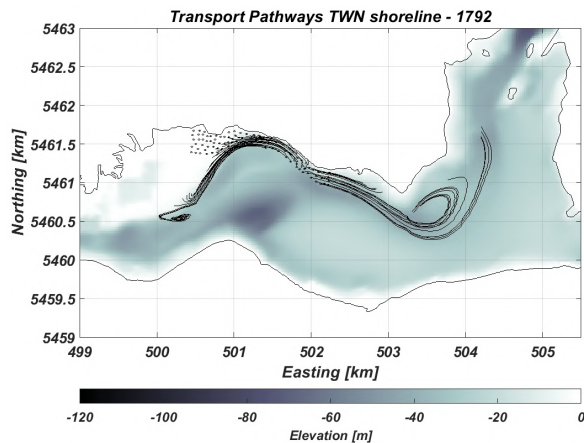
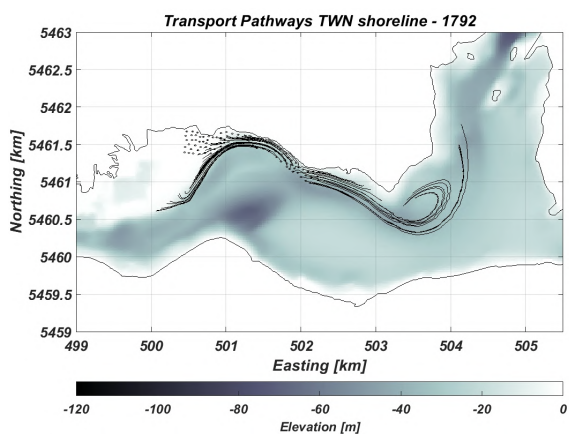
Figure H.5: SedTRAILS performed of Burrard Inlet for tidal flats of 2m high.



(a)

(b)

Figure H.6: a) Trajectories originating from Cates Park, intertidal areas 1m high. b) Trajectories originating from Cates Park, intertidal areas 2m high.



(a)

(b)

Figure H.7: a) Trajectories originating from the shorelines in front of the TWN reserve, intertidal areas 1m high. b) Trajectories originating from the shorelines in front of the TWN reserve, intertidal areas 2m high.